Regenerable Liquid Desiccants for High Efficiency Humidity Control in Microgravity

The University of North Texas

X-Hab Team: Gerardo Castro, Laura Barbe, Martin Vu, Jeffery Asencio, Joshua Joblin

Graduate Students: Chirag Byanjankar, Alex Sarvadi

Faculty Advisor: Dr. Huseyin Bostanci (PI), Dr. Cable Kurwitz (Co-PI, Texas A&M University)

NASA Mentor: Grace Belancik, NASA Ames Research Center

Final Report

May 2023

Table of Contents

List of Figures

List of Tables

Nomenclature

Table 1: Nomenclature	Symbol	Variable	Units
Material Property Variables	ρg	density of gas phase	kg/m^3
	ρ1	inlet liquid density	kg/m^3
	µl	dynamic viscosity of fluid @ liq. inlet	N*s/m
	ν	kinematic viscosity of liquid	m^2/s
	σ	surface tension force	N/m
Input Variables	$\tilde{V}$	liquid flow rate into nozzle	LPM
	VF	fluid volume	L
Geometric Variables	A	liquid inlet area of nozzle	m^2
	As	surface area of cylinder	m^2
	D	cylinder diameter	m
	Dz	height inlet nozzle to baffle plate	m
	h	height of nozzle inlet	m
	H	height of cylinder	m
	R	separator inner radius	m
	wd	liquid inlet width	m
Bubble Analysis and Infill Variables	AAT	axial and tangential flow area	m^2
	ab	bubble acceleration	m/s^2
	Bo	Bond number	--
	CD1	drag coeff for 20 < Reb < 1500	--
	D1	core diameter	m
	Fd	drag force	N
	Fb	buoyant force	N
	Fr	Froude number	--
	Fres	resultant force	N
	Fw	weight force	N
	L	distance, separator axis to bubble center	m
	LN	sq. rt. liq. inlet area of nozzle A	m
	m	mass of liquid	kg
	$\dot{m}$	flow rate	kg*m/s
	ω	rotational fluid speed inside separator	RPM
	ωmin	min. ω for successful vortex separation	RPM
	$\dot{p}$	inlet momentum rate	N
	r	bubble radius	M
	Reb	Reynolds Number around the bubble	--
	ReN	Reynolds Number at liquid inlet	--
	ta	axial transit time nozzle to baffle plate	s
	tr	radial transit time outside to VPS vortex center	s
	V	liquid inlet velocity	m/s
	V1	liquid fill level	m
	vrad	radial velocity of a bubble	m/s
	Vsph	volume of bubble	m^3
	vterm	terminal velocity of the bubble	m/s
	vz	average axial velocity	m/s
	We	Weber number	--

EXECUTIVE SUMMARY

The NASA X-Hab project aims to design, manufacture, test, and prove functionality of an air humidity control subsystem to dehumidify and re-humidify air from a space cabin. The method of regulating cabin air humidity utilizes vortex phase separation, which uses an ionic liquid (IL) desiccant for air-water phase separation. This subsystem is intended to be integrated with a CO_2 removal system requiring de-humidified air to operate efficiently. The air humidity control subsystem is composed of a cold-desiccant or cold-side Vortex Phase Separator (VPS) that dehumidifies the cabin air. The dehumidified air exits the cold-side (CS) VPS chamber to flow into the CO_2 removal module, and the cold, water-laden liquid desiccant flows to a regenerative heat exchanger. From the heat exchanger the liquid desiccant continues to the heater. After heating, the desiccant flows into a hot-desiccant or hot-side (HS) VPS as the dehumidified air from CO_2 removal module enters through the HS VPS air inlet. The re-humidified air exits the HS VPS into the space cabin. One pump installed at the liquid exit of the CS VPS and one pump installed at the liquid exit of the HS VPS transport the fluid through the system. To evaluate the system's efficiency and effectiveness, the temperature, pressure, flow rate and relative humidity are read, recorded, and analyzed at critical points along the module.

1. INTRODUCTION

The following sections describe the project objective, motivation, and approach.

1.1. Objective

The goal of this project is to develop a sub-system that regulates humidity from a deep-space cabin. The sub-system utilizes a hot and cold VPS to humidify and dehumidify the processed cabin air. A liquid desiccant was selected, and the humidity control VPS system was designed, manufactured, and tested. Before designing the components of the sub-system, the chemical, thermal, and physical properties of the desiccant were needed to characterize and predict the behavior of the liquid desiccant in context of aircraft humidity removal. Once these properties were identified, the material was selected for the VPS chambers, nozzles, and tubing. [1][2][3][4] The major targets for this humidity control module include:

1) The use of a liquid desiccant to absorb humidity, preferably an IL
2) The use of a cold VPS that will mix the desiccant with the cabin air to separate the humidity from
   cabin air before it is decarbonated
3) The use of a hot VPS that will mix the desiccant with the decarbonated air to add the humidity back
   into it before it is directed into the cabin.
4) High reliability
5) Safe operation
6) High efficiency
7) The ability of the desiccant to release all absorbed moisture, or to regenerate.

1.2. Motivation

The motivation for this project is to produce an efficient and reliable sub-system that can dehumidify and re-humidify space cabin air in a microgravity environment.

1.3. Approach

The approach taken for this project begins with selection of a liquid desiccant. Properties such as water-miscibility, density, kinematic and dynamic viscosities, vapor pressure were considered during liquid desiccant selection. The desiccant's thermodynamic properties are important in optimizing VPS system performance for dehumidification and re-humidification. To ensure that the system is safe, effective, and reliable long-term, the desiccant must be:

1) Non-combustible
2) Non-corrosive
3) Non-toxic and odorless
4) Regenerative
5) Thermally stable

Once the liquid desiccant is chosen, calculations are performed to determine the physical performance of the VPS with the chosen desiccant(s) and to characterize parameters for optimal VPS geometry. EXCEL and MATLAB were used to complete calculations. Previous iterations of VPS designs were analyzed to determine the VPS design. The following parameters determined the VPS design:

1) VPS chamber geometry
2) Inlet nozzle geometry
3) VPS baffle plate geometry
4) Liquid inlet dynamics
5) Bubble transit time and average bubble size
6) Liquid flow rate inside the VPS
7) Infill volume
8) Manufacturability
9) IL corrosivity

Once Calculations were finalized for the design of the VPS sub-system, the components were designed in Fusion360 and SolidWorks. The VPS chamber, baffle plate, and inlet liquid and gas nozzles were designed separately.

After the design was finalized, the VPS and accompanying components were manufactured. Subtractive manufacturing was the primary method considered for the VPS chamber and gas/liquid nozzles. Additive manufacturing was also used to create components with complex geometry. Fusion360 CAM software was used to create the programs for CNC milling and wire EDM cutting at the UNT machine shop. Mechanical engineering students have access to the Wire EDM, along with HAAS CNC 3-axis mill and lathe machines. Dimensions and tolerances were measured, evaluated, and adjusted for throughout manufacturing and inspection.

Parts, instruments, and components were chosen and ordered for the remainder of the subsystem. Once the components were consolidated, the sub-system was assembled. The assembly includes a VPS for the hot side of the system (along with its respective nozzles, fittings, sensors, heater, and heat exchanger), a VPS for the cold side of the system (along with its respective nozzles, fittings, sensors, chiller, and heat exchanger), and the accompanying stainless-steel tubing used to transport processed liquid desiccant and plastic tubing for cabin air. Tests were run on the final assembly, and results were compared to the predicted outcomes.

2. PROJECT TIMELINE

This section illustrates the distribution of tasks and completion schedule. A comprehensive Gantt Chart was created to set tasks, helping the team visualize the project over time by listing tasks and subtasks by task group. The number of days available and effective dates for task completion are also noted. The X-Hab project was expected to take 8 months to complete. The first half of the project is dedicated to researching and selecting a liquid desiccant, understanding the calculations required to design the VPS, designing the VPS, and selecting materials, fittings, and instruments to order, starting 19th of September 2022, and ending 9th of December 2022. The second half of the project is dedicated to finalizing the design, consolidating materials, testing sensors, running experiments, manufacturing components, assembling the prototype, testing the system, and analyzing the results, starting the 19th of January 2023, and ending the 28th of April 2023.

2.1. Gantt Chart

M2M X-HAB 2023

NASA

Project Start Date: 9/19/2022 (Monday) | Display Week: 1 | Project Lead: Gerardo Castro

WBS	TASK	TASK LEAD	START	END	DAYS	% DONE	WORK DAYS
1	**Experiment Set-Up**			-			-
1.1	Design Experiment	All	Mon 12/19/22	Fri 12/23/22	5	100%	5
1.1.1	Redesign Tee fittings for RH sensors	Jeff & Martin	Mon 12/19/22	Wed 12/21/22	3	100%	3
1.1.2	Adjust Fittings at UNT Machine Shop	Gerardo & Laura	Wed 12/21/22	Wed 1/04/23	15	100%	11
1.2	Assemble Experiment	Jeff Josh & Gerardo	Sun 1/01/23	Fri 2/03/23	34	90%	25
1.4	Run Experiment with Water	All	Mon 1/02/23	Sun 2/05/23	35	0%	25
2	**Optimize Prototype Design**			-			-
2.1	Meet with Dr. Kurwitz	All	Thu 1/05/23	Fri 1/06/23	2	100%	2
2.1.1	Finalize Calcs for Nozzles	Gerardo & Laura	Thu 1/05/23	Thu 1/12/23	8	100%	6
2.1.2	Finalize Calcs for Baffle Plate	Martin	Thu 1/05/23	Thu 1/12/23	8	100%	6
2.1.3	Finalize Calcs for Chamber	Jeff	Thu 1/05/23	Thu 1/12/23	8	100%	6
2.2	Order All Components & Materials	All	Wed 1/11/23	Wed 1/11/23	1	26%	1
2.3	Consolidate all in-house Components	All	Wed 1/11/23	Sat 1/14/23	4	100%	3
3	**Fabrication**						
3.1	Manufacture VPS (Cold & Hot)	All	Tue 1/17/23	Fri 3/17/23	60	0%	44
3.1.1	Order all Tools and Fixtures needed	All	Tue 1/17/23	Fri 3/17/23	60	0%	44
3.2	Machine Chamber	Laura & Gerardo	Tue 1/17/23	Fri 3/17/23	60	0%	44
3.2.1	Machine Baffle	Laura	Tue 1/17/23	Fri 3/17/23	60	0%	44
3.2.2	Machine Baffle Spacers	Josh	Tue 1/17/23	Fri 3/17/23	60	0%	44
3.2.3	Machine End Plates	Josh	Tue 1/17/23	Fri 3/17/23	60	0%	44
3.3	Manufacture Nozzles (Gas & Liquid)	Gerardo	Tue 1/17/23	Fri 3/17/23	60	0%	44
4	**Assembly**						
4.1	Assemble VPS (Cold & Hot)	All	Wed 3/15/23	Wed 4/05/23	21	0%	15
4.2	Set up plumbing	All	Wed 3/15/23	Wed 4/05/23	21	0%	15
4.3	Install Sensors	All	Wed 3/15/23	Wed 4/05/23	21	0%	15
4.4	Install Pumps, HX, Heater, Chiller,	All	Wed 3/15/23	Wed 4/05/23	21	0%	15
5	**Testing Prototype**						
5.1	Create LabView program for prototype	All	Wed 3/21/23	Fri 5/05/23	23	0%	17
5.2	Run prototype with water	All	Wed 3/21/23	Sat 5/06/23	23	0%	17
5.1	Perform test runs	All	Wed 4/12/23	Fri 5/05/23	23	0%	17
5.2	Collect data from sensors	All	Wed 4/12/23	Fri 5/05/23	23	0%	17
6	**NASA Milestones**						
6.1	Kickoff Meeting	All	Thu 9/22/22	Thu 9/22/22	1	100%	1
6.2	SDR Presentation	All	Thu 10/27/22	Thu 10/27/22	1	100%	1
6.3	PDR Presentation	All	Thu 12/01/22	Thu 12/01/22	1	100%	1
6.4	CDR Presentation	All	Fri 2/24/23	Fri 2/24/23	1	0%	1
6.5	PCR Presentation	All	Sat 3/11/23	Sat 3/11/23	1	0%	1
6.6	Project Completion and Evaluation by NASA	All	Sat 5/06/23	Sat 5/06/23	1	0%	1
7	**Report**						
7.1	Sections I - III	--	Sun 10/02/22	Thu 10/20/22	19	75%	14
7.1.1	Section I	Gerardo	Sun 10/02/22	Thu 10/20/22	19	100%	14
7.1.2	Section II	Martin	Sun 10/02/22	Thu 10/20/22	19	100%	14
7.1.3	Section III pt. 1	--	Sun 10/02/22	Thu 10/20/22	19	100%	14
7.1.3.1	III.a	Josh	Sun 10/02/22	Thu 10/20/22	19	75%	14
7.1.3.2	III.b	Laura	Sun 10/02/22	Thu 10/20/22	19	100%	14
7.1.3.3	III.c	Jeff	Sun 10/02/22	Thu 10/20/22	19	100%	14
7.1.4	References (Append A)	All	Sun 10/02/22	Mon 10/31/22	30	90%	21
7.1.5	Consolidation	Gerardo	Sun 10/02/22	Thu 10/20/22	19	100%	14
7.1.6	Review/ Format/ Edit I	Laura	Sun 10/02/22	Thu 10/20/22	19	100%	14

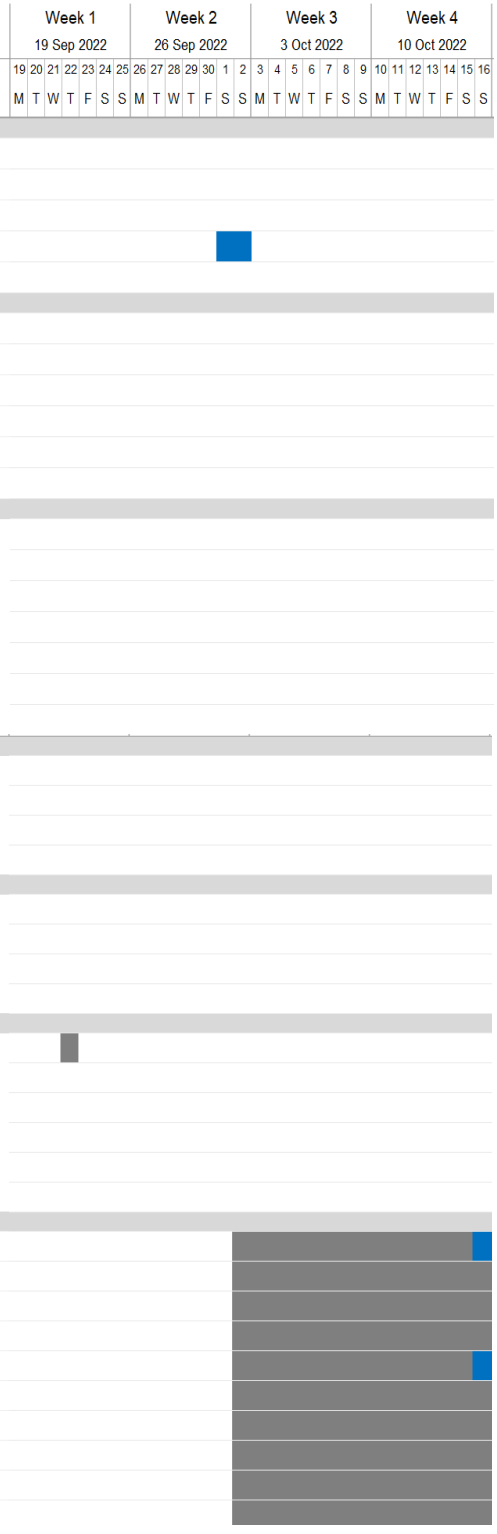

Figure 1: Gantt Chart – Weeks 1-4

M2M X-HAB 2023

NASA

Project Start Date: 9/19/2022 (Monday) | Display Week: 5
Project Lead: Gerardo Castro

WBS	TASK	TASK LEAD	START	END	DAYS	% DONE	WORK DAYS
1	**Experiment Set-Up**			-			-
1.1	Design Experiment	All	Mon 12/19/22	Fri 12/23/22	5	100%	5
1.1.1	Redesign Tee fittings for RH sensors	Jeff & Martin	Mon 12/19/22	Wed 12/21/22	3	100%	3
1.1.2	Adjust Fittings at UNT Machine Shop	Gerardo & Laura	Wed 12/21/22	Wed 1/04/23	15	100%	11
1.2	Assemble Experiment	Jeff Josh & Gerardo	Sun 1/01/23	Fri 2/03/23	34	90%	25
1.4	Run Experiment with Water	All	Mon 1/02/23	Sun 2/05/23	35	0%	25
2	**Optimize Prototype Design**			-			-
2.1	Meet with Dr. Kurwitz	All	Thu 1/05/23	Fri 1/06/23	2	100%	2
2.1.1	Finalize Calcs for Nozzles	Gerardo & Laura	Thu 1/05/23	Thu 1/12/23	8	100%	6
2.1.2	Finalize Calcs for Baffle Plate	Martin	Thu 1/05/23	Thu 1/12/23	8	100%	6
2.1.3	Finalize Calcs for Chamber	Jeff	Thu 1/05/23	Thu 1/12/23	8	100%	6
2.2	Order All Components & Materials	All	Wed 1/11/23	Wed 1/11/23	1	26%	1
2.3	Consolidate all in-house Components	All	Wed 1/11/23	Sat 1/14/23	4	100%	3
3	**Fabrication**						
3.1	Manufacture VPS (Cold & Hot)	All	Tue 1/17/23	Fri 3/17/23	60	0%	44
3.1.1	Order all Tools and Fixtures needed	All	Tue 1/17/23	Fri 3/17/23	60	0%	44
3.2	Machine Chamber	Laura & Gerardo	Tue 1/17/23	Fri 3/17/23	60	0%	44
3.2.1	Machine Baffle	Laura	Tue 1/17/23	Fri 3/17/23	60	0%	44
3.2.2	Machine Baffle Spacers	Josh	Tue 1/17/23	Fri 3/17/23	60	0%	44
3.2.3	Machine End Plates	Josh	Tue 1/17/23	Fri 3/17/23	60	0%	44
3.3	Manufacture Nozzles (Gas & Liquid)	Gerardo	Tue 1/17/23	Fri 3/17/23	60	0%	44
4	**Assembly**						
4.1	Assemble VPS (Cold & Hot)	All	Wed 3/15/23	Wed 4/05/23	21	0%	15
4.2	Set up plumbing	All	Wed 3/15/23	Wed 4/05/23	21	0%	15
4.3	Install Sensors	All	Wed 3/15/23	Wed 4/05/23	21	0%	15
4.4	Install Pumps, HX, Heater, Chiller,	All	Wed 3/15/23	Wed 4/05/23	21	0%	15
5	**Testing Prototype**						
5.1	Create LabView program for prototype	All	Wed 3/21/23	Fri 5/05/23	23	0%	17
5.2	Run prototype with water	All	Wed 3/21/23	Sat 5/06/23	23	0%	17
5.1	Perform test runs	All	Wed 4/12/23	Fri 5/05/23	23	0%	17
5.2	Collect data from sensors	All	Wed 4/12/23	Fri 5/05/23	23	0%	17
6	**NASA Milestones**						
6.1	Kickoff Meeting	All	Thu 9/22/22	Thu 9/22/22	1	100%	1
6.2	SDR Presentation	All	Thu 10/27/22	Thu 10/27/22	1	100%	1
6.3	PDR Presentation	All	Thu 12/01/22	Thu 12/01/22	1	100%	1
6.4	CDR Presentation	All	Fri 2/24/23	Fri 2/24/23	1	0%	1
6.5	PCR Presentation	All	Sat 3/11/23	Sat 3/11/23	1	0%	1
6.6	Project Completion and Evaluation by NASA	All	Sat 5/06/23	Sat 5/06/23	1	0%	1
7	**Report**						
7.1	Sections I - III	--	Sun 10/02/22	Thu 10/20/22	19	75%	14
7.1.1	Section I	Gerardo	Sun 10/02/22	Thu 10/20/22	19	100%	14
7.1.2	Section II	Martin	Sun 10/02/22	Thu 10/20/22	19	100%	14
7.1.3	Section III pt. 1	--	Sun 10/02/22	Thu 10/20/22	19	100%	14
7.1.3.1	III.a	Josh	Sun 10/02/22	Thu 10/20/22	19	75%	14
7.1.3.2	III.b	Laura	Sun 10/02/22	Thu 10/20/22	19	100%	14
7.1.3.3	III.c	Jeff	Sun 10/02/22	Thu 10/20/22	19	100%	14
7.1.4	References (Append A)	All	Sun 10/02/22	Mon 10/31/22	30	90%	21
7.1.5	Consolidation	Gerardo	Sun 10/02/22	Thu 10/20/22	19	100%	14
7.1.6	Review/ Format/ Edit I	Laura	Sun 10/02/22	Thu 10/20/22	19	100%	14

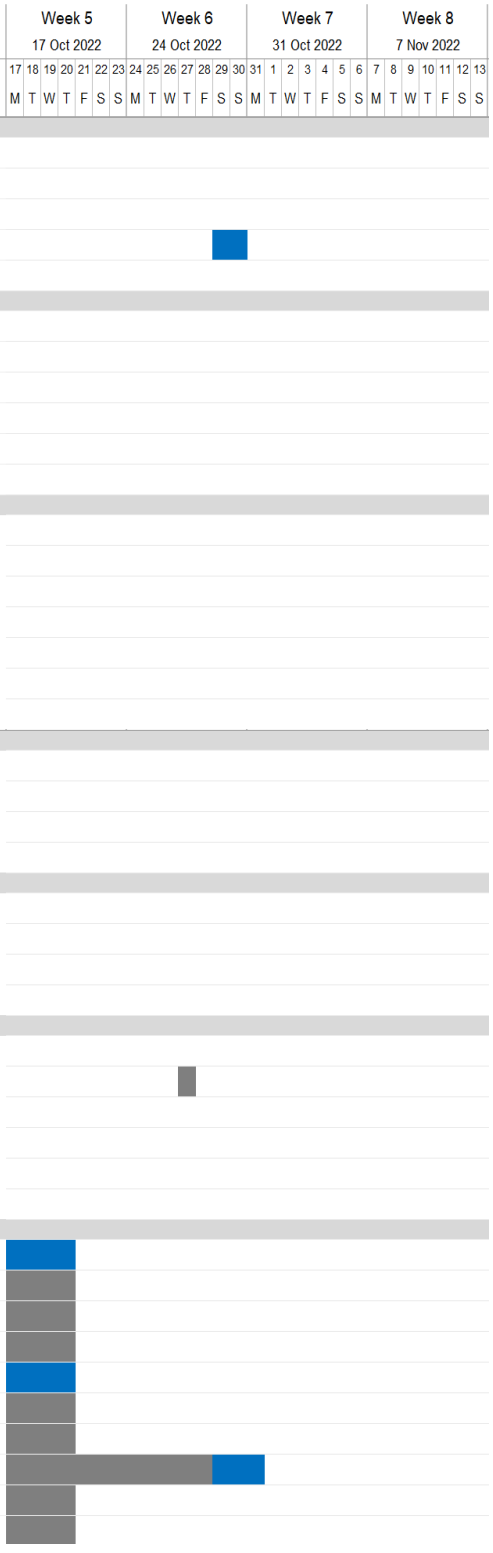

Figure 2: Gantt Chart – Weeks 5-8

M2M X-HAB 2023

NASA

Project Start Date: 9/19/2022 (Monday) | Display Week: 9
Project Lead: Gerardo Castro

WBS	TASK	TASK LEAD	START	END	DAYS	% DONE	WORK DAYS
1	**Experiment Set-Up**			-			-
1.1	Design Experiment	All	Mon 12/19/22	Fri 12/23/22	5	100%	5
1.1.1	Redesign Tee fittings for RH sensors	Jeff & Martin	Mon 12/19/22	Wed 12/21/22	3	100%	3
1.1.2	Adjust Fittings at UNT Machine Shop	Gerardo & Laura	Wed 12/21/22	Wed 1/04/23	15	100%	11
1.2	Assemble Experiment	Jeff Josh & Gerardo	Sun 1/01/23	Fri 2/03/23	34	90%	25
1.4	Run Experiment with Water	All	Mon 1/02/23	Sun 2/05/23	35	0%	25
2	**Optimize Prototype Design**			-			-
2.1	Meet with Dr. Kurwitz	All	Thu 1/05/23	Fri 1/06/23	2	100%	2
2.1.1	Finalize Calcs for Nozzles	Gerardo & Laura	Thu 1/05/23	Thu 1/12/23	8	100%	6
2.1.2	Finalize Calcs for Baffle Plate	Martin	Thu 1/05/23	Thu 1/12/23	8	100%	6
2.1.3	Finalize Calcs for Chamber	Jeff	Thu 1/05/23	Thu 1/12/23	8	100%	6
2.2	Order All Components & Materials	All	Wed 1/11/23	Wed 1/11/23	1	26%	1
2.3	Consolidate all in-house Components	All	Wed 1/11/23	Sat 1/14/23	4	100%	3
3	**Fabrication**						
3.1	Manufacture VPS (Cold & Hot)	All	Tue 1/17/23	Fri 3/17/23	60	0%	44
3.1.1	Order all Tools and Fixtures needed	All	Tue 1/17/23	Fri 3/17/23	60	0%	44
3.2	Machine Chamber	Laura & Gerardo	Tue 1/17/23	Fri 3/17/23	60	0%	44
3.2.1	Machine Baffle	Laura	Tue 1/17/23	Fri 3/17/23	60	0%	44
3.2.2	Machine Baffle Spacers	Josh	Tue 1/17/23	Fri 3/17/23	60	0%	44
3.2.3	Machine End Plates	Josh	Tue 1/17/23	Fri 3/17/23	60	0%	44
3.3	Manufacture Nozzles (Gas & Liquid)	Gerardo	Tue 1/17/23	Fri 3/17/23	60	0%	44
4	**Assembly**						
4.1	Assemble VPS (Cold & Hot)	All	Wed 3/15/23	Wed 4/05/23	21	0%	15
4.2	Set up plumbing	All	Wed 3/15/23	Wed 4/05/23	21	0%	15
4.3	Install Sensors	All	Wed 3/15/23	Wed 4/05/23	21	0%	15
4.4	Install Pumps, HX, Heater, Chiller,	All	Wed 3/15/23	Wed 4/05/23	21	0%	15
5	**Testing Prototype**						
5.1	Create LabView program for prototype	All	Wed 3/21/23	Fri 5/05/23	23	0%	17
5.2	Run prototype with water	All	Wed 3/21/23	Sat 5/06/23	23	0%	17
5.1	Perform test runs	All	Wed 4/12/23	Fri 5/05/23	23	0%	17
5.2	Collect data from sensors	All	Wed 4/12/23	Fri 5/05/23	23	0%	17
6	**NASA Milestones**						
6.1	Kickoff Meeting	All	Thu 9/22/22	Thu 9/22/22	1	100%	1
6.2	SDR Presentation	All	Thu 10/27/22	Thu 10/27/22	1	100%	1
6.3	PDR Presentation	All	Thu 12/01/22	Thu 12/01/22	1	100%	1
6.4	CDR Presentation	All	Fri 2/24/23	Fri 2/24/23	1	0%	1
6.5	PCR Presentation	All	Sat 3/11/23	Sat 3/11/23	1	0%	1
6.6	Project Completion and Evaluation by NASA	All	Sat 5/06/23	Sat 5/06/23	1	0%	1
7	**Report**						
7.1	Sections I - III	--	Sun 10/02/22	Thu 10/20/22	19	75%	14
7.1.1	Section I	Gerardo	Sun 10/02/22	Thu 10/20/22	19	100%	14
7.1.2	Section II	Martin	Sun 10/02/22	Thu 10/20/22	19	100%	14
7.1.3	Section III pt. 1	--	Sun 10/02/22	Thu 10/20/22	19	100%	14
7.1.3.1	III.a	Josh	Sun 10/02/22	Thu 10/20/22	19	75%	14
7.1.3.2	III.b	Laura	Sun 10/02/22	Thu 10/20/22	19	100%	14
7.1.3.3	III.c	Jeff	Sun 10/02/22	Thu 10/20/22	19	100%	14
7.1.4	References (Append A)	All	Sun 10/02/22	Mon 10/31/22	30	90%	21
7.1.5	Consolidation	Gerardo	Sun 10/02/22	Thu 10/20/22	19	100%	14
7.1.6	Review/ Format/ Edit I	Laura	Sun 10/02/22	Thu 10/20/22	19	100%	14

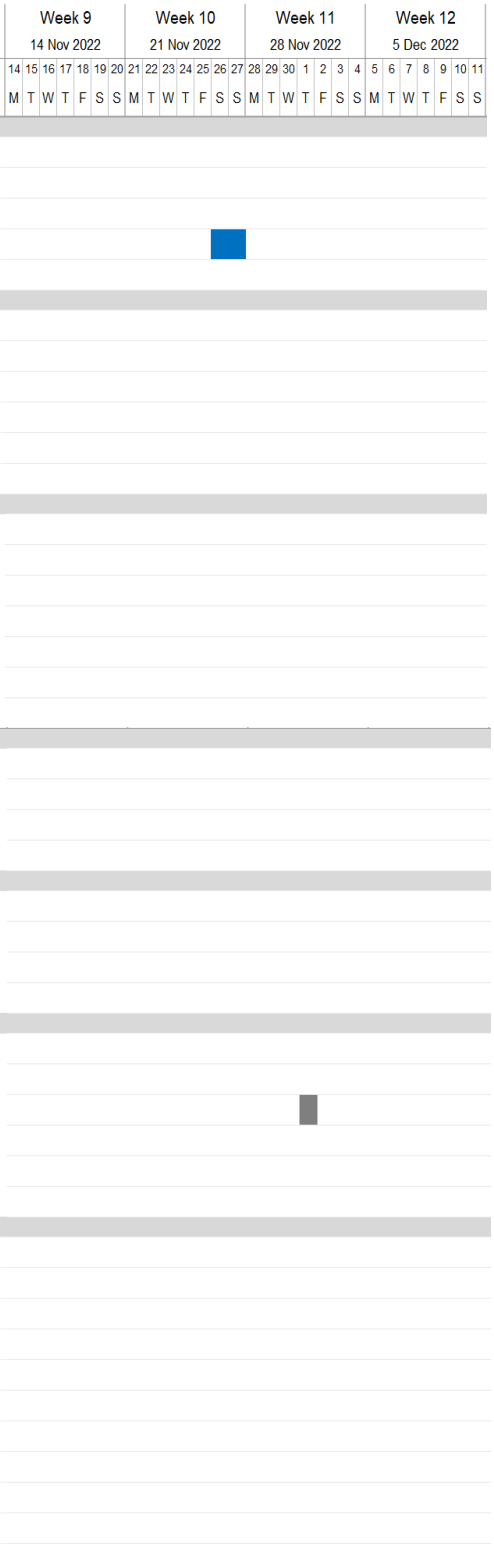

Figure 3: Gantt Chart – Weeks 9-12

M2M X-HAB 2023

NASA

Project Start Date: 9/19/2022 (Monday) | Display Week: 13
Project Lead: Gerardo Castro

WBS	TASK	TASK LEAD	START	END	DAYS	% DONE	WORK DAYS
1	**Experiment Set-Up**			-			-
1.1	Design Experiment	All	Mon 12/19/22	Fri 12/23/22	5	100%	5
1.1.1	Redesign Tee fittings for RH sensors	Jeff & Martin	Mon 12/19/22	Wed 12/21/22	3	100%	3
1.1.2	Adjust Fittings at UNT Machine Shop	Gerardo & Laura	Wed 12/21/22	Wed 1/04/23	15	100%	11
1.2	Assemble Experiment	Jeff Josh & Gerardo	Sun 1/01/23	Fri 2/03/23	34	90%	25
1.4	Run Experiment with Water	All	Mon 1/02/23	Sun 2/05/23	35	0%	25
2	**Optimize Prototype Design**			-			-
2.1	Meet with Dr. Kurwitz	All	Thu 1/05/23	Fri 1/06/23	2	100%	2
2.1.1	Finalize Calcs for Nozzles	Gerardo & Laura	Thu 1/05/23	Thu 1/12/23	8	100%	6
2.1.2	Finalize Calcs for Baffle Plate	Martin	Thu 1/05/23	Thu 1/12/23	8	100%	6
2.1.3	Finalize Calcs for Chamber	Jeff	Thu 1/05/23	Thu 1/12/23	8	100%	6
2.2	Order All Components & Materials	All	Wed 1/11/23	Wed 1/11/23	1	26%	1
2.3	Consolidate all in-house Components	All	Wed 1/11/23	Sat 1/14/23	4	100%	3
3	**Fabrication**						
3.1	Manufacture VPS (Cold & Hot)	All	Tue 1/17/23	Fri 3/17/23	60	0%	44
3.1.1	Order all Tools and Fixtures needed	All	Tue 1/17/23	Fri 3/17/23	60	0%	44
3.2	Machine Chamber	Laura & Gerardo	Tue 1/17/23	Fri 3/17/23	60	0%	44
3.2.1	Machine Baffle	Laura	Tue 1/17/23	Fri 3/17/23	60	0%	44
3.2.2	Machine Baffle Spacers	Josh	Tue 1/17/23	Fri 3/17/23	60	0%	44
3.2.3	Machine End Plates	Josh	Tue 1/17/23	Fri 3/17/23	60	0%	44
3.3	Manufacture Nozzles (Gas & Liquid)	Gerardo	Tue 1/17/23	Fri 3/17/23	60	0%	44
4	**Assembly**						
4.1	Assemble VPS (Cold & Hot)	All	Wed 3/15/23	Wed 4/05/23	21	0%	15
4.2	Set up plumbing	All	Wed 3/15/23	Wed 4/05/23	21	0%	15
4.3	Install Sensors	All	Wed 3/15/23	Wed 4/05/23	21	0%	15
4.4	Install Pumps, HX, Heater, Chiller,	All	Wed 3/15/23	Wed 4/05/23	21	0%	15
5	**Testing Prototype**						
5.1	Create LabView program for prototype	All	Wed 3/21/23	Fri 5/05/23	23	0%	17
5.2	Run prototype with water	All	Wed 3/21/23	Sat 5/06/23	23	0%	17
5.1	Perform test runs	All	Wed 4/12/23	Fri 5/05/23	23	0%	17
5.2	Collect data from sensors	All	Wed 4/12/23	Fri 5/05/23	23	0%	17
6	**NASA Milestones**						
6.1	Kickoff Meeting	All	Thu 9/22/22	Thu 9/22/22	1	100%	1
6.2	SDR Presentation	All	Thu 10/27/22	Thu 10/27/22	1	100%	1
6.3	PDR Presentation	All	Thu 12/01/22	Thu 12/01/22	1	100%	1
6.4	CDR Presentation	All	Fri 2/24/23	Fri 2/24/23	1	0%	1
6.5	PCR Presentation	All	Sat 3/11/23	Sat 3/11/23	1	0%	1
6.6	Project Completion and Evaluation by NASA	All	Sat 5/06/23	Sat 5/06/23	1	0%	1
7	**Report**						
7.1	Sections I - III	--	Sun 10/02/22	Thu 10/20/22	19	75%	14
7.1.1	Section I	Gerardo	Sun 10/02/22	Thu 10/20/22	19	100%	14
7.1.2	Section II	Martin	Sun 10/02/22	Thu 10/20/22	19	100%	14
7.1.3	Section III pt. 1	--	Sun 10/02/22	Thu 10/20/22	19	100%	14
7.1.3.1	III.a	Josh	Sun 10/02/22	Thu 10/20/22	19	75%	14
7.1.3.2	III.b	Laura	Sun 10/02/22	Thu 10/20/22	19	100%	14
7.1.3.3	III.c	Jeff	Sun 10/02/22	Thu 10/20/22	19	100%	14
7.1.4	References (Append A)	All	Sun 10/02/22	Mon 10/31/22	30	90%	21
7.1.5	Consolidation	Gerardo	Sun 10/02/22	Thu 10/20/22	19	100%	14
7.1.6	Review/ Format/ Edit I	Laura	Sun 10/02/22	Thu 10/20/22	19	100%	14

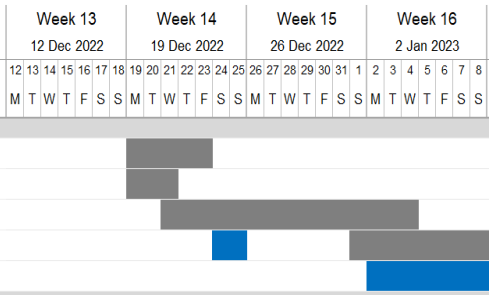

Figure 4: Gantt Chart – Weeks 13-16

M2M X-HAB 2023

NASA

Project Start Date: 9/19/2022 (Monday) | Display Week: 17
Project Lead: Gerardo Castro

WBS	TASK	TASK LEAD	START	END	DAYS	% DONE	WORK DAYS
1	**Experiment Set-Up**			-			-
1.1	Design Experiment	All	Mon 12/19/22	Fri 12/23/22	5	100%	5
1.1.1	Redesign Tee fittings for RH sensors	Jeff & Martin	Mon 12/19/22	Wed 12/21/22	3	100%	3
1.1.2	Adjust Fittings at UNT Machine Shop	Gerardo & Laura	Wed 12/21/22	Wed 1/04/23	15	100%	11
1.2	Assemble Experiment	Jeff Josh & Gerardo	Sun 1/01/23	Fri 2/03/23	34	90%	25
1.4	Run Experiment with Water	All	Mon 1/02/23	Sun 2/05/23	35	0%	25
2	**Optimize Prototype Design**			-			-
2.1	Meet with Dr. Kurwitz	All	Thu 1/05/23	Fri 1/06/23	2	100%	2
2.1.1	Finalize Calcs for Nozzles	Gerardo & Laura	Thu 1/05/23	Thu 1/12/23	8	100%	6
2.1.2	Finalize Calcs for Baffle Plate	Martin	Thu 1/05/23	Thu 1/12/23	8	100%	6
2.1.3	Finalize Calcs for Chamber	Jeff	Thu 1/05/23	Thu 1/12/23	8	100%	6
2.2	Order All Components & Materials	All	Wed 1/11/23	Wed 1/11/23	1	26%	1
2.3	Consolidate all in-house Components	All	Wed 1/11/23	Sat 1/14/23	4	100%	3
3	**Fabrication**						
3.1	Manufacture VPS (Cold & Hot)	All	Tue 1/17/23	Fri 3/17/23	60	0%	44
3.1.1	Order all Tools and Fixtures needed	All	Tue 1/17/23	Fri 3/17/23	60	0%	44
3.2	Machine Chamber	Laura & Gerardo	Tue 1/17/23	Fri 3/17/23	60	0%	44
3.2.1	Machine Baffle	Laura	Tue 1/17/23	Fri 3/17/23	60	0%	44
3.2.2	Machine Baffle Spacers	Josh	Tue 1/17/23	Fri 3/17/23	60	0%	44
3.2.3	Machine End Plates	Josh	Tue 1/17/23	Fri 3/17/23	60	0%	44
3.3	Manufacture Nozzles (Gas & Liquid)	Gerardo	Tue 1/17/23	Fri 3/17/23	60	0%	44
4	**Assembly**						
4.1	Assemble VPS (Cold & Hot)	All	Wed 3/15/23	Wed 4/05/23	21	0%	15
4.2	Set up plumbing	All	Wed 3/15/23	Wed 4/05/23	21	0%	15
4.3	Install Sensors	All	Wed 3/15/23	Wed 4/05/23	21	0%	15
4.4	Install Pumps, HX, Heater, Chiller,	All	Wed 3/15/23	Wed 4/05/23	21	0%	15
5	**Testing Prototype**						
5.1	Create LabView program for prototype	All	Wed 3/21/23	Fri 5/05/23	23	0%	17
5.2	Run prototype with water	All	Wed 3/21/23	Sat 5/06/23	23	0%	17
5.1	Perform test runs	All	Wed 4/12/23	Fri 5/05/23	23	0%	17
5.2	Collect data from sensors	All	Wed 4/12/23	Fri 5/05/23	23	0%	17
6	**NASA Milestones**						
6.1	Kickoff Meeting	All	Thu 9/22/22	Thu 9/22/22	1	100%	1
6.2	SDR Presentation	All	Thu 10/27/22	Thu 10/27/22	1	100%	1
6.3	PDR Presentation	All	Thu 12/01/22	Thu 12/01/22	1	100%	1
6.4	CDR Presentation	All	Fri 2/24/23	Fri 2/24/23	1	0%	1
6.5	PCR Presentation	All	Sat 3/11/23	Sat 3/11/23	1	0%	1
6.6	Project Completion and Evaluation by NASA	All	Sat 5/06/23	Sat 5/06/23	1	0%	1
7	**Report**						
7.1	Sections I - III	--	Sun 10/02/22	Thu 10/20/22	19	75%	14
7.1.1	Section I	Gerardo	Sun 10/02/22	Thu 10/20/22	19	100%	14
7.1.2	Section II	Martin	Sun 10/02/22	Thu 10/20/22	19	100%	14
7.1.3	Section III pt. 1	--	Sun 10/02/22	Thu 10/20/22	19	100%	14
7.1.3.1	III.a	Josh	Sun 10/02/22	Thu 10/20/22	19	75%	14
7.1.3.2	III.b	Laura	Sun 10/02/22	Thu 10/20/22	19	100%	14
7.1.3.3	III.c	Jeff	Sun 10/02/22	Thu 10/20/22	19	100%	14
7.1.4	References (Append A)	All	Sun 10/02/22	Mon 10/31/22	30	90%	21
7.1.5	Consolidation	Gerardo	Sun 10/02/22	Thu 10/20/22	19	100%	14
7.1.6	Review/ Format/ Edit I	Laura	Sun 10/02/22	Thu 10/20/22	19	100%	14

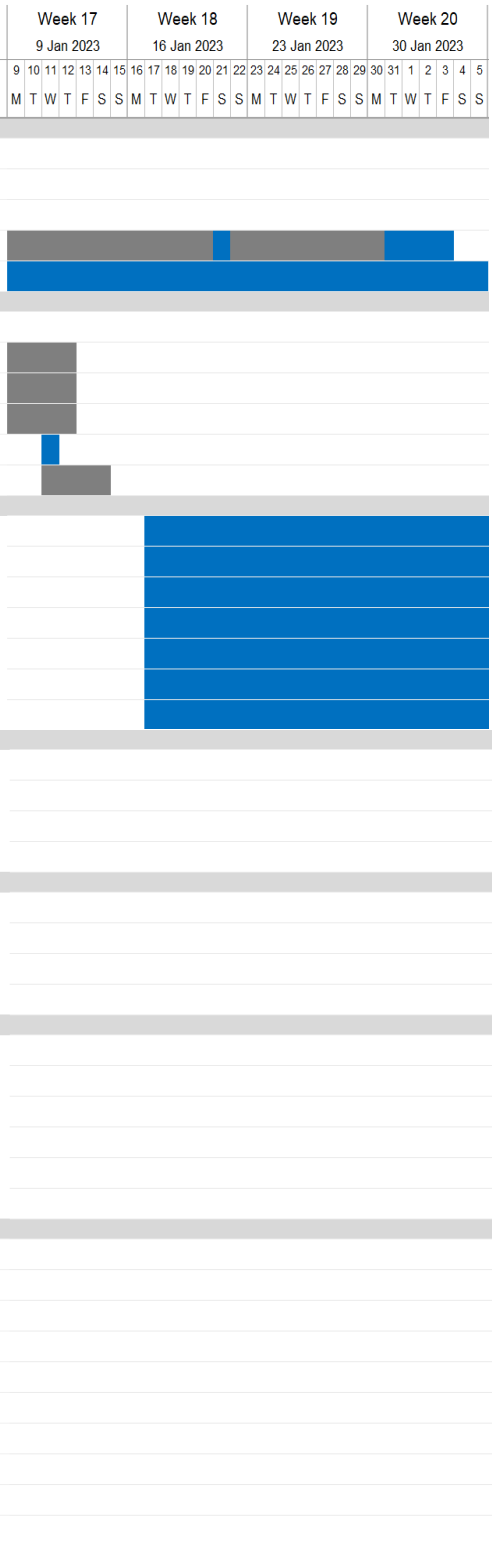

Figure 5: Gantt Chart – Weeks 17-20

M2M X-HAB 2023

NASA

Project Start Date: 9/19/2022 (Monday) | Display Week: 21
Project Lead: Gerardo Castro

WBS	TASK	TASK LEAD	START	END	DAYS	% DONE	WORK DAYS
1	**Experiment Set-Up**			-			-
1.1	Design Experiment	All	Mon 12/19/22	Fri 12/23/22	5	100%	5
1.1.1	Redesign Tee fittings for RH sensors	Jeff & Martin	Mon 12/19/22	Wed 12/21/22	3	100%	3
1.1.2	Adjust Fittings at UNT Machine Shop	Gerardo & Laura	Wed 12/21/22	Wed 1/04/23	15	100%	11
1.2	Assemble Experiment	Jeff Josh & Gerardo	Sun 1/01/23	Fri 2/03/23	34	90%	25
1.4	Run Experiment with Water	All	Mon 1/02/23	Sun 2/05/23	35	0%	25
2	**Optimize Prototype Design**			-			-
2.1	Meet with Dr. Kurwitz	All	Thu 1/05/23	Fri 1/06/23	2	100%	2
2.1.1	Finalize Calcs for Nozzles	Gerardo & Laura	Thu 1/05/23	Thu 1/12/23	8	100%	6
2.1.2	Finalize Calcs for Baffle Plate	Martin	Thu 1/05/23	Thu 1/12/23	8	100%	6
2.1.3	Finalize Calcs for Chamber	Jeff	Thu 1/05/23	Thu 1/12/23	8	100%	6
2.2	Order All Components & Materials	All	Wed 1/11/23	Wed 1/11/23	1	26%	1
2.3	Consolidate all in-house Components	All	Wed 1/11/23	Sat 1/14/23	4	100%	3
3	**Fabrication**						
3.1	Manufacture VPS (Cold & Hot)	All	Tue 1/17/23	Fri 3/17/23	60	0%	44
3.1.1	Order all Tools and Fixtures needed	All	Tue 1/17/23	Fri 3/17/23	60	0%	44
3.2	Machine Chamber	Laura & Gerardo	Tue 1/17/23	Fri 3/17/23	60	0%	44
3.2.1	Machine Baffle	Laura	Tue 1/17/23	Fri 3/17/23	60	0%	44
3.2.2	Machine Baffle Spacers	Josh	Tue 1/17/23	Fri 3/17/23	60	0%	44
3.2.3	Machine End Plates	Josh	Tue 1/17/23	Fri 3/17/23	60	0%	44
3.3	Manufacture Nozzles (Gas & Liquid)	Gerardo	Tue 1/17/23	Fri 3/17/23	60	0%	44
4	**Assembly**						
4.1	Assemble VPS (Cold & Hot)	All	Wed 3/15/23	Wed 4/05/23	21	0%	15
4.2	Set up plumbing	All	Wed 3/15/23	Wed 4/05/23	21	0%	15
4.3	Install Sensors	All	Wed 3/15/23	Wed 4/05/23	21	0%	15
4.4	Install Pumps, HX, Heater, Chiller,	All	Wed 3/15/23	Wed 4/05/23	21	0%	15
5	**Testing Prototype**						
5.1	Create LabView program for prototype	All	Wed 3/21/23	Fri 5/05/23	23	0%	17
5.2	Run prototype with water	All	Wed 3/21/23	Sat 5/06/23	23	0%	17
5.1	Perform test runs	All	Wed 4/12/23	Fri 5/05/23	23	0%	17
5.2	Collect data from sensors	All	Wed 4/12/23	Fri 5/05/23	23	0%	17
6	**NASA Milestones**						
6.1	Kickoff Meeting	All	Thu 9/22/22	Thu 9/22/22	1	100%	1
6.2	SDR Presentation	All	Thu 10/27/22	Thu 10/27/22	1	100%	1
6.3	PDR Presentation	All	Thu 12/01/22	Thu 12/01/22	1	100%	1
6.4	CDR Presentation	All	Fri 2/24/23	Fri 2/24/23	1	0%	1
6.5	PCR Presentation	All	Sat 3/11/23	Sat 3/11/23	1	0%	1
6.6	Project Completion and Evaluation by NASA	All	Sat 5/06/23	Sat 5/06/23	1	0%	1
7	**Report**						
7.1	Sections I - III	--	Sun 10/02/22	Thu 10/20/22	19	75%	14
7.1.1	Section I	Gerardo	Sun 10/02/22	Thu 10/20/22	19	100%	14
7.1.2	Section II	Martin	Sun 10/02/22	Thu 10/20/22	19	100%	14
7.1.3	Section III pt. 1	--	Sun 10/02/22	Thu 10/20/22	19	100%	14
7.1.3.1	III.a	Josh	Sun 10/02/22	Thu 10/20/22	19	75%	14
7.1.3.2	III.b	Laura	Sun 10/02/22	Thu 10/20/22	19	100%	14
7.1.3.3	III.c	Jeff	Sun 10/02/22	Thu 10/20/22	19	100%	14
7.1.4	References (Append A)	All	Sun 10/02/22	Mon 10/31/22	30	90%	21
7.1.5	Consolidation	Gerardo	Sun 10/02/22	Thu 10/20/22	19	100%	14
7.1.6	Review/ Format/ Edit I	Laura	Sun 10/02/22	Thu 10/20/22	19	100%	14

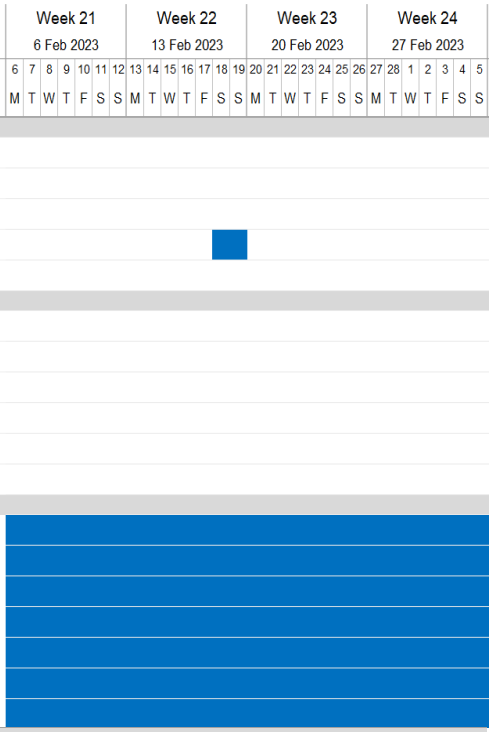

Figure 6: Gantt Chart – Weeks 21-4

M2M X-HAB 2023

NASA

Project Start Date: 9/19/2022 (Monday) | Display Week: 25
Project Lead: Gerardo Castro

WBS	TASK	TASK LEAD	START	END	DAYS	% DONE	WORK DAYS
1	**Experiment Set-Up**			-			-
1.1	Design Experiment	All	Mon 12/19/22	Fri 12/23/22	5	100%	5
1.1.1	Redesign Tee fittings for RH sensors	Jeff & Martin	Mon 12/19/22	Wed 12/21/22	3	100%	3
1.1.2	Adjust Fittings at UNT Machine Shop	Gerardo & Laura	Wed 12/21/22	Wed 1/04/23	15	100%	11
1.2	Assemble Experiment	Jeff Josh & Gerardo	Sun 1/01/23	Fri 2/03/23	34	90%	25
1.4	Run Experiment with Water	All	Mon 1/02/23	Sun 2/05/23	35	0%	25
2	**Optimize Prototype Design**			-			-
2.1	Meet with Dr. Kurwitz	All	Thu 1/05/23	Fri 1/06/23	2	100%	2
2.1.1	Finalize Calcs for Nozzles	Gerardo & Laura	Thu 1/05/23	Thu 1/12/23	8	100%	6
2.1.2	Finalize Calcs for Baffle Plate	Martin	Thu 1/05/23	Thu 1/12/23	8	100%	6
2.1.3	Finalize Calcs for Chamber	Jeff	Thu 1/05/23	Thu 1/12/23	8	100%	6
2.2	Order All Components & Materials	All	Wed 1/11/23	Wed 1/11/23	1	26%	1
2.3	Consolidate all in-house Components	All	Wed 1/11/23	Sat 1/14/23	4	100%	3
3	**Fabrication**						
3.1	Manufacture VPS (Cold & Hot)	All	Tue 1/17/23	Fri 3/17/23	60	0%	44
3.1.1	Order all Tools and Fixtures needed	All	Tue 1/17/23	Fri 3/17/23	60	0%	44
3.2	Machine Chamber	Laura & Gerardo	Tue 1/17/23	Fri 3/17/23	60	0%	44
3.2.1	Machine Baffle	Laura	Tue 1/17/23	Fri 3/17/23	60	0%	44
3.2.2	Machine Baffle Spacers	Josh	Tue 1/17/23	Fri 3/17/23	60	0%	44
3.2.3	Machine End Plates	Josh	Tue 1/17/23	Fri 3/17/23	60	0%	44
3.3	Manufacture Nozzles (Gas & Liquid)	Gerardo	Tue 1/17/23	Fri 3/17/23	60	0%	44
4	**Assembly**						
4.1	Assemble VPS (Cold & Hot)	All	Wed 3/15/23	Wed 4/05/23	21	0%	15
4.2	Set up plumbing	All	Wed 3/15/23	Wed 4/05/23	21	0%	15
4.3	Install Sensors	All	Wed 3/15/23	Wed 4/05/23	21	0%	15
4.4	Install Pumps, HX, Heater, Chiller,	All	Wed 3/15/23	Wed 4/05/23	21	0%	15
5	**Testing Prototype**						
5.1	Create LabView program for prototype	All	Wed 3/21/23	Fri 5/05/23	23	0%	17
5.2	Run prototype with water	All	Wed 3/21/23	Sat 5/06/23	23	0%	17
5.1	Perform test runs	All	Wed 4/12/23	Fri 5/05/23	23	0%	17
5.2	Collect data from sensors	All	Wed 4/12/23	Fri 5/05/23	23	0%	17
6	**NASA Milestones**						
6.1	Kickoff Meeting	All	Thu 9/22/22	Thu 9/22/22	1	100%	1
6.2	SDR Presentation	All	Thu 10/27/22	Thu 10/27/22	1	100%	1
6.3	PDR Presentation	All	Thu 12/01/22	Thu 12/01/22	1	100%	1
6.4	CDR Presentation	All	Fri 2/24/23	Fri 2/24/23	1	0%	1
6.5	PCR Presentation	All	Sat 3/11/23	Sat 3/11/23	1	0%	1
6.6	Project Completion and Evaluation by NASA	All	Sat 5/06/23	Sat 5/06/23	1	0%	1
7	**Report**						
7.1	Sections I - III	--	Sun 10/02/22	Thu 10/20/22	19	75%	14
7.1.1	Section I	Gerardo	Sun 10/02/22	Thu 10/20/22	19	100%	14
7.1.2	Section II	Martin	Sun 10/02/22	Thu 10/20/22	19	100%	14
7.1.3	Section III pt. 1	--	Sun 10/02/22	Thu 10/20/22	19	100%	14
7.1.3.1	III.a	Josh	Sun 10/02/22	Thu 10/20/22	19	75%	14
7.1.3.2	III.b	Laura	Sun 10/02/22	Thu 10/20/22	19	100%	14
7.1.3.3	III.c	Jeff	Sun 10/02/22	Thu 10/20/22	19	100%	14
7.1.4	References (Append A)	All	Sun 10/02/22	Mon 10/31/22	30	90%	21
7.1.5	Consolidation	Gerardo	Sun 10/02/22	Thu 10/20/22	19	100%	14
7.1.6	Review/ Format/ Edit I	Laura	Sun 10/02/22	Thu 10/20/22	19	100%	14

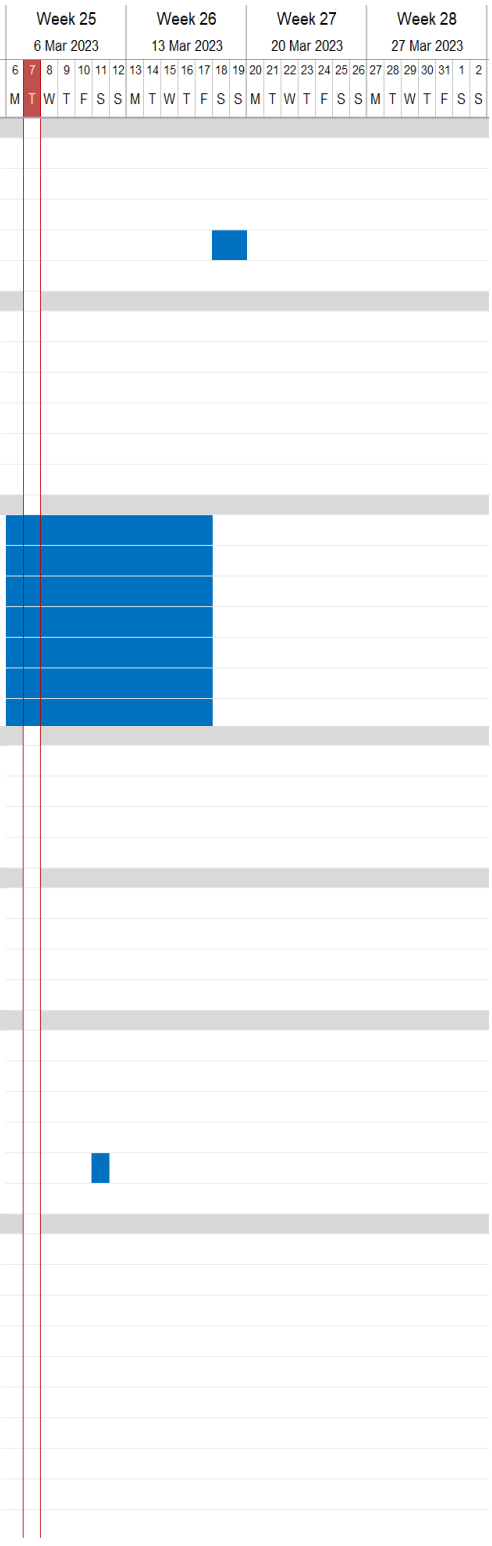

Figure 7: Gantt Chart – Weeks 24-28

M2M X-HAB 2023

NASA

Project Start Date: 9/19/2022 (Monday) | Display Week: 29
Project Lead: Gerardo Castro

WBS	TASK	TASK LEAD	START	END	DAYS	% DONE	WORK DAYS
1	**Experiment Set-Up**			-			-
1.1	Design Experiment	All	Mon 12/19/22	Fri 12/23/22	5	100%	5
1.1.1	Redesign Tee fittings for RH sensors	Jeff & Martin	Mon 12/19/22	Wed 12/21/22	3	100%	3
1.1.2	Adjust Fittings at UNT Machine Shop	Gerardo & Laura	Wed 12/21/22	Wed 1/04/23	15	100%	11
1.2	Assemble Experiment	Jeff Josh & Gerardo	Sun 1/01/23	Fri 2/03/23	34	90%	25
1.4	Run Experiment with Water	All	Mon 1/02/23	Sun 2/05/23	35	0%	25
2	**Optimize Prototype Design**			-			-
2.1	Meet with Dr. Kurwitz	All	Thu 1/05/23	Fri 1/06/23	2	100%	2
2.1.1	Finalize Calcs for Nozzles	Gerardo & Laura	Thu 1/05/23	Thu 1/12/23	8	100%	6
2.1.2	Finalize Calcs for Baffle Plate	Martin	Thu 1/05/23	Thu 1/12/23	8	100%	6
2.1.3	Finalize Calcs for Chamber	Jeff	Thu 1/05/23	Thu 1/12/23	8	100%	6
2.2	Order All Components & Materials	All	Wed 1/11/23	Wed 1/11/23	1	26%	1
2.3	Consolidate all in-house Components	All	Wed 1/11/23	Sat 1/14/23	4	100%	3
3	**Fabrication**						
3.1	Manufacture VPS (Cold & Hot)	All	Tue 1/17/23	Fri 3/17/23	60	0%	44
3.1.1	Order all Tools and Fixtures needed	All	Tue 1/17/23	Fri 3/17/23	60	0%	44
3.2	Machine Chamber	Laura & Gerardo	Tue 1/17/23	Fri 3/17/23	60	0%	44
3.2.1	Machine Baffle	Laura	Tue 1/17/23	Fri 3/17/23	60	0%	44
3.2.2	Machine Baffle Spacers	Josh	Tue 1/17/23	Fri 3/17/23	60	0%	44
3.2.3	Machine End Plates	Josh	Tue 1/17/23	Fri 3/17/23	60	0%	44
3.3	Manufacture Nozzles (Gas & Liquid)	Gerardo	Tue 1/17/23	Fri 3/17/23	60	0%	44
4	**Assembly**						
4.1	Assemble VPS (Cold & Hot)	All	Wed 3/15/23	Wed 4/05/23	21	0%	15
4.2	Set up plumbing	All	Wed 3/15/23	Wed 4/05/23	21	0%	15
4.3	Install Sensors	All	Wed 3/15/23	Wed 4/05/23	21	0%	15
4.4	Install Pumps, HX, Heater, Chiller,	All	Wed 3/15/23	Wed 4/05/23	21	0%	15
5	**Testing Prototype**						
5.1	Create LabView program for prototype	All	Wed 3/21/23	Fri 5/05/23	23	0%	17
5.2	Run prototype with water	All	Wed 3/21/23	Sat 5/06/23	23	0%	17
5.1	Perform test runs	All	Wed 4/12/23	Fri 5/05/23	23	0%	17
5.2	Collect data from sensors	All	Wed 4/12/23	Fri 5/05/23	23	0%	17
6	**NASA Milestones**						
6.1	Kickoff Meeting	All	Thu 9/22/22	Thu 9/22/22	1	100%	1
6.2	SDR Presentation	All	Thu 10/27/22	Thu 10/27/22	1	100%	1
6.3	PDR Presentation	All	Thu 12/01/22	Thu 12/01/22	1	100%	1
6.4	CDR Presentation	All	Fri 2/24/23	Fri 2/24/23	1	0%	1
6.5	PCR Presentation	All	Sat 3/11/23	Sat 3/11/23	1	0%	1
6.6	Project Completion and Evaluation by NASA	All	Sat 5/06/23	Sat 5/06/23	1	0%	1
7	**Report**						
7.1	Sections I - III	--	Sun 10/02/22	Thu 10/20/22	19	75%	14
7.1.1	Section I	Gerardo	Sun 10/02/22	Thu 10/20/22	19	100%	14
7.1.2	Section II	Martin	Sun 10/02/22	Thu 10/20/22	19	100%	14
7.1.3	Section III pt. 1	--	Sun 10/02/22	Thu 10/20/22	19	100%	14
7.1.3.1	III.a	Josh	Sun 10/02/22	Thu 10/20/22	19	75%	14
7.1.3.2	III.b	Laura	Sun 10/02/22	Thu 10/20/22	19	100%	14
7.1.3.3	III.c	Jeff	Sun 10/02/22	Thu 10/20/22	19	100%	14
7.1.4	References (Append A)	All	Sun 10/02/22	Mon 10/31/22	30	90%	21
7.1.5	Consolidation	Gerardo	Sun 10/02/22	Thu 10/20/22	19	100%	14
7.1.6	Review/ Format/ Edit I	Laura	Sun 10/02/22	Thu 10/20/22	19	100%	14

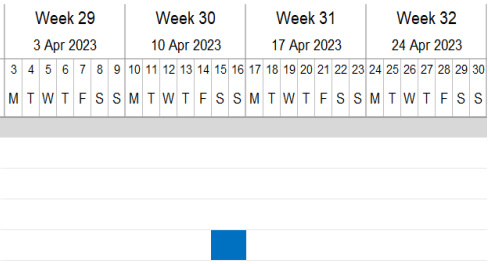

Figure 8: Gantt Chart – Weeks 29-32

3. DESIGN EVOLUTION

This section discusses some competitive developments. The phases of the design are also referenced. This analysis illustrates that the dual-phase VPS design may be an ideal solution for space cabin air humidity control for long-term use. Naturally, there are safety considerations. Safety is the number one priority for the designers, fabricators, and users of this system. Ethics and professionalism must be considered and are discussed in this section. The system's life cycle is also estimated, along with its cost breakdown. As this prototype is the first of its kind to be developed, the cost breakdown and life cycle analyses evaluated are not reflective of the prototype's production costs and life cycle predictions, as improvements in these areas would likely be made in future iterations.

3.1. Summary of Competitive Developments

This section discusses competitive designs for a spacecraft humidity control subsystem. Since this X-Hab Spacecraft Humidity Control Module is the first subsystem iterated for NASA's latest CO_2 removal module, there is not currently a commercial market of deliberately "competitive" products. To place the X-Hab Spacecraft Humidity Control Subsystem into the context of aerospace developments, other current spacecraft humidity control systems are examined and compared to the Mars X-Hab VPS.

3.1.1. Temperature and Humidity Control (THC) Subsystem

The ISS's Environmental Control and Life Support System (ECLSS) controls and monitors humidity with the THC, a complex system of air channels and isolation valves which control air circulation through the heat exchangers in the ISS's Active Thermal Control System (ACTS) to maintain the air humidity leaving the ECLSS at 60% RH. [5]

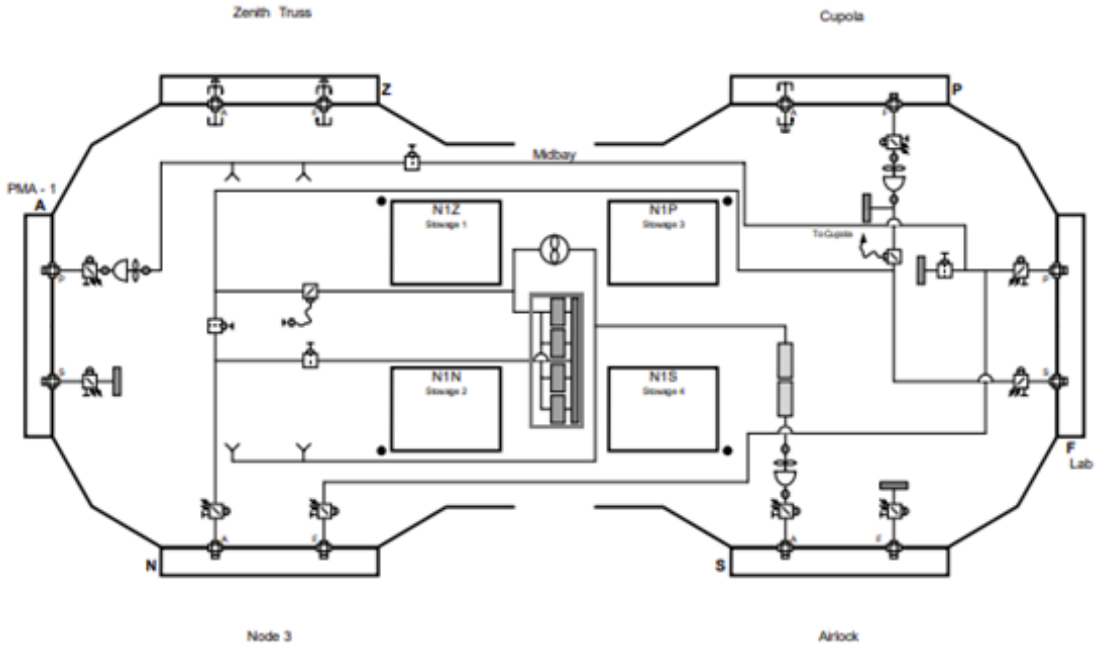

Figure 9*: The ISS THC in Node 1*

The THC's Inlet Orbital Replacement Unit (ORU) directs cabin air into four bacteria and microbial control filters, which must be manually cleaned twice per week. Then, the THC's valve control system allows air to move through several other ECLSS subsystems via the THC's isolation control valves, and then through the various cabin vents both in the ISS's interior chambers and at the various docking points and exit airlock chambers. [5]

The THC is an appropriate system to use for a large SS with many locations of highly variant air conditions, and its integrated design makes sense for the ECLSS. For the humidity control of one large chamber, however, the integrated layout of the THC is not ideal. To compare: The Mars X-Hab VPS module is a separate subsystem isolating all air humidification and dehumidification within its 2 VPS chambers and thermal control units, which makes it simpler to install and easier to monitor if necessary. Its smaller and lighter footprint also makes it more efficient.

3.1.2. Paragon Space Development Control Corporation-Space Humidity Control System

A patent was filed by Taber K. MacCallum at the Paragon Space Development Corp. in Tucson, AZ, for a Space Humidity Control System designed to filter water vapor from cabin air through a chemically selective membrane. An air conductor moves air into the containment wall, which has a chemically selective water-permeable membrane made of Teflon and $C_9HF_{13}O_5S$. The membrane captures the water as the air moves through it. The air is then pulled through by a vacuum vent. The system relies on heat from the attached CO_2 separation module to prevent the water from condensing. [6]

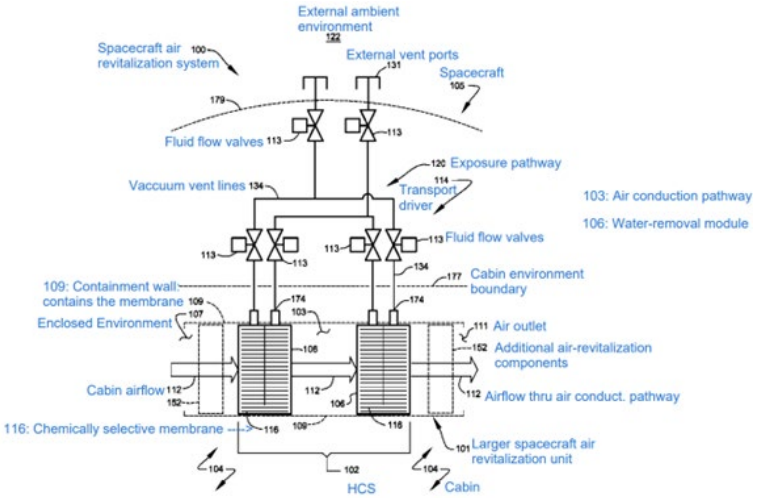

Figure 10: *Full HCS System*

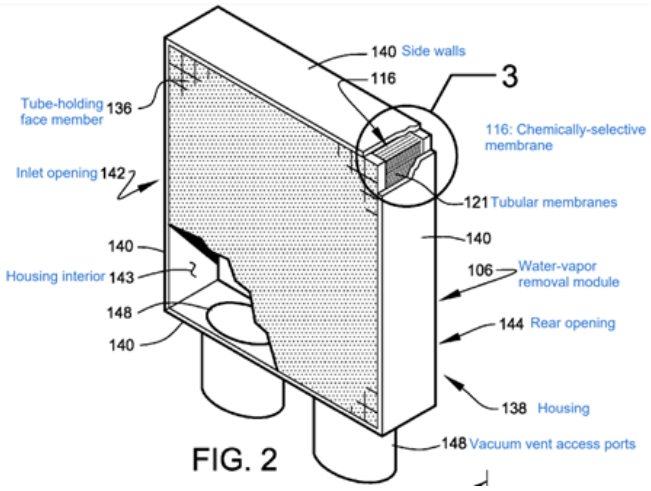

Figure 11: *Water-vapor removal module*

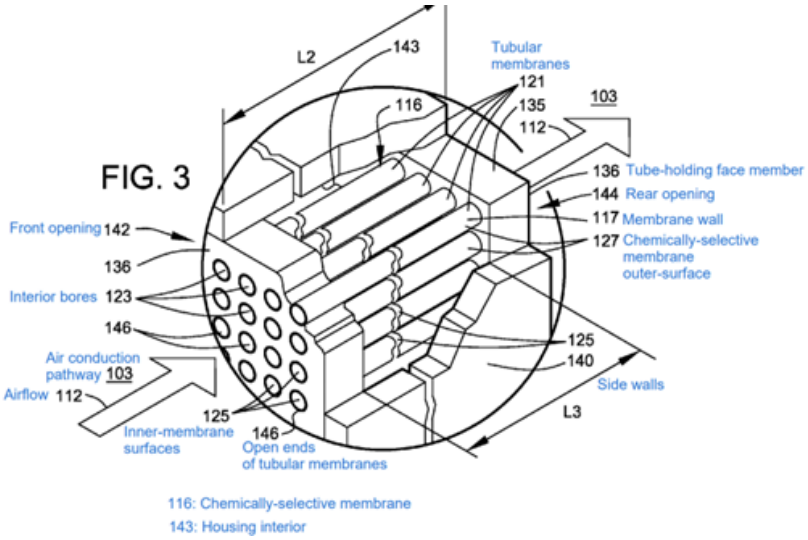

Figure 12*: Partial section view of the water-vapor removal module*

This passive system resembles that of NASA's comparable contactor design for an iteration of NASA's CO_2 deposition system design [1], which also used hollow tubes as the chemically selective membranes. NASA's X-Hab team encountered significant limitations that could not be solved. The slow rates of mass transfer through the membrane and the eventual particle-buildup inside the membrane tubes decreased the flow surface area and thus hindered performance and efficiency. These limitations are tied to the nature of the system's geometry and would therefore likely be encountered in MacCallum's similar SHC design.

The Mars X-Hab VPS module remedies these issues because its flowrate can always be improved via upscaling, and its continuous flowrate prevents particle deposition in the system. Its regenerative heat exchanger controls the liquid heating system, and thus the magnitude and rate of condensation, so it is not dependent on an exterior module, as is the case with MacCallum's SHC. [6]

3.2. Phases of the Project Design

There are two major phases to the project overall: liquid desiccant selection and system design for the selected desiccants. This desiccant section phase incorporates research of IL desiccants and theoretical calculations to predict their performance in a VPS system. The selection process is discussed in section 3.3.

The VPS has research dating back to 1988 at Texas A&M University, in experiments with two-phase systems in low gravity environments. [7] The MVS is a centripetal driven system which uses buoyancy forces to make a gas-liquid vortex. There are two nozzles tangent in the middle of the circular cylinder that are opposite of each other in direction of the injection. The tangential liquid inlet nozzle injects a liquid stream causing a rotating liquid layer on the inside wall. The nozzle in the opposite location of the liquid nozzle is the gas inlet nozzle that directs a gas stream into the chamber, releasing bubbles that are smaller than 1mm (about 0.04 in) which interact with the liquid stream.

The VPS design used in the X-Hab air humidity control module also took inspiration from Alex Sarvadi's design, shown in figure 13. [4] Sarvadi's VPS is machined from aluminum and has two nozzles welded onto the outer wall of the VPS. In the new dual-phase VPS system, a safe and regenerable ionic liquid (IL) catalyzes phase-separation of the water and air for dehumidification and re-evaporates the water into the dry air for re-humidification. The IL's negligible vapor pressure and variable thermodynamic properties allow it to optimize humidity removal as its temperature is decreased during dehumidification and increased during re-humidification. [9]

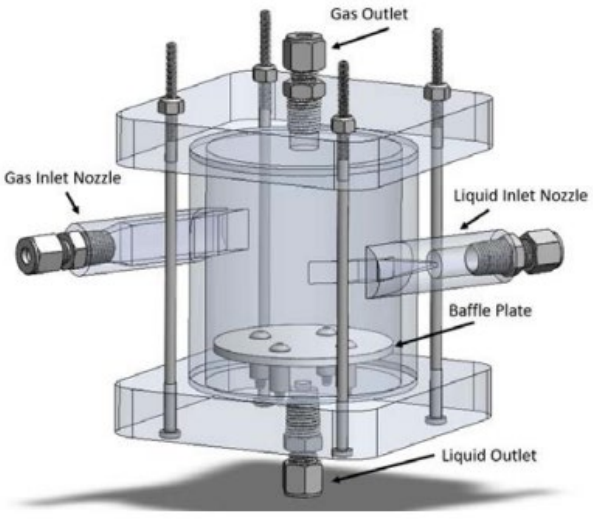

Figure 13: *VPS Model for Liquid Amine CO_2 Removal [4]*

A schematic of the dual-phase X-Hab climate humidity control module is shown below in fig. 14. Humid cabin air enters the cold VPS from the inlet (left side). The cold VPS dehumidifies the air entering the chamber. Fresh desiccant from the chiller is used to absorb the humidity, and this water-laden desiccant leaves the chamber and is then pumped from the cold VPS into a regenerative heat exchanger, then into a heater. The regenerated desiccant leaves the heater and enters the hot VPS. The heated desiccant re-humidifies the air. The incoming air in the hot side flows directly from the cold side VPS outlet. The hot liquid desiccant is then pumped back through the heat exchanger, then through a chiller, and back through the cold VPS inlet.

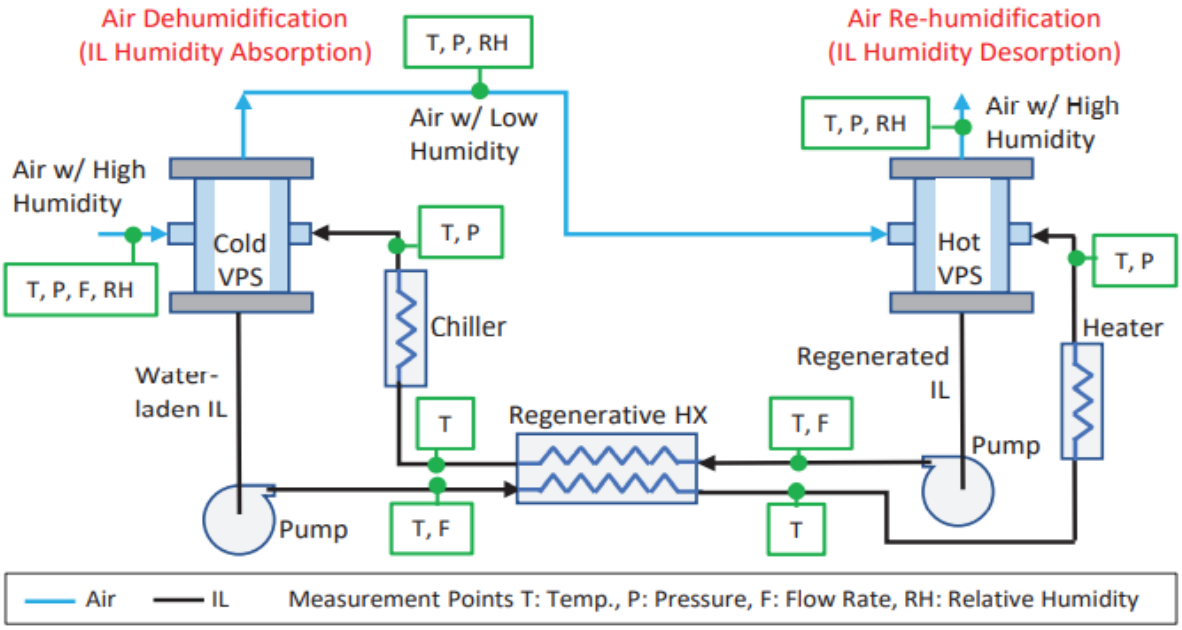

Figure 14: *Schematic of Dehumidification/ Re-humidification Test System [1]*

3.2.1. Liquid Nozzle Design Phases:

Iteration 1, shown in fig. 8: the liquid nozzle had a rectangular cut extrude of 0.44” x 0.18” for 1.00” deep for its inlet hole. The exit hole, in which the liquid would exit and proceed into the VPS, is tapered. The OD of the nozzle was 0.75” and its length was 2.00”.

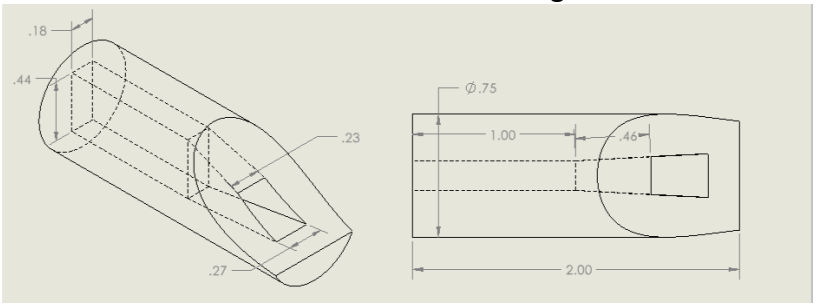

Figure 8: *Liquid Nozzle Iteration 1*

Iteration 2, shown in fig. 9: The exit nozzle hole was modified to a reduced cross-sectional area to improve the performance at which the fluid exits the nozzle and acts within the VPS. All other geometric properties were kept the same.

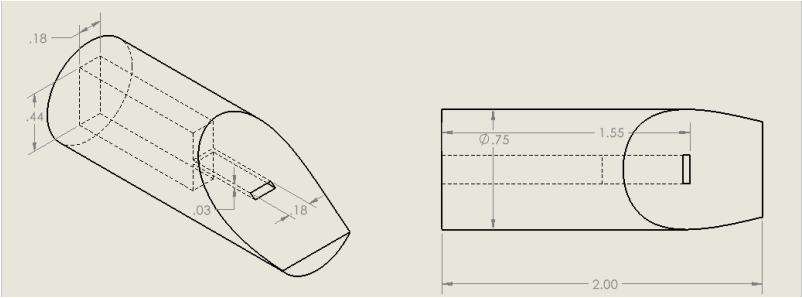

Figure 9: *Liquid Nozzle Iteration 2*

Iteration 3, shown in fig. 10: The inlet hole of the liquid nozzle was changed to 0.27”. The exit hole of the liquid nozzle was changed to back to the first iteration shape but with a slightly larger area.

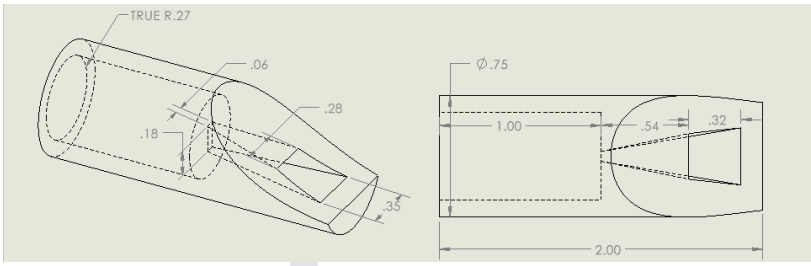

Figure 10*: Liquid Nozzle Iteration 3*

Iteration 4, shown in fig. 11: The inlet hole diameter of the liquid nozzle was decreased to 0.21” and all other geometric properties were kept the same.

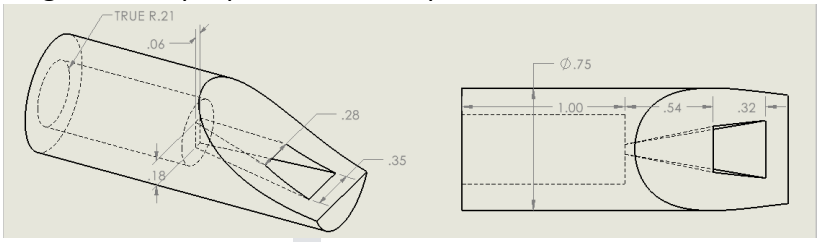

Figure 11: *Liquid Nozzle Iteration 4*

Iteration 5, shown in fig. 12: It was concluded that the fourth iteration could be improved to reduce turbulence of flow. Here, two components make up the nozzle: The shell is CNC-machined 316 stainless steel tubing and is welded to the chamber. The insert is designed to encourage a smoother flow transition from the tube’s circular cross-section to the rectangular cross-section needed for tangential flow. This geometry, while not machinable, could be manufactured using 3D printing techniques, which is more cost-effective to Direct Metal Laser Sintering (DMLS) or Selective Laser Sintering (SLS) techniques with stainless steel powder. After researching various polymer filament options, ultem PEI was chosen for its performance in corrosion resistance. The material passed testing when in contact in [EMIM][EtSO4] and KCOOH, and the results were characterized in this report.

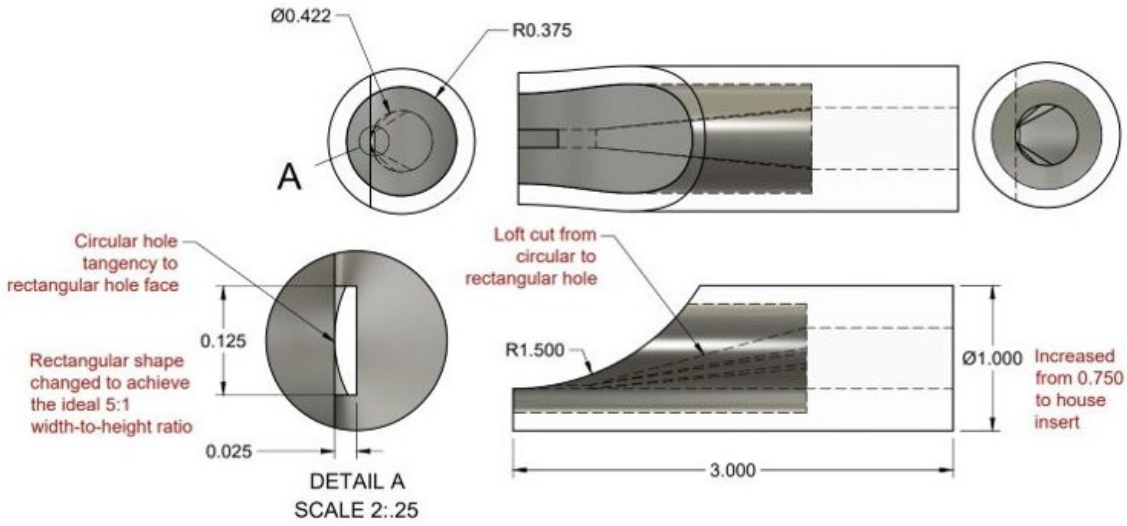

Figure 12: *Liquid Nozzle Iteration 5*

3.2.2. Gas Nozzle Design Phases:

Iteration 1, shown in fig. 13: A 2.80" x 1.00" rod was extruded with a 0.50" diameter hole for the inlet gas hole. The exit gas hole was a rectangular 0.62" x 0.32" extruded hole.

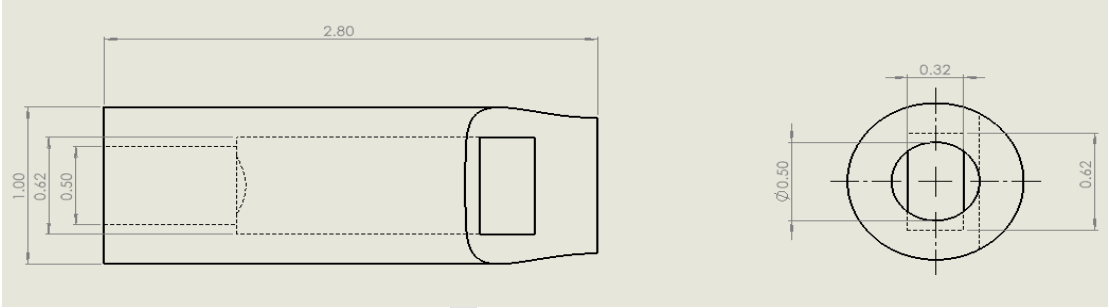

Figure 13: Gas Nozzle Iteration 1

Iteration 2, shown in fig. 14 and 15: The gas inlet hole was changed to 0.68" hole 1.00" deep. Fillets were added to the gas exit hole to allow the nozzle to be CNC machined, instead of EDM-cut. The corners would be square filed manually.

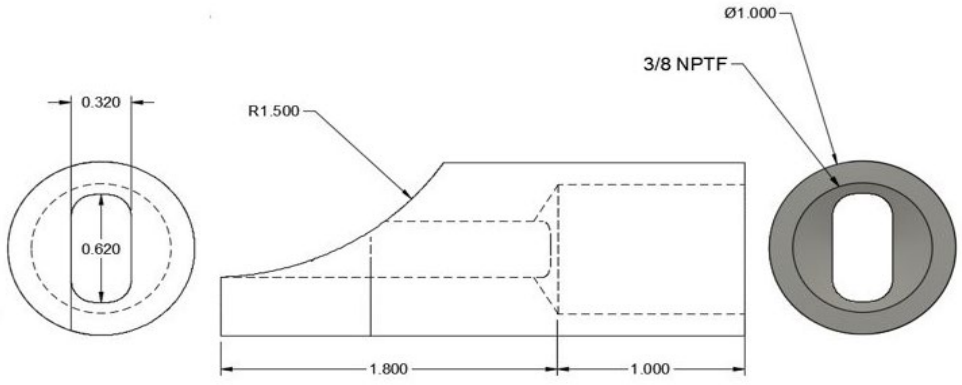

Figure 14: Gas Nozzle Iteration 2

Iteration 3, shown in figure 15: The sudden change of cross-sectional area in iteration 2 would have resulted in a large pressure-drop. To minimize the pressure-drop a design feature was added. This feature can be seen as a transition from the large cross-section to the smaller cross-section. A 60° drill bit is used to achieve the designed shape.

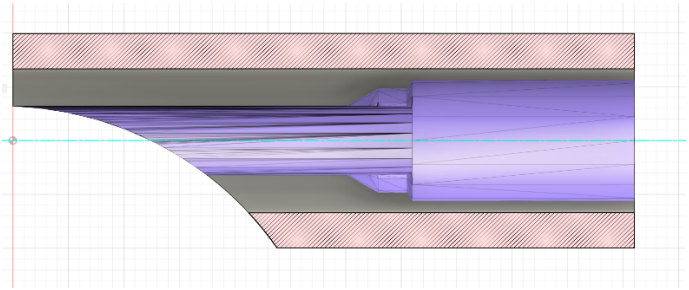

Figure 15: Gas Nozzle Iteration 3 – Cross-Section View

3.2.3. Chamber Design Phases:

Iteration 1, shown in fig. 16: The chamber is a 3.00” x 3.00” OD cylinder had a cut extrude of 2.50”. The holes were cut-extruded from a custom plane for nozzle height. The gas inlet hole was cut at 0.35” by 0.266” height.

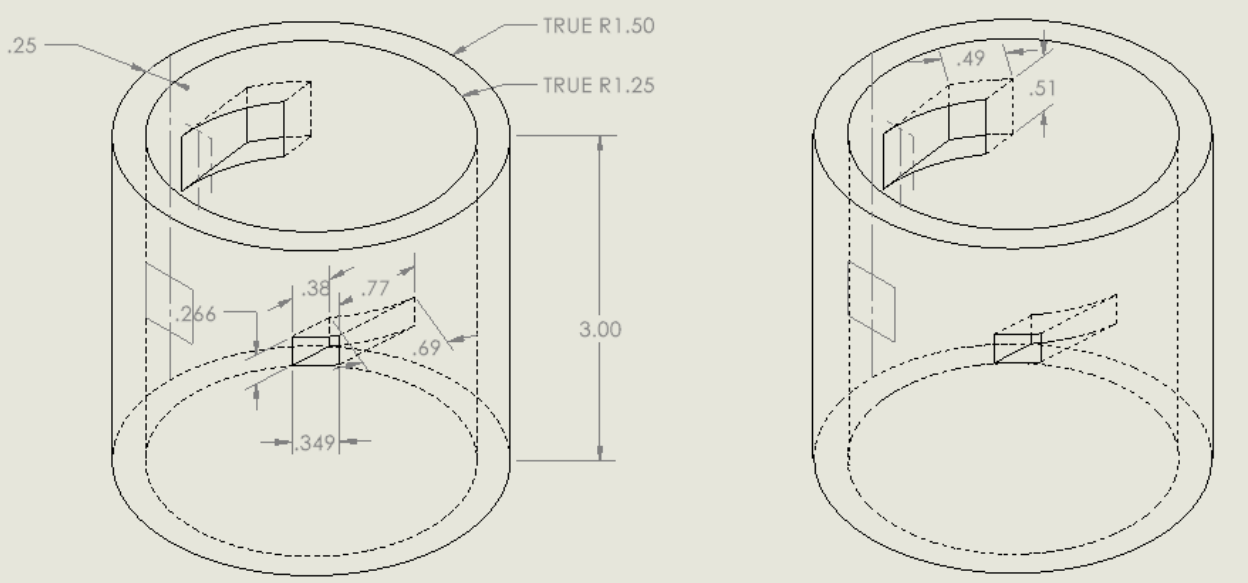

Figure 16: Chamber Iteration 1

Iteration 2, shown in fig. 17: The OD was increased to 3.50” and the ID was changed to 3.00”. The hole was tangent to the ID to be a straight cut. The nozzle height was also changed to 1.98” from the bottom of the chamber.

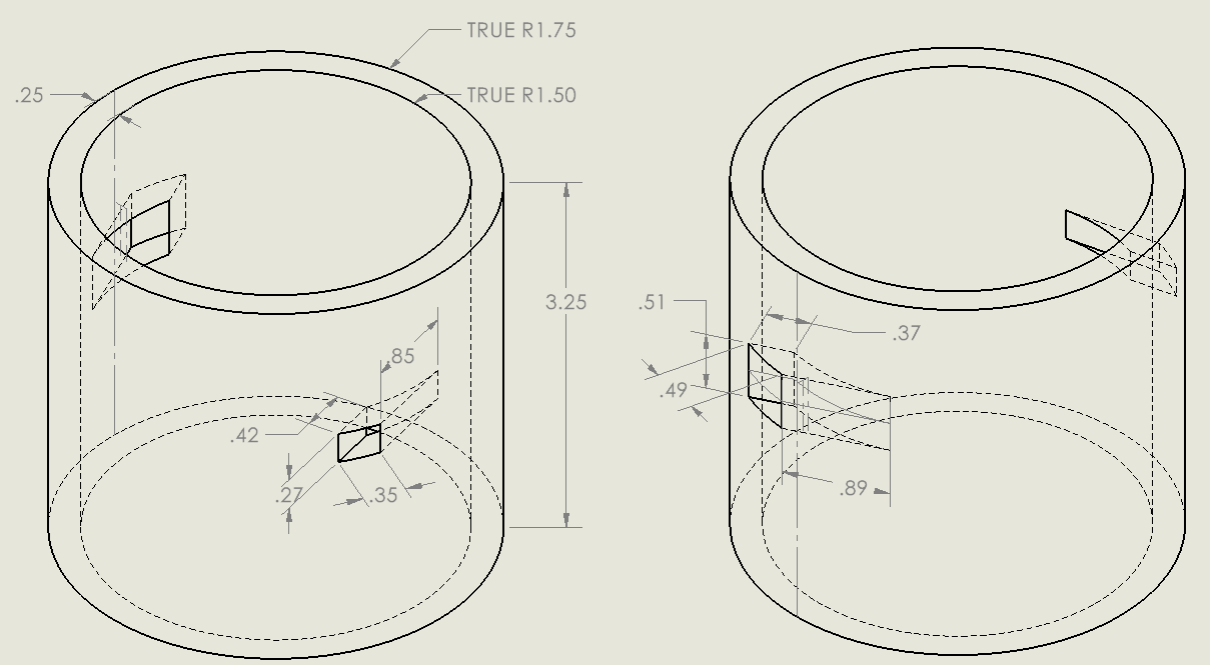

Figure 17: Chamber Iteration 2

Iteration 3, shown in fig. 18: The chamber height was changed to 3.93” to increase the volume and compensate for the chamber edges seated inside the caps. The nozzle holes were also slightly modified in cross-sectional areas and to be directly opposite of each other.

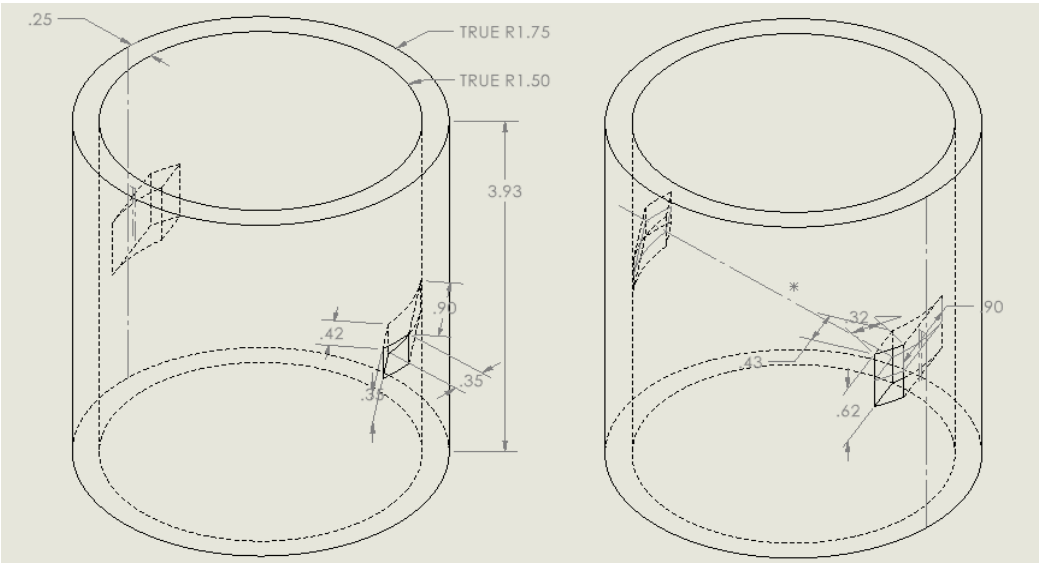

Figure 18: Chamber Iteration 3

Iteration 4, shown in fig. 19: The nozzle holes were changed to align the nozzles with the inside diameter of the chamber, which would ensure a consistent flow from the nozzle to the chamber, and allow the chamber to made in one piece, reducing areas of potential leaking and reducing manufacturing time.

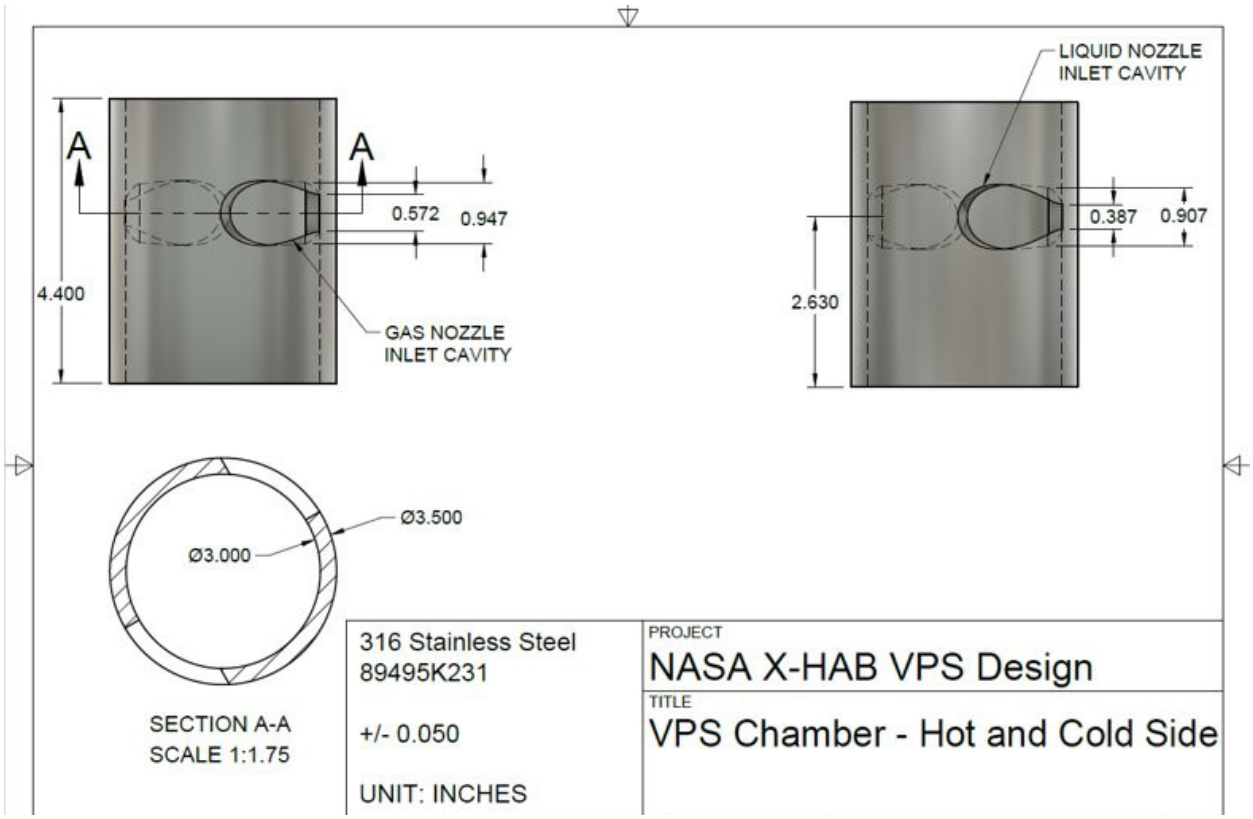

Figure 19: Chamber Iteration 4

3.2.4. Baffle Plate Design Phases:

Iteration 1, shown in fig. 20: The circular disk of 2.75” diameter had ten 0.16” holes rotating around the plate. Then four 0.21” threaded holes were created to bolt into the bottom cap. The baffle plate was 0.13” thick with a fillet of 0.05” radius.

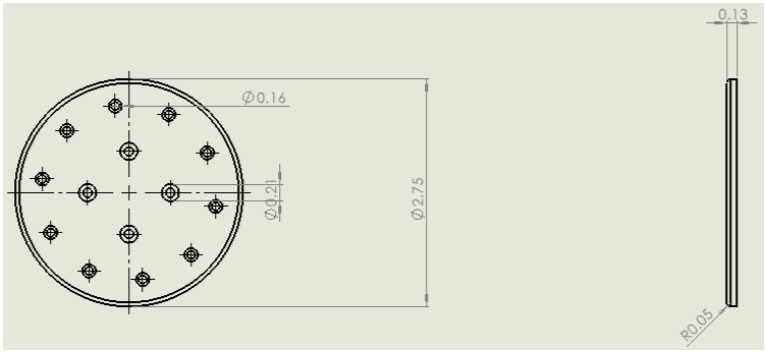

Figure 20: Baffle Plate Iteration 1

Iteration 2, shown in fig. 21: The holes around the edge of the baffle plate were removed to improve functionality.

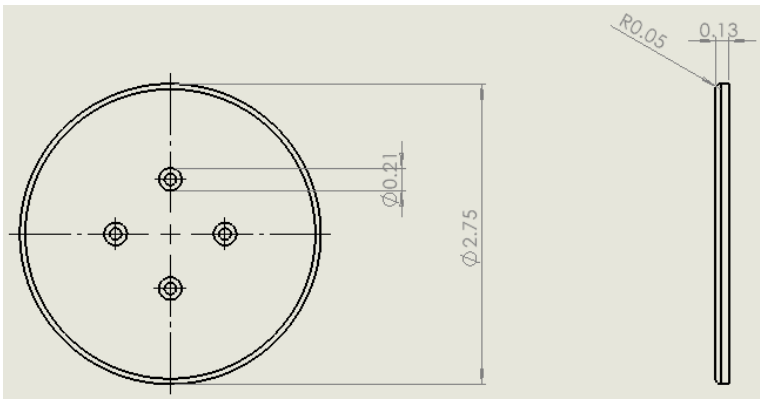

Figure 21: Baffle Plate Iteration 2

Iteration 3, shown in fig. 22: Adding a conical taper allows gas bubbles to travel back up into the chamber, preventing carry-under. The pockets provide clearance for the baffle spacers.

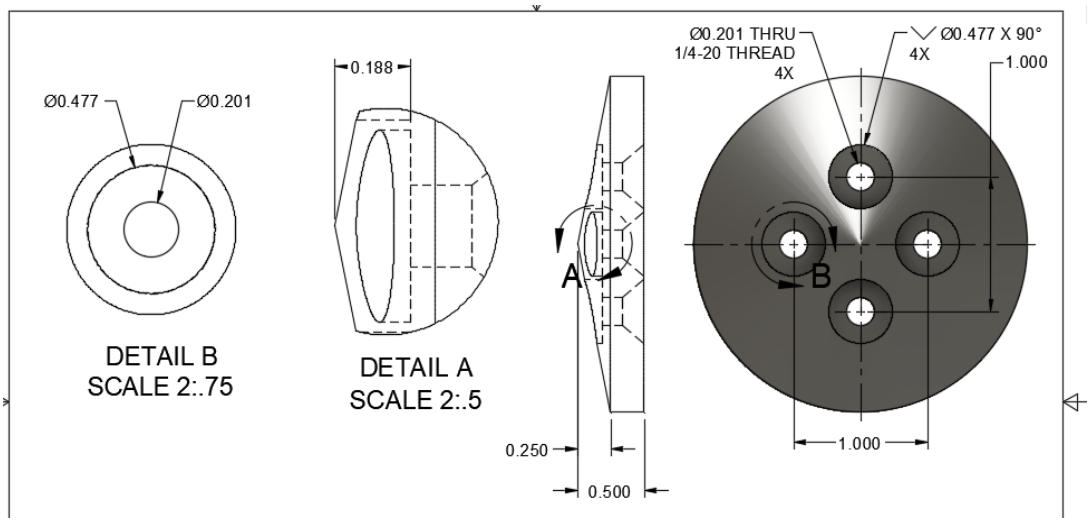

Figure 22: Baffle Plate Iteration 3

3.2.5. Top and Bottom Cap Design Phases:

The Top and Bottom Caps each have a 1/4” hole in the center for gas and liquids to exit. The four holes in the cap corners run bolts through them to hold the VPS together. The circular slot cut in each cap seats the chamber top and bottom. Four holes closer toward the center of the bottom cap hold in the baffle plate.

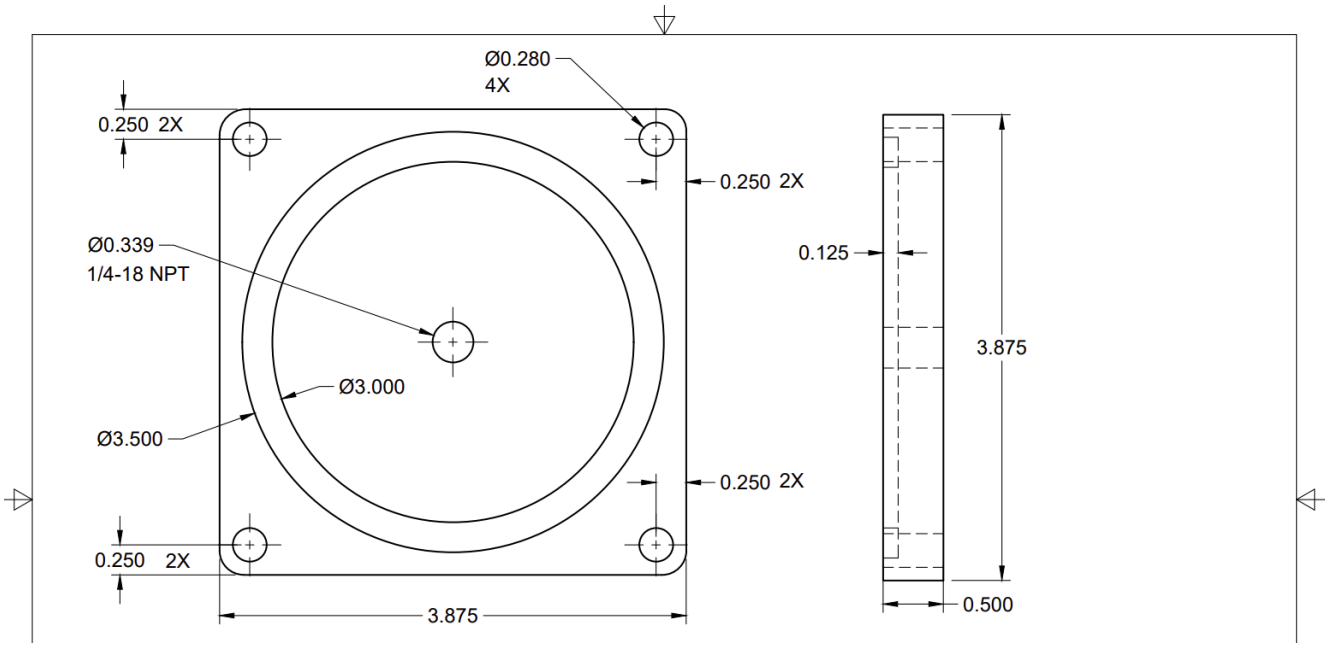

Figure 23: Top Cap Iteration 1

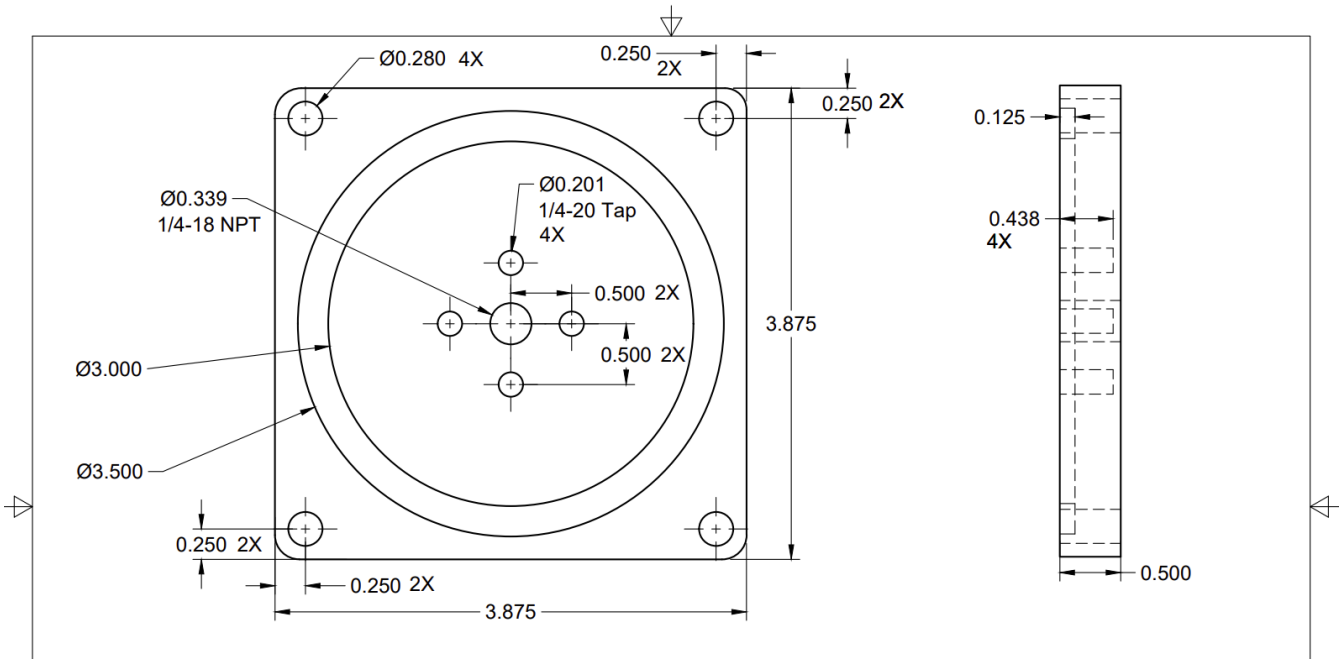

Figure 24: Bottom Cap Iteration 1

3.3. Analysis

3.3.1. Liquid Desiccant Selection:

The VPS system utilizes liquid desiccant for the phase-separation process explained in section (3.2). The desiccant is cooled to 289K and mixed with cabin air (temperature and humidity ranges shown in table 2). The desiccant condenses and absorbs the air's humidity. It

is regenerated in a heat exchanger, heated to 343K in a heating tank and remixed with the dehumidified air. The operating conditions listed are sourced from NASA's L*ife Support Baseline Values and Assumptions Document* describing expected space cabin conditions. [10]

Cabin Air Initial Conditions	*Units*	*Lower*	*Nominal*	*Upper*
Total Cabin Pressure	kPa	48	101	102.7
Temperature	K	291	296	300
RH	%	25	40	75

Table 2: Baseline Assumed Air Properties [34]

Thus, the liquid desiccant must have specific properties conducive to dehumidifying and re-humidifying air. The liquid desiccant must:

- Absorb water effectively when cooled and mixed with air.
- Release water effectively when reheated and mixed with air.
- Have thermal stability sufficient to minimize changes in its chemical and thermophysical properties as it undergoes temperature and humidity changes.
- Have molecular stability – remain in liquid form within the system's temperature parameters.
- Be Minimally corrosive to non-corrosive – The system requires minimal maintenance/ deterioration.
- Be Non-Combustible – There can be no chance of combustion present on board.
- Be Regenerable – The desiccant will be relieved of the absorbed water and "reset" as it is reheated, and it must be able to repeatedly undergo this regeneration without losing its chemical stability.
- Be CO_2 rejecting – Because the desiccant is not relieved of CO_2 until it passes through the main X-Hab system, it must not be able to absorb significant quantities of CO_2 during the separation phase. [11]
- Be Non-Toxic – The desiccant will interact with air and water that recirculate into the cabin, so it must be safe for the respiratory systems of the crew members.
- Be Odorless – The crew members will breathe the cabin air, so it cannot be irritating in the longrun.

Using the correct desiccant is key for this system, as it affects the functionality and efficiency of both the subsystem and CO_2 deposition system. [11]

Researched Desiccants:

- LiCl – Lithium Chloride
- LiBr – Lithium Bromide
- CaCl – Calcium Chloride
- [EMIM][OAc] - 1-Ethyl-3-methylimidazolium acetate

- [EMIM][EtSO4] - 1-Ethyl-3-methylimidazolium ethyl sulfate
- [[EMIM][BF4] - 1-ethyl-3-methyl-imidazolium tetrafluoroborate
- [EMIM]Cl - 1-Ethyl-3-methylimidazolium chloride
- [EMIM][MeSO3] - 1-Ethyl-3-methylimidazolium methanesulfonate
- [EMIM][MeSO4] - 1-Ethyl-3-methylimidazolium ethyl sulfate
- [EMIM][TFA] - 1-Ethyl-3-methylimidazolium trifluoroacetate
- [EMIM][OTf] - 1-Ethyl-3-methylimidazolium trifluoromethanesulfonate
- [P4441][DMPO4] - tributyl(methyl)phosphonium dimethyl phosphate
- [P4442OH][Tf2N] - tributylmethylphosphonium bis(trifluoromethylsulfonyl)imide
- [P4444][DEPDT] - tetra-n-butylphosphonium O,O'-diethylphosphorodithioate
- [P444,12][MCBS] - tri-n-butyldodecylphosphonium 3,5-bis(methoxycarbonyl)benzenesulfonate
- KCOOH – Potassium formate
- TEG – Triethyl glycol

Research Analysis

Preliminary research found that certain room-temperature ionic liquids (RTILs or ILs) are desirable options. ILs are salts in the liquid phase at standard temperature and pressure. ILs are characterized by highly stable properties at various temperatures, have negligible vapor pressure and low dew point driving temperatures, and are regenerable. To narrow down the search for possible candidates, research documents focusing on physiochemical properties and experimental results regarding water absorbability were collected. These properties reduced the large variety of binary combinations of ILs and desiccants to those listed above, which include all desiccants mentioned in all research documents referenced. [12]

Various ILs have been tested for use as desiccants in terrestrial air conditioning systems, which have the same requirements for effective use. Commonly used desiccants such as LiCl and LiBr and $CaCl_2$ were ruled out first due to their low vapor pressures (relative to ILs) and strong corrosivity to ferrous and non-ferrous metals, despite well-documented effective water absorption capacities. [13][14]

To find non-corrosive options, IL candidates for corrosion inhibitors, including [EMIM][BF4] and [EMIM][EtSO4] were found in the corrosion experiments performed by Araújo, et. al. [15] Further research ruled out [EMIM][BF4] because it is also a promising candidate for CO_2 absorption, which is counterintuitive to the scope of this challenge. [16] Thermophysical and thermochemical properties were acquired for [EMIM][EtSO4]. [12][17][18][19][20][25] These studies included [EMIM][MeSO4] and [EMIM][OAc].

Further research of IL candidates for use as desiccants in terrestrial HVAC systems also pointed toward [EMIM][OAc] [21], and thermophysical and thermochemical properties for this IL were acquired. [18][22]

In the terrestrial HVAC category of ILs, [EMIM]Cl and [EMIM][MeSO3] were also found. [23][24] [EMIM]Cl was quickly ruled out due to its acute respiratory toxicity [27]. Despite the promising water-absorption capabilities of [EMIM][MeSO3] [5][9][24][26][27], its Prio-ionic Safety Data Sheet showed it to also be severely unsafe to breathe for prolonged periods, which ruled it out as a candidate. [26]

Further research regarding CO_2 absorption rates for [EMIM][EtSO4] also showed results for [EMIM][TFA], and [EMIM][OTf] by Rodriguez, et. Al. [12]: [EMIM][EtSO4] was less absorbent of CO_2 than both [EMIM][TFA] and [EMIM][OTf]. Because CO_2 absorption should be as low as possible, [EMIM][TFA] and [EMIM][OTf] were ruled out.

Other research to find properties for [EMIM][EtSO4] thermophysical properties included CO_2 absorption research performed Qazi et. Al. [19] on [EMIM][EtSO4], [EMIM][OAc], and [EMIM][MeSO4]. These ILs were tested for CO_2 absorption via an absorption membrane. [EMIM][MeSO4], despite its promising thermal stability, negligible vapor pressure, and reasonable price, also showed to be highly CO_2 absorbent [25]. Because [EMIM][MeSO4] is also highly toxic when inhaled, it was subsequently ruled out. [30]

Further research found some lesser-known non-toxic room-temperature ionic liquids (RTILs) to have promising properties for regenerability and thermal stability, including [P4442OH][Tf2N], [P4444][DEPDT], and [P444,12] [MCBS], and a novel RTIL [P4441][DMPO4], which forms a plastic crystal phase between 279K and 290K. [P4441][DMPO4] proved to be the only significantly water-miscible RTIL of those studied by Yoshii, et. al. [31]

KCOOH also became an IL desiccant candidate when it showed similar thermodynamic properties and regenerable qualities to those of LiCl, a commonly used IL for terrestrial air conditioning systems, but was found to be less corrosive than traditional aqueous solution desiccants such as LiCl and LiBr in corrosion tests. [32][33] KCOOH was thus chosen as a desiccant to compare the behavior of an IL desiccant to that of a non-IL desiccant within the scope of dehumidification and regenerability.

In researching these desiccants, thermodynamic properties were collected at the temperatures the VPS system was expected to operate in at the time of research – 289K at the separator, 313K at the re-humidifier. The following tables show the properties available in research. The desiccants not listed were ruled out before their properties were acquired. Specific data regarding the water absorption capacity of the desiccant options were not all available. The candidates available for purchase will be experimented on for their respective water absorption capacities and regenerable temperatures.

To determine if the desiccant could be used, the more apparent barriers were considered first, including:

- Water-miscibility - can the desiccant absorb water at all?

- Price – The desiccant must be priced within reasonable considerations of the budget allotted.
- Corrosivity – The system must require minimal to no maintenance.
- Combustibility – There can be no chance of combustion present on board.
- Toxicity – The desiccant will interact with air and water that recirculate into the cabin, so it must be safe for the respiratory systems of the crew members.
- Odor – The crewmembers will breathe the cabin air, so it cannot be irritating.

Desirable Properties IL	Significantly Odorless?	Significant Respiratory Toxicity?	Water-Miscible?	Significantly Combustible?	Al and Mild Steel Corrosivity	CO2 Absorption Capability	$/mL
[emim][EtSO4]	No	No	Yes	No	None [21]	Low	
[emim][OAc]	No Data	No	Yes	No	None [21]	High	
[emim][MeSO4]	Yes	Yes	Yes	Yes	Less than LiBr [19]	High	
[emim][OTf]	Yes	Yes	Yes	No	No Data	High	
[emim][TFA]	Yes	No	Yes	Yes	No Data	High	
30% LiCl Aq. Sol.	Yes	No	Yes	No	Significant in high concentrations	No Data	
[emim]Cl	No Data	Yes	Yes	Yes	No Data	No Data	
[P4441][DMPO4]	Yes	No Data	Yes	No Data	None [16]	No Data	
75% Aq. Sol. KCOOH	No Data	Not severe	Yes	No	Less than LiCl [19]	No Data	
[emim][MeSO3]	Yes	Yes	Yes	No Data	No Data	No Data	
Triethylene Glycol	Yes	No	Yes	Yes	Yes	No Data	

Posed Major health or safety Risk
High corrosivity or CO2 absorption
Too Costly or Unavailable
Meet all criteria

Table 3: Physical Properties

The results of Table 3 necessitated ruling out desiccants which were clearly unsafe, including [EMIM][MeSO4], [EMIM][OTf], [EMIM]Cl, and [EMIM][TFA]. Desiccants which are unavailable for purchase were ruled out, including [EMIM][OAc] and the promising RTIL [P4441][DMPO4].

Temperature and Pressure-Dependent Properties			
Temperature (K):	303		
IL	Density	Dynamic Viscosity	Kinematic Viscosity
Units	kg/m^3	Pa*s	m^2/s
[P4441][DMPO4]	1030	0.379	0.000367961

Table 4: Temperature and Pressure Dependent Properties of [P4441][DMPO4]

Temperature (K):	289		
IL	Density	Dynamic Viscosity	Kinematic Viscosity
Units	kg/m^3	Pa*s	m^2/s
[emim][EtSO4]	1243.841679	0.2592133	0.000208397
95% Aq. Sol. [emim][OAc]	1125	0.269046371	0.000239152
[emim][MeSO4]	1229.5002	0.2715595	0.00022087
[emim][OTf]	1384.3174	0.0593	4.2837E-05
[emim][TFA]	1298.12915	0.04664	3.59286E-05
30% LiCl Aq. Sol.	1154	0.0295	2.55633E-05
80% [emim]Cl Aq. Sol.	1092	0.01195	1.09432E-05
[P4441][DMPO4]	No Data	No Data	
75% Aq. Sol. KCOOH	1261.772308	0.0157966	1.25194E-05
[EMIM][MeSO3]	1248.19	0.2828835	0.000226635
Triethylene Glycol	1124	0.04156	3.69751E-05

Table 5: Temperature and Pressure Dependent Properties at 289K

Temperature (K):	313		
IL	Density	Dynamic Viscosity	Kinematic Viscosity
Units	kg/m^3	Pa*s	m^2/s
[emim][EtSO4]	1227.594923	0.08636667	7.03544E-05
95% Aq. Sol. [emim][OAc]	1100	0.06070617	5.51874E-05
[emim][MeSO4]	1199.75	0.1042	8.68514E-05
[emim][OTf]	1371.1848	0.02512	1.83199E-05
[emim][TFA]	1279.0185	0.02009	1.57074E-05
30% LiCl Aq. Sol.	1147	0.019	1.6565E-05
80% [emim]Cl Aq. Sol.	1092	0.01119	1.02473E-05
[P4441][DMPO4]	No Data	No Data	No Data
75% Aq. Sol. KCOOH	No Data	0.007367	N/A
[EMIM][MeSO3]	1231.4	0.069	5.60338E-05
Triethylene Glycol	1108.8	0.01979	1.78481E-05

Table 6: Temperature and Pressure Dependent Properties at 313K

The properties tabulated above are used in theoretical calculations to predict the behavior of the desiccants within estimated temperature parameters, which, if purchased, will be used in the moisture absorption experiments and in the prototype VPS. The moisture absorption data was highly diverse in the research documents studied, and thermodynamic data was missing for several candidates.

Thermophysical Properties		(Freezing Point for ILs)				
		Boiling Point	Melting Point	Crystallization	Glass Transition	Flash Point
IL	Molar Weight	K	K	K	K	K
Units	kg/mol					
[emim][EtSO4]	0.23629	678	N/A [26]	N/A [26]	194.6	435
95% Aq. Sol. [emim][OAc]	0.17021	No Data	228	N/A	No Data	427.65
[emim][MeSO4]	0.1110971	> 623	268.9	N/A [26]	181.1	No Data
[emim][OTf]	0.26023	> 623	264	< 253	No Data	491.5
[emim][TFA]	0.22418	1655	< 218	No Data	< 320	No Data
30% LiCl Aq. Sol.	0.0424	1633	< 249.4	N/A	N/A	No Data
[emim]Cl	0.14662	No Data	226.5	< 193	No Data	461
[P4441][DMPO4]	0.3424	No Data	290	No Data	202	No Data
75% Aq. Sol. KCOOH	0.0841157	No Data	215	270.78	No Data	No Data
[emim][MeSO3]	0.20626 [24]	403-471	293 [24]	No Data	No Data	No Data
Triethylene Glycol	0.15017	558.15	268.8722	No Data	No Data	450.15

Table 7: Freezing Point for ILs

Thermophysical Properties	Water Absorption Capability
IL	
Units	
[emim][EtSO4]	
95% Aq. Sol. [emim][OAc]	[6] At initial water content of 1265 ppm, average max. absorption reached wt.% 67.66 (Moisture absorption = IL/(IL + H2O) * 100.)
[emim][MeSO4]	
[emim][OTf]	
[emim][TFA]	0.004 kg/kg Humidity Ratio
30% LiCl Aq. Sol.	Dehydration cconcentration of 30 - 40% [iii]
[emim]Cl	
[P4441][DMPO4]	At humidity ratio of 32 %/g, Dehumidification Capacity of 10,944%/mol, with a dehumidification rate of 781%min/mol
75% Aq. Sol. KCOOH	
[emim][MeSO3]	[23] Stronger Interaction energy with water than between water molecules, shows gas dehydration capabilities [28]
Triethylene Glycol	20°C to 60°C => Liquid to gas 0.03 to 0.14

Table *8*: Water Absorption Data and Thermophysical Properties

3.3.2. VPS Geometry

This section covers the considerations for the VPS system's design geometry. Several issues can occur resulting from incorrect geometry:

3.3.2.1 Carry-over – wherein liquid escapes through the gas outlet. If too much liquid flows tangentially along the chamber walls, it will shrink the vortex in the center it collapses and the fluid flows over and out of the air outlet hole. To avoid this, a correct amount of liquid must be used. [4][8]

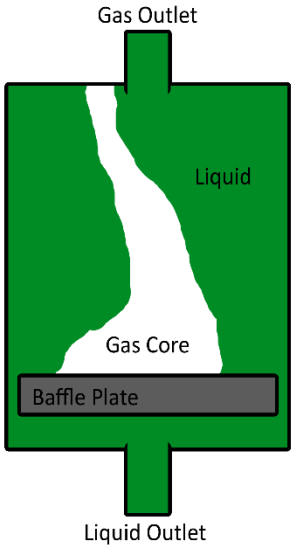

Figure 25: Carry-Over Illustrated

Adequate fill level can be derived from its relationship between the gas core diameter, calculated by the fluid thickness along the chamber inner wall. The derivations to acquire this are listed in operational order.

$$V = \frac{\tilde{V}}{A} \quad (1)$$

$$\dot{m} = \rho_l * A * V \quad (2)$$

$$m = V_F * \rho_l \quad (3)$$

$$t_f = \frac{m}{A_s * \rho_l} \quad (4)$$

$$D_1 = 2R - 2t_f \quad (5)$$

$$V_1 = \frac{D_1^2 * H}{2R^2} + H \quad (6)$$

The graph investigates if there is a property-based discrepancy between the two fluids for fill level and volume. The linear positive relationship between the two variables indicates that there is no point within the considered fill-volumes in which the fill level increases exponentially.

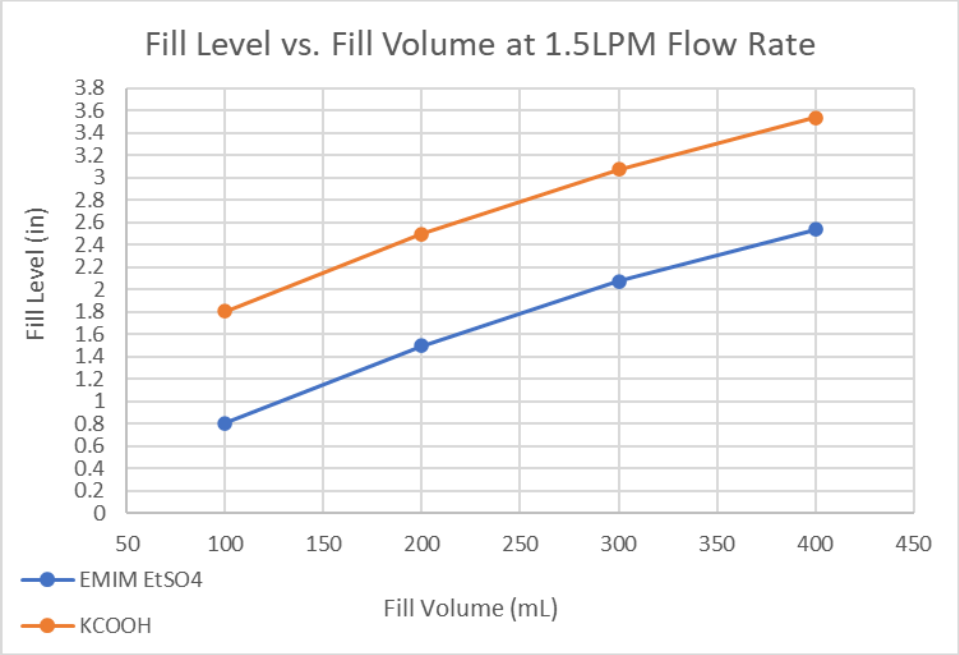

Figure 26: Fill Level Vs. Fill Volume at 1.5LPM: KCOOH data shifted 1" on Y-axis for clarity

The Gas Core diameter is shown as a function of fill volume. As expected, the gas core decreases as the chamber fills with fluid. The linear relationship between the two variables indicates that there is no point within the considered fill volumes in which the gas core diameter decreases exponentially.

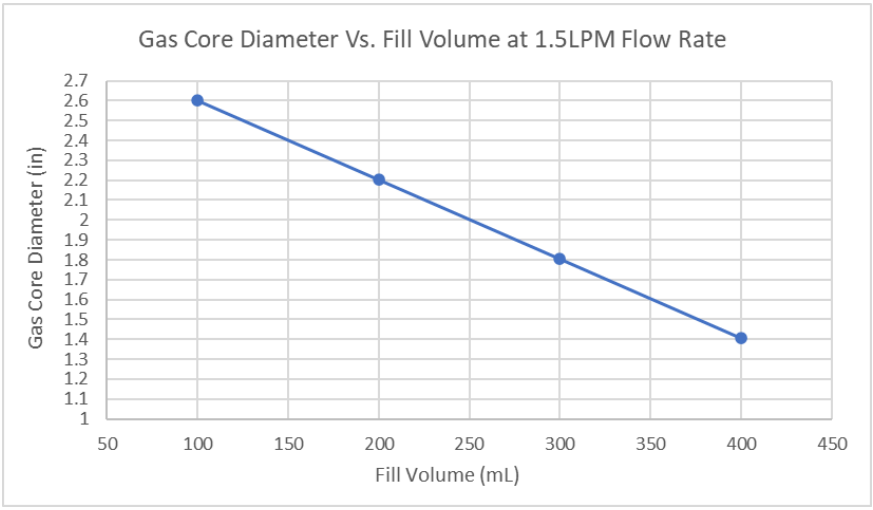

Figure 27: Gas Core Diameter Vs. Fill Volume at 1.5LPM: Same for both desiccants

The gas outlet diameter of 0.375” cannot be wider than the gas core diameter, so the data indicates that carry-over due to gas core diameter collapse theoretically should not occur within these parameters. To account for variability due to turbulence, potential differences in theoretical and real property values of the desiccant in the VPS system, and the variability in flow rates and temperatures, the system will be tested at $\leq$ 200mL fill volume.

3.3.2.2 Carry-under – occurs when gas escapes through the liquid exit. Gas bubbles travel simultaneously radially (toward the center of the chamber) and axially (up or down the chamber wall). If a bubble takes longer to travel radially than axially, it can travel beneath the baffle plate and out of the liquid exit.

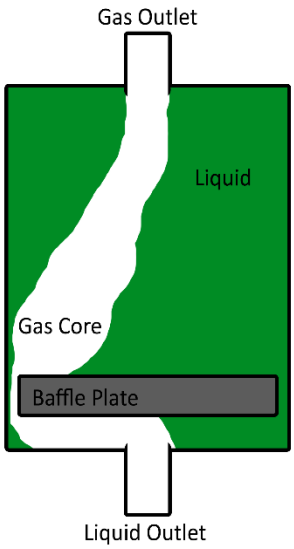

Figure 28: Carry-Under Illustrated

The following equations describing how the radial and axial bubble transit times would be calculated:

3.3.2.3 Radial Bubble Transit – As buoyant and weight forces act on the bubble, a resultant force on the bubble accelerates it radially through the chamber toward the center. [4][8] As it does so, a drag force acts on the bubble, which characterizes its radial velocity and the subsequent axial transit time. The following equations would illustrate this:

$$F_B = (\rho_l - \rho_g) * \omega^2 * L * V_s \quad (7)$$

$$F_W = \rho_l * \omega^2 * L * V_s \quad (8)$$

$$F_D = \frac{1}{2} * C_D * \rho_l * v_{rad} * \pi * r^2 \quad (9)$$

$$F_{res} = [(\rho_l - \rho_l) * \omega^2 * L * V] + (6 * \rho_l * v_{rad} * \pi * r) \quad (10)$$

$$a_b = \frac{F_{res}}{\rho_g * V} = \left[\left(1 - \frac{\rho_g}{\rho_l}\right) * \omega^2 * L\right] + \left(\frac{9 * \mu_l * v_{rad}}{2 * \rho_g * r^2}\right) \quad (11)$$

$$t_r = \frac{9 * \mu_l}{r^2 * \omega^2 * (\rho_l - \rho_g)} \quad (12)$$

The minimum velocity for radial bubble travel is characterized by the following variables:

$$v_{term} = \frac{2 * R^2}{9 * \mu_l} * (\rho_l - \rho_g) * \omega^2 * L \quad (13)$$

3.3.2.4 Axial Bubble Transit – The bubble travels simultaneously toward the center and across the height of the chamber (axially). The area of axial transit determines the bubble's velocity as it moves axially, which provides the axial transit time of the bubble in relation to the nozzle height from the baffle plate. [8]

$$A_{AT} = \pi * \left(\frac{D^2}{4} - \frac{R^2}{4}\right) \quad (14)$$

$$v_z = \frac{\tilde{V}}{A_{AT}} \quad (15)$$

$$t_a = \frac{D_z}{v_z} \quad (16)$$

From the axial transit time, radial velocity can be acquired.

$$v_{rad} = L * t_a \quad (17)$$

The minimum rotational speed required for phase separation to occur is calculated when the axial and radial transit times are equated.

$$\omega_{min} = \sqrt{\frac{9 * \mu_l * v_z}{D_z * r^2 * (\rho_l - \rho_g)}} \quad (18)$$

Another important value is the inlet momentum rate, as it acts as a force on the inside surface of the chamber and is included in pressure-induced forces which act on the bubble and chamber.

$$\dot{p} = \rho_l * A * V^2 \quad (19)$$

3.3.2.5 The geometry of the VPS – Is determined by the physical behavior of the liquid desiccant as it moves through the chamber. The rotational speed of the fluid increases with flow rate, and the rate of increase also increases as the chamber inside diameter decreases:

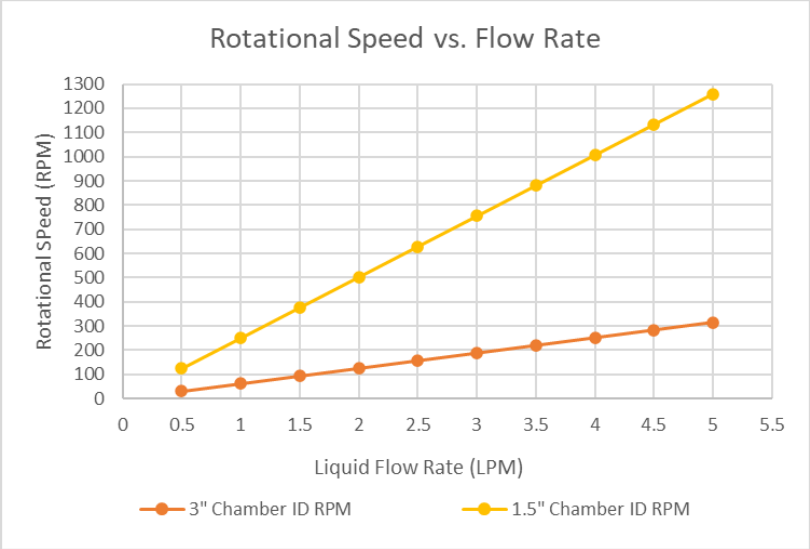

Figure 29: Rotational Speed Vs. Flow Rate at 2 different chamber inside-diameters

Rotational speed is a function of Reynold's number at the liquid inlet nozzle. The derivations are listed in operational order.

$$\mathrm{ReN} = \frac{\rho_l * \sqrt{A} * V}{\mu_l} \tag{20}$$

$$\omega = \frac{\mathrm{ReN} * \mu_l}{\rho_l * R^2} \tag{21}$$

$$\mathrm{Bo} = \frac{(\rho_l - \rho_g) * (D_1/2)^2 * 9.871}{\sigma} \tag{22}$$

$$\mathrm{Fr} = \frac{\omega * R^2}{D_1 * 9.871} \tag{23}$$

$$\mathrm{We} = \mathrm{Bo} * \mathrm{Fr} \tag{24}$$

Other calculations were performed to acquire other geometric features, however, due to the similarity in desiccants and preliminary design to Alex's VPS, the VPS was modeled after his design to ensure real-world functionality.

The equations used to derive the geometric features and predict bubble behavior are listed below. Experiments performed for [EMIM][EtSO4] showed its minimum regenerable temperature to be 343K (70^{o}C). Thus, it was determined that the properties would be used for the IL at this temperature, shown in table 9. For further analysis of these equations, Sarvadi's thesis is referenced. [4]

3.3.3. Experimental Testing to acquire unknown thermodynamic properties:

The following preliminary experiment is designed to acquire the last 2 unknown thermophysical properties of each desiccant candidates:

1) The water-absorption capacity at various temperatures, and

2) The ideal temperature for full regeneration.

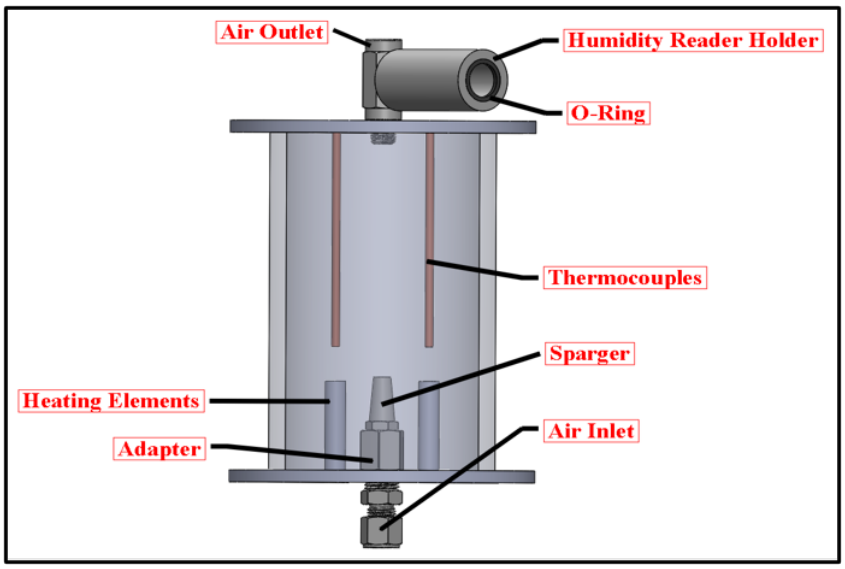

The figure above shows a schematic of the experimental set-up used to identify unknown thermodynamic properties for the liquid desiccants. Before testing begins, the desiccant is added to the chamber, submerging both the sparger and cartridge heaters. The chamber is weighed before and after each test to determine how much water is added to the desiccant after absorption, and how much is removed after regeneration.

Overview:

To acquire the desiccant's water absorption capacity in experiment 1, the desiccant is left in room temperature until the air outlet relative humidity (RH) sensor has a stable reading. Then the sparger valve is opened: The sparger allows humid air to flow into the desiccant in a chamber, and the bottom end valve is closed to not allow humid air to escape. Each desiccant run was weighed before and after regeneration. The change in the humidity level of air stream indicates the desiccant's water-absorption capacity. In experiment 2, the desiccant pool is then gradually heated to evaporate water from the saturated desiccant to find proper temperature for the desiccant's regenerability.

3.3.4. Theoretical Calculations Results:

Excel was used to list the variables and derivations. The results of the calculations performed provide insight into the parameters of operation the VPS will operate in while in use.

[EMIM][EtSO4]	Temperature: 16C (289K)			Flow Rate: 1.5 LPM	
Input Variable	Symbol	Value	Unit	Conv.	Conv. Unit
Cylinder Diameter	D	0.0762	m	3.0000	in
dynamic viscosity of fluid @ liq. Inlet	μl	0.1590	N*s/m^2		
mass of liquid	m	0.1243	kg		
density of gas phase	ρg	1.3660	kg/m^3		
Inlet liquid density	ρ1	1243.00	kg/m^3		
core diameter	D1	0.0683	m	2.6880	in
fluid volume	Vf	0.0001	m^3	0.1000	L
Reynolds Number at inle	ReN	137.92			
Fluid Thickness	t	0.0040	m	0.1560	in
Liquid Fill Level	Vl	0.0208	m	0.8184	in
"rotational fluid speed inside separator	ω	12.1534	Hz	116.06	RPM
Min ω for Successful Vortex Separation	ωmin	0.6548	Hz	6.2532	RPM
(liq. Inlet area of nozzle A)^1/2	LN	0.0014	m		
Liquid Inlet Velocity	V	12.4248	m/s		
radial transit time of bubble - from outsides to center of VPS vortex	tr	0.0315	s		
axial transit time of bubble - vertically from nozzle to baffle plate	ta	10.8377	s		
Average axial velocity	vz	0.0073	m/s		
"Axial and tangential flow area	AAT	0.0034	m^2		

Figure 30: [EMIM][EtSO4] Excel Calculations – 289K

[EMIM][EtSO4]	Temperature: 70C (343K)			Flow Rate: 1.5 LPM	
Input Variable	Symbol	Value	Unit	Conv.	Conv. Unit
Cylinder Diameter	D	0.0762	m	3.0000	in
dynamic viscosity of fluid @ liq. Inlet	μl	0.0187	N*s/m^2		
mass of liquid	m	0.1206	kg		
density of gas phase	ρg	1.3660	kg/m^3		
Inlet liquid density	ρ1	1206.00	kg/m^3		
core diameter	D1	0.0683	m	2.6880	in
fluid volume	Vf	0.0001	m^3	0.1000	L
Reynolds Number at inle	ReN	1136.37			
Fluid Thickness	t	0.0040	m	0.1560	in
Liquid Fill Level	Vl	0.0208	m	0.8184	in
"rotational fluid speed inside separator	ω	12.1534	Hz	116.06	RPM
Min ω for Successful Vortex Separation	ωmin	0.2281	Hz	2.1785	RPM
(liq. Inlet area of nozzle A)^1/2	LN	0.0014	m		
Liquid Inlet Velocity	V	12.4248	m/s		
radial transit time of bubble - from outsides to center of VPS vortex	tr	0.0038	s		
axial transit time of bubble - vertically from nozzle to baffle plate	ta	10.8377	s		
Average axial velocity	vz	0.0073	m/s		
"Axial and tangential flow area	AAT	0.0034	m^2		

Figure 31: [EMIM][EtSO4] Excel Calculations – 343K

3.3.5. Material Selection

Research was performed to select VPS materials which can withstand the corrosive effects of ILs. The results of Uerdingen's research on the corrosivity of seven ILs on Carbon-Steel, 304 stainless steel (304 SS), Hastelloy C22, brass, copper, and aluminum, showed that the corrosion impact on 304 SS and the Ni-based alloy Hastelloy C22 was much lower than on other materials tested, with 304 SS showing the least change when exposed to the effects of acidic corrosion of diluted ILs. [29] Because Hastelloy is less common to find, difficult to manufacture, and isn't used to make fittings commercially, stainless steel was the better candidate for the scope of the challenge. To ensure minimal corrosivity of ILs for long-term use, austenitic 316 stainless steel was chosen.

3.4. Safety Considerations

The subsystem is intended to re-humidify/dehumidify cabin air for crew members to breathe, so preventing risks and ensuring safe operations are prioritized. Some safety considerations and risk prevention methods involve selecting a compatible liquid desiccant, proper hardware assembly, and functioning sensors.

One of the main components to the subsystem is liquid desiccant. The desiccant needs to be non-toxic because it mixes with the air leaving and re-entering the cabin. The desiccant also needs to be compatible with the material of the subsystem. A corrosive desiccant would compromise the subsystem's structure by corroding the components such as the tubing and chambers, leading to improper desiccant regeneration, flow, and functionality. A non-flammable/combustible desiccant is also required for this system. Liquid desiccants with poor thermal stabilities that generate large quantities of heat are a risk, even if operating temperatures for this subsystem are not extreme. It is therefore necessary for a desiccant to be highly thermally stable. If a desiccant researched was incompatible to these standards, it was not considered for subsystem operations. Detailed risk and safety considerations, the following consequence, and mitigation approaches are tabulated below.

Risk / Safety	Consequence	Mitigation Approach
Pump Failure	Liquid desiccant regeneration sequence will halt	Backup Pump
Nozzle	Gas/liquid will not enter VPS	Filters
Piping Leakage	Incorrect pressure in system	Locate and repair leak
Heater Failure • Electronics not communicating • Heating higher than needed • Heating lower than needed • Lack of flow through heater	Re-humidification will not function properly, and correct humidity cannot be reached	Backup heater
Chiller Failure • Electronics not communicating • Cooling higher than needed • Cooler lower than needed • Lack of flow through chiller	Dehumidification will not function efficiently, and correct humidity cannot be reached	Backup cooler
Excessive Pressure	System structure will be compromised	Relief valve to reduce excess pressure
Gas escapes through IL outlet or IL escapes through gas outlet	Phase Separation Issues	• Use a proper liquid fill • Have indicator light to show liquid level changes
Sensor Failure • Incorrect readings • Sensor compromised	• Phase Separation Issues • Excess pressure in system • System won't function properly	Backup sensors

Table 9: Risk Management and Safety Review

Another safety consideration is Leakage: The components in the system need to be properly secured to prevent leaks in the system. Leaks could potentially lead to excessive pressure in the system, causing structural instabilities in the tubing and desiccant flow. Neglecting correct assembly would compromise the entire system – desiccant flow must be consistent and balanced throughout operation. Ensuring the other components such as the pumps, heater, chiller, heat exchangers, and sensors are secured correctly will therefore be crucial. The humidity regulation functions of the system will depend on the proper assembly of these major components.

Functioning sensors are key to reading and regulating the pressure, temperature, flow rate, and humidity at critical points throughout the system. A dysfunctional sensor would give incorrect readings which can cause issues with gathering data or pinpointing where a problem is occurring in the system.

3.5. Ethical/Professional Considerations

Ethical principles and practices guide and influence productivity, decision making, and outcomes. Taking proper ethical and professional considerations sets a standard for personnel involved with this project. Ethical considerations include meeting sponsor expectations, setting quality/engineering standards, and establishing resource management.

NASA guidelines were followed to meet proper sponsor expectations and qualities. Past designs, formulas, hardware, theses, research papers, code, and CAD models were utilized for this project, and taking care to source information from accurate and reliable references is an ethical consideration. Analytical and experimental results gathered were recorded so that they can be properly used for future reference.

A Gantt chart aided time management to ensure time was used efficiently and deadlines were met on time, while taking into consideration personnel availability, resources supplied, and the time given. A trade analysis is conducted to select safe components for the system and a bill of materials is used to maintain organization for any costs.

3.6. Estimated Life Cycle of Development

Regeneration is a key factor of the VPS system. The system is designed to continuously work with little to no maintenance. The estimated prototype lifespan depends on the condition of the supporting components. The components most likely to cause system failure are the pumps, heat exchanger, and heater/chiller. Each instrument has a specified method of use and is sensitive. Most wear will be caused by the desiccant's corrosivity. Therefore, the material for the supporting instruments was carefully chosen.

The pumps are made of AISI 316 to ensure maximum corrosion resistance. [29] The heat exchangers are brazed flat and are made up of primarily stainless steel.

3.6.1. Pump Life Cycle:

Most pumps are rated for a 10-to-15-year operation life. Over multiple cycles of operations the internal components of the pump will start to wear. For the project's duration, the pumps will not have to be replaced. One source of accelerated wear would be improper

pump usage, which will reduce life cycles. Each pump comes with a datasheet with its optimal conditions including, but not limited to, speed limit, temperature range, and minimum/max flow rate. A magnet drive gear pump was chosen for the system. It has a minimum flow rate of 20 l/h and a maximum flow rate of 250 l/h. For this project's purposes, the flow rates range will be between 90 l/h to 150 l/h, which is well within the pump's operational range.

3.6.2. Heat Exchanger Life Cycle:

Most heat exchangers have an expected life cycle of 15-to-20 years. Improper usage of the heat exchanger would reduce life expectancy. Meeting the optimal operational conditions and using the heat exchanger correctly ensures that the heat exchanger will not need to be replaced. However, some key conditions the team will have to lookout for are fouling, temperature ranges and flow rates. A brazed plate heat exchanger was chosen for this system. One of the benefits of using this type of heat exchanger is the highly turbulent flow created by the corrugated geometry of the internal plates. The turbulent flow allows for Cleaning in Place (CIP), or self-cleaning of the heat exchanger. Having a clean heat exchanger will reduce fouling and increase life expectancy.

3.6.3. Heater/Chiller Life Cycle:

The life expectancy for the heater and chiller is also about 15-to-20 years with proper usage. The critical condition to monitor when operating these devices is temperature control. At the chiller, the temperature must be monitored to ensure the device’s internal components do not freeze. For the heater, corrosion becomes a potential issue. At higher temperatures, corrosion of material is greatly accelerated. Ensuring proper operatorial temperature ranges are maintained will allow for a longer operating life from both the heater and chiller. The chiller used for this system is a ThermoChill II Recirculating Chiller, which has an operating temperature between -10°C to 30°C. The lowest temperature necessary for our prototype is 15°C, which is within the chiller’s temperature range. The heater being used for this system is a MENCO cartridge heater system provided by Dr. Bostanci’s lab. This heater has been used in similar applications and has proven to be effective and reliable.

3.6.4. VPS Life Cycle:

Besides supporting instruments, the most likely component to fail on the VPS protype are sealing points. Welding locations and O-rings can be sources of leaks and could reduce the lifespan of the VPS and, consequently, the rest of the system. These critical points were identified and addressed during fabrication and assembly. Proper welding techniques were employed to prevent leaks, including proper material preparation to minimize porosity, and proper gas shielding conditions. O-ring size and dimensioning charts were used to ensure proper fitment.

3.7. Cost Breakdown of Development

The costs of the system are divided into several subassemblies which comprise the overall VPS system.

3.7.1. Desiccant:

2L of each were ordered to ensure there would be enough for both experimentation and prototype testing, accounting for potential desiccant loss due to an inability to fully regenerate and leaks. An adequate fill level is also needed to fill the experiment chamber and fully submerge the sparger.

Item #	Name	Material	Volume	EDP #	Manufacturer	Qty. Needed	Total ($)
Desiccant							
1	[EMIM][EtSO4]	N/A	2L	51682-1KG-F	Sigma Aldrich	2L	[redacted]
2	KCOOH	N/A	2L	294454-1KG	Sigma Aldrich	2L	

Table 10: BOM – Desiccants

3.7.2. Components of the VPS Chambers:

The chamber was built from 316 stainless steel. To avoid galvanic corrosion, only steel fittings were chosen.

Item #	Name	Material	Dimensions	EDP #	Manufacturer	Qty. Needed	Total ($)
Components of the VPS Chambers							
3	Chamber Material	316 Stainless Steel Round Tube	3-1/2" OD x 0.25" Wall Thickness x 24" Length	STR316S/3500250	Metal Supermarkets	1	[redacted]
4	End Caps - Opaque	316 Stainless Steel Sheet	12" x 12"x 1/2" thick	9195K42	MCmaster-Carr	1	
5	End Caps - Transvescent	Ultem 9085 or PolyCarb Plate	12" x 12"x 1/2" thick	8585K522 or 8707K159	MCmaster-Carr	1	
6	Baffle Plates	316 Stainless Round Bar	2-1/2" DIA. X 12" long berstock	SR316/2500	Metal Supermarkets	1	
7	Gas Nozzles	316 Stainless Round Bar	1" OD X 3' Long	SR316/1	Metal Supermarkets	1	
8	Liquid Nozzles - Shell	316 Stainless Round Bar	----------	SR316/1	Metal Supermarkets	1	
9	Shell-Insert Adhesive	521 Marine Grade Epoxy	Quart Size Fast Hardener	521 epoxy	ProMarine	1	
10	Liquid Nozzles - Insert	3D-Printed Ultem PEI filament	3/4" OD X 2' Long	N/A	Fortus 450	1	
Associated Hardware							
11	Chamber Connecting Rods	Carbon Steel	6" Overall Length, 1/4"-20 Thread	6516K263	McMaster-Carr	12	[redacted]
12	Lock Nuts	Grade 8 Steel Nylon-Insert	1/4"-20 2B Thread	90630A110	McMaster-Carr	2	
13	Baffle Plate Connecting Screws	316 Stainless Steel	1-1/4" Long, 1/4"-20 Slotted Flat Head	91858A544	McMaster-Carr	2	
Sensors							
14	Pressure Sensors	Stainless Steel	1/4" Port, 0-5V DC, Range 0-100psi	PX309-100G5V	OMEGA	5	[redacted]
15	Relative Humidity (RH) Sensors		±2% Analog humidity and temperature sensor	SHT31-ARP-B	Sensirion	4	
16	Thermocouples	304 Stainless Steel Sheath	2" Length, 1/16 ' Diameter	KMTSS-062U-2	OMEGA	10	
17	Flowmeter for IL	glass tube	N/A	TBD	Brooks Instruments	2	
18	Flowmeter for air	glass tube	N/A	TBD	Brooks Instruments	2	
Hardware							
19	On/Off Inline Hydraulic Valve	316 Stainless Steel	1/4" NPTF inlet/outlet	4SAL07	Grainger	6	[redacted]
20	Standard-Wall Steel Pipe Nipple	316 Stainless Steel	1/4" NPT both sides, 0.364 ' ID	4548K131	McMaster-Carr	18	
21	Yor-Lok Straight Adaptor	316 Stainless Steel	3/8" Tube OD x 1/4" NPT Male	5182K119	McMaster-Carr	32	
22	Yor-Lok Straight Adaptor Thermocouple	316 Stainless Steel	1/8" Tube OD x 1/4" NPT Male	5529K34	McMaster-Carr	10	
23	Steel Pipe Fitting Cross Connector	316 Stainless Steel	1/4" NPTF Female	48805K631	McMaster-Carr	6	
24	Tee Connector	316 Stainless Steel	1/4" NPTF Female	48805K471	McMaster-Carr	8	
25	Yor-Lok Straight Adaptor	316 Stainless Steel	3/8" Tube OD x 1/8" NPT Male	5182K811	McMaster-Carr	4	
26	Bushing Reducing Adaptor NPTF to NPTM	316 Stainless Steel	3/8" NPTM X 1/4" NPTF	48805k525	McMaster-Carr	2	

Table 11: BOM – Components of VPS Chambers

3.7.3. Tubing Components:

To avoid galvanic corrosion, steel tubing was chosen.

Item #	Name		Dimensions	EDP #	Manufacturer	Qty. Needed	Total ($)
Tubing Components							
27	Tubing	316 Stainless Steel	3/8"OD X 0.305"ID X 4'	89495K345	McMaster-Carr	5	[redacted]

Table 12: BOM – Tubing Components

3.7.4. Preliminary Desiccant Properties Experiment:

The experiment was performed to test the liquid desiccant's thermophysical properties.

Item #	Name	Material	Dimensions	EDP #	Manufacturer	Qty. Needed	Total ($)
Preliminary Desiccant Properties Experiment - Components							
4	Experimental Chamber	316 Stainless Steel	5"Height x 3"ID	N/A	N/A	1	[redacted]
5	Baffle Plate	316 Stainless Steel	2-1/2"D X 1/2"	N/A	N/A	1	
6	Sparger	Bronze Body, Steel Fitting	1-1/8" Height x 1/8" NPT Thread	4450K1	McMaster-Carr	1	
7	RH sensor O-Ring - Square-Profile	Viton® Fluoroelastomer O-Ring	1/16" Width, Dash No. 015	1170N25	McMaster-Carr	2	
8	Digital humicity reader	N/A	N/A	FLUKE971	Fluke	2	
9	Cartridge Heaters	N/A	N/A	N/A	UNT TML	1	
10	Thermocouple	Steel	N/A	N/A	UNT TML	2	
11	Ball Valve - Air cut-off	Steel	1/4" NPTF to 1/4" NPTM	27420421718080	Dernord	2	
12	Yor-Lok	316 Stainless Steel	1/16" Tube OD x 1/16" NPT Male	5182K834	McMaster-Carr	2	
13	Yor-Lok Straight Adaptor	316 Stainless Steel	3/8" Tube OD x 1/4" NPT Male	5182K119	McMaster-Carr	2	
14	RH sensor tee fitting	304 Stainless Steel	1/4" NPT female thread	4464K48	McMaster-Carr	2	
15	Plug with External Hex Drive	316 Stainless Steel	1/4" NPT male thread	4452K142	McMaster-Carr	2	
16	Fitting connector	316 Stainless Steel	1/4" NPT male straight connector	5232T316	McMaster-Carr	4	

Table 13: BOM – Preliminary Experiment Components

3.7.5 Heating and Cooling Systems:

These were specified for the expected performance and conditions of the VPS prototype.

Item #	Name	Material	Dimensions	EDP #	Manufacturer	Qty. Needed	Total ($)
Heating and Cooling Components							
1	Chiller	Multiple	24.4"x14.2"x23.6" Temp ±0.1°C	197111010000	Thermofisher	1	[redacted]
2	Heat Exchanger	Copper	8"x3"x1.3"	BL14-10D	WiseWater	2	
3	Immersion Heater	304 Stainless Steel	6 3/8"x1 1/8"	3656K186	McMaster-Carr	1	

Table 14: BOM – Heating and Cooling Components

3.7.6 Fluid Control Components:

These were specified for the expected performance and conditions of the VPS prototype.

Item #	Name	Material	Specifications	EDP #	Manufacturer	Qty. Needed	Total ($)
Fluid Control Components							
17	DC Motor M42x30/I Brushed motor	Zinc-plated	24V 22W Output Power 6.5 Ncm nom. Torque	N/A	Kahlig Antriebstechnick	2	[redacted]
18	Gear Pump	316 SS housing/PTFE Gears	Max P 290psi, Max vacumm 724mmHg	MG204XDOPT00000	fluidctech	2	

Table 15: BOM – Fluid Control Components

4. FABRICATION

The fabrication phase of the X-Hab humidity control module involves both the machining of VPS chamber components and nozzles, and the assembly of hardware, tubing, operational equipment, and testing instruments.

4.1. Fabrication Methods

The following methods were used for VPS system fabrication.

1. Waterjet Cutting – A method of cutting metals and polymers in which high-pressure water is mixed with garnet abrasive media and ejected through a nozzle to cut material. The machine's toolpath is read from code generated by software.

2. Horizontal Band Saw Cutting – A hydraulic power saw which uses a long, toothed saw band, stretched between two rolling wheels, to cut material stock.

3. Manual Milling – The process of feeding a workpiece into a rotating cutting tool (inside of a spindle) which uses cutting flutes or inserts to remove the material. The workpiece is moved in the X and Y axes on a power-operated moveable worktable, and the cutter moves on the Z axis.

4. Manual Lathe Turning – The process of feeding the cutting edge of an insert on the X axis into a workpiece turning inside a lathe chuck about the Z axis.

5. Computer Numerical Control (CNC) Milling– Mill machining process in which the mill operates from code written by software that allows the machinist to control the surface speed and revolutions per minute. The machinist can also adjust speed and geometric tool parameters at the machine during runtime.

6. TIG Welding – A method of welding in which a metal filler joins two or more workpieces. The filler wire is heated and melted with a torch and held within a critical distance to the workpieces. An electrode in the torch creates an arc of electricity between the workpieces to heat them. The melted filler wire joins the melted points of workpiece metal, creating a bond between the workpieces and filler.

7. 3D Printing – A form of additive manufacturing in which polymer filament is heated in and jetted through a nozzle to land on a printing bed, thus constructing a print layer. As the filament drops, the nozzle moves on the Z axis while the print bed moves in the X and Y axes, which creates the part. The printer reads the coordinates from a program generated by software which slices the part to be made into the 3D print layers.

8. Wire Electrical Discharge Machine (EDM) Cutting – Electrical discharges are fired in rapid succession between a "tool" electrode and a "workpiece" electrode to cut stock into a desired shape. This method of machining works well with ferrous materials as the

electrical discharge must have a path of least resistance from the wire to the work piece. The following table summarizes the fabrication stages of each component.

Part	Fabrication Method	Operation
Chamber	Horizontal Band Saw	Cuts stock to 5-1/2” stock
	Manual Lathe	Faces stock and turns the ends down for fit to end cap slots
	CNC Mill	Creates the Nozzle holes
Baffle Plate	Horizontal Band Saw	Cuts 6” baffle plate stock into 2-1/2” pieces (so that the chuck has material to hold)
	Manual Lathe	Creates the cone feature
	CNC Mill	Faces off the sawed side and drills/countersinks the countersink screw holes
	Manual Lathe	Faces the flat side down to the correct 1/2” length
Top and Bottom Caps	Waterjet	Cuts contours, center holes and lead screw holes of all parts from stock plate
	Manual Mill	Faces Stock and manually taps NPT and baffle plate holes
	CNC Mill	Drills Bottom stock holes and forms gasket/chamber slot
Liquid Nozzle Pocket	Horizontal Band Saw	Cuts stock to length
	Manual Lathe	Faces Stock, forms pocket feature, drills NPT tapped hole
	Wire EDM	Cuts radius feature on outlet side of nozzle
Liquid Nozzle Insert	3D printer	Prints the insert with the geometry for the liquid inlet hole using Ultem filament
Gas Nozzle	Horizontal Band Saw	Cuts stock to length
	Wire EDM	Cuts radius feature on outlet side of nozzle
	CNC Mill	Creates gas nozzle pocket features
	Manual Lathe	Faces Stock and drills the NPT tapped hole

Table 16: Fabrication Stages by Component

4.1.1. Manual Machining vs CNC Machining

The manual lathe was used to face all components' stock because it can face both sides with accurate perpendicularity between stock faces and sides. This ensures accuracy and precision of work-holding during subsequent CNC milling operations. Several facing operations were switched to the manual lathe after further consideration. The baffle plate's conical shape was fastest to achieve on the manual lathe, as it is radially symmetrical and has no high-precision dimensions requiring CNC accuracy. The liquid nozzle pocket was also made on the manual lathe as the features were all radially symmetric, and drilled operations required manual feedrate calibration to avoid losing drills to the work hardening effects of 316 Stainless Steel.

The following table illustrates the general costs and benefits of each method.

	Manual Machining (mill and lathe)	CNC Machining (mill and lathe)
Benefits	• Short set-up time • Simple operation • No program necessary • Easily adjustable – Manual operation allows minute adjustments to be made during operation to optimize finish and accuracy	• Precise and consistent machining • Multiple operations per machining cycle • Consistent coolant flow • Rigid work-holding
Costs	• Less repeatability • Less precision in feature dimensions • More vibration and less rigid workholding due to structural imperfections. • Limited in what features can be made	• Requires a model and CAM program to run • Program requires step-through – increases set-up time • Less modular to change approach when fixtures or tools don't work • Feeds and speeds are limited in adjustability

Table 17: Benefits and Cost, Manual Vs CNC

4.1.2. Machining vs Water Jetting

The top and bottom caps were initially going to be exclusively manually machined and CNC drilled and milled. However, because all parts could be made on one plate stock, both plates shared five holes and contour dimensions, and tooling order delays created a time constraint, it was determined that the parts could be water jetted.

The following table illustrates the general costs and benefits of each technique.

	Machining	Water jetting
Benefits	• Adjustable in tooling diameter and height between cycles or operations – allows repeated feature cutting • Controllable cutting parameters	• No tooling necessary • Guaranteed consistent cooling • Large work area allows large stock to be cut into many parts
Costs	• Requires tooling • Limited work holding and work area • Requires more involved programming • Longer set-up time than water jetting	• Cannot fix dimensional errors after cutting • Less precise perpendicularity between faces and walls.

Table 18: Benefits and Cost, Machining Vs Waterjet

4.1.3. Manual Lathe Part-off vs Horizontal Band Saw Cutting

The baffle plates were saw-cut because the lathe part-off tooling provided was not sufficient for 316 stainless steel stock. However, the saw cutter cut the material at an angle, resulting in a two-step operation in which the part is cut off in the band saw and then faced off in the CNC mill. The benefits and costs of the lathe versus the band saw are analyzed and shown.

	Manual Lathe – Part-off Operations	Horizontal Band Saw Cutting
Benefits	• Higher precision and accuracy of cut. • Cut can be finished with a facing pass. • Cutting Length can be adjusted and repeated.	• Simpler operation. • More room to cut – can cut larger stock. • Can cut various stock types. • Cheaper machine.
Costs	• Stock diameter to cut is limited by the part-off tool. • Cooling issues are more common and can cause tool failure and poor finish. • Set-up time is longer. • Feeds are controlled by-hand, not hydraulically – can cause tool failure.	• No adjustability of cut. • Slanted cuts are common for harder stock materials. • Stock length must be significantly longer than the distance from work holding to saw blade.

Table 19: Benefits and Cost, Manual Lathe Vs Horzontal Band Saw

4.1.4. CNC Machining vs Wire EDM

Due to time constraints and availability of the wire EDM, it was used to create the nozzle cutout feature. This was beneficial, as the cutout was easier and cheaper to cut on the EDM, and the EDM has a lower risk of producing scrap making simpler cuts than a CNC milling machine has, overall. The benefits and costs of using each machine **for single-toolpath/ two-axis cuts** are considered and recorded.

	CNC Mill Machining – two axis cuts	Wire EDM – two axis cuts
Benefits	• Adjustable tooling diameter and height offsets during operation allow recutting of feature to avoid scrap. • Adjustable cycle time makes for potentially faster cycles.	• No tooling necessary. • Guaranteed consistent cooling via water. • Faster set-up time. • Less force pushing on material to cause error.
Costs	• Requires tooling, which can raise costs and pose risks of tool failure and scrap. • Requires more involved programming. • Potential issues with vibration, chatter, cooling, or G-code.	• Longer cycle times. • Cannot adjust cutting once cycle starts.

Table 20: Benefits and Cost, CNC Vs Wire EDM

4.1.5. 3D Printing vs 'Subtractive Manufacturing' Processes

The feature designed to reduce and flatten the fluid stream entering the VPS chamber required the inlet pocket begin as the circular NPT tap-sized hole, and gradually extrude into a rectangular pocket shape, wherein the bottom of the rectangular flat is tangent to the bottom edge of the round hole. This could not be made using subtractive manufacturing methods, so the decision was made to 3D print the insert using Ultem filament.

	Subtractive Manufacturing	3D Printing
Benefits	• Adjustable tooling diameter and height offsets during operation allow recutting of feature to avoid scrap. • Adjustable cycle time makes for potentially faster cycles.	• Can create features which are impossible to make using Subtractive Manufacturing methods. • Can be cheaper without the expense of tooling/ work holding. • Easier to run lights out.
Costs	• Can require tooling and work holding. • Potential issues with vibration, chatter, or cooling. • Limits to what features can be made.	• Longer cycle times. • Cannot adjust cutting once cycle starts. • Any error during the printing process results in a failed part.

Table 21: Benefits and Cost, Subtrative Machining Vs 3D Priniting

4.2 Fabrication Stages

4.2.1. Waterjet Cutting

Top and Bottom Caps: The following show the successful and unsuccessful cuts from the stock plate. The scrap was caused by incorrect x-axis and y-axis home-positioning before starting the cutting cycle. 4 of 8 parts are within spec.

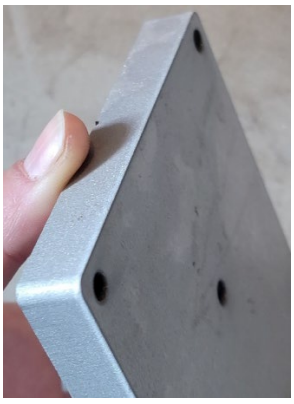

4.2.2. Wire EDM

Creating the cutout of both the liquid and gas nozzles.

The liquid and gas nozzles are each positioned on the left side of the machine. The wire is touched off on the lowest point of the part to determine y-origin along with the right most point of the part to determine x-origin. The hatch door is closed to fully submerge the part under water helping to control the heat generated by the wire. The middle picture and the picture on the right show the liquid and gas nozzles, respectively, post machining.

4.2.3. Manual Lathe Turning

Creating the conical baffle plate feature:

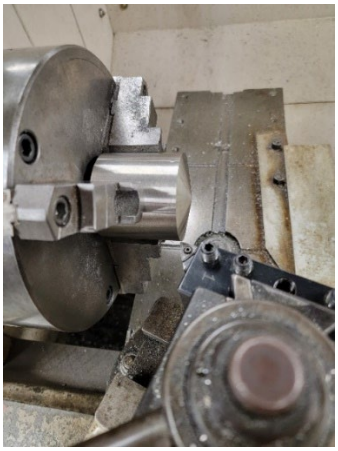

Facing the chambers to part length:

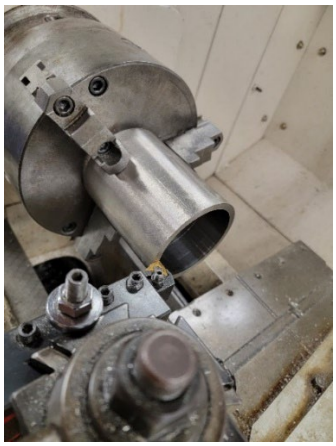

Creating the pocket and NPT drill hole of each liquid nozzle: The best lubrication method for drilling operations into the 316 stainless steel is tap lube, while water-based coolant sprayed through an air-pressurized mister (shown here) yielded the best results for the boring operations.

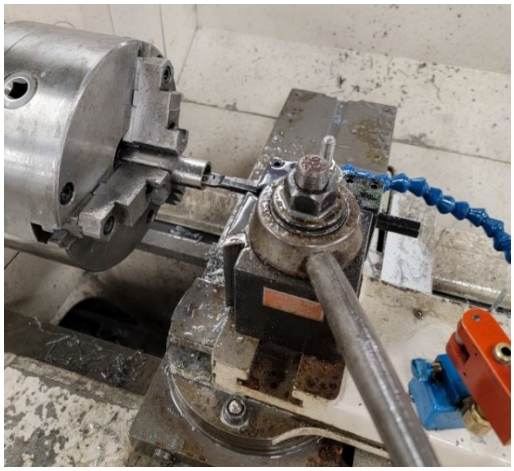

The following shows the liquid nozzle insert test-fitted into the pocket. Actual pocket depth = 2.0005”

After the gas nozzle pockets were CNC milled, the holes in the back for the NPT fittings are drilled.

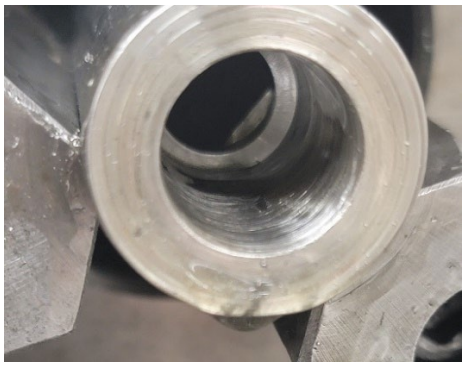

4.2.4. CNC Machining

Baffle Plate: The holes are drilled and countersunk.

Gas Nozzle: The outlet of the gas into the chamber is drilled and pocketed.

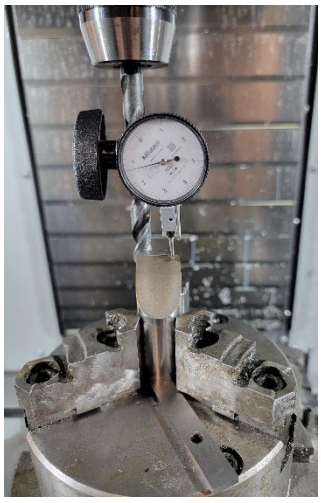

Chamber: Due to time constraints, the chamber was outsourced to be CNC machined by Henry Justiniano, CEO of Sadie Mae Manufacturing. A 1/4” TiCN long-reach reduced-shank end mill is used to create the nozzle holes.

End Caps: A 3/16” end mill cuts the chamber and gasket slot in each cap.

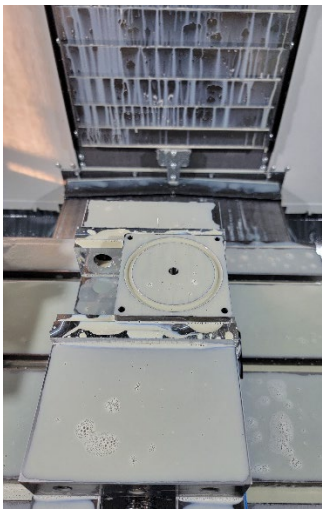

4.2.5. Manual Milling

The end caps are tapped for the baffle plate and NPT fittings.

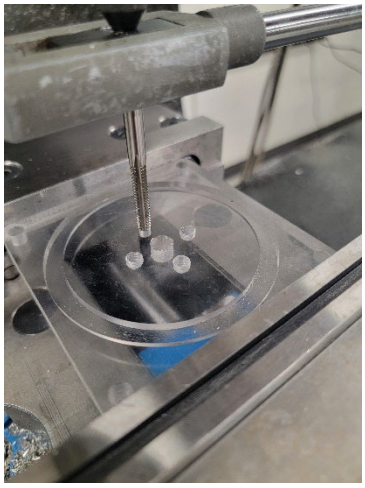

4.2.6. 3D Printing

The liquid nozzle inserts are 3D printed to achieve the feature desired for the system.

5. TESTING

This project requires multiple phases of testing:

Before fabrication could occur, materials had to be chosen for use in the VPS system. However, no research data was found regarding how these materials would interact with IL. To ensure that the VPS components could withstand the corrosive effects of the IL, a material compatibility test is designed and performed on materials chosen for the VPS components.

To acquire unknown thermodynamic properties that characterize the IL desiccant, an additional preliminary test is designed, fabricated, and performed.

Because the theoretical calculations did not reflect the infill levels and flow rates necessary for the VPS to operate without carry-under during real-world testing, the infill levels, and liquid and air flow rates are obtained through experimentation to achieve consistent flow that distributes fluid evenly on both sides of the system, as well as vortices on both sides which avoid carry-over and carry-under. Vortex formation requires proper pump voltage application and leak prevention. Thus, the prototype is also tested for leaks. To preserve the IL during leak and vortex testing, water is used for the prototype.

5.1. Testing Plan

5.1.1. Testing Plan for Liquid Nozzle Inserts - material compatibility

A puck submersion test is designed to determine the corrosion resistance of the liquid nozzle inserts against the liquid desiccants used. The liquid nozzle is made with a 3D-printed insert due to the feature geometry of the liquid inlet. This insert is epoxy-coated and housed inside the liquid nozzle shell which attaches to the chamber. However, because the desiccant is highly corrosive, highly corrosion-resistant 3D-printing filament and epoxy resin are used. To find the best material to use for the liquid nozzle inserts, the toughest polymer filaments available are tested, with and without the epoxy coating. These include Nylon 12 CF and Ultem.

Materials for the experiment:

- A scale
- glass beakers
- Latex Gloves
- Ultem Pucks
- Nylon 12 CF Pucks
- 70% Isopropyl Alcohol
- 75% KCOOH Solution
- [EMiM][EtSO4]
- Tweezers

Setup: 8 pucks are printed for experimentation – 4 Nylon 12 CF and 4 Ultem. 2 of each puck material are coated with epoxy resin and 2 of each are left uncoated. The setup is as follows:

Desiccant	Epoxy + Ultem (TotalBoat)	Uncoated Ultem	Epoxy + Nylon 12 CF (JB Weld)	Uncoated Nylon 12 CF
[EMiM][EtSO4] 50mL	Unaffected	Unaffected	Unaffected	Unaffected
KCOOH 50 mL	Unaffected	Unaffected	Unaffected	Unaffected

Table 22: 3D Material and IL Compatability

Step 1: Each puck and SS were cleaned with alcohol and weighed before submersion.



Step 2: The liquid desiccants are poured into the beakers and weighed before submersion.


Step 3: Each puck is added to its respective beaker of desiccant. It is submerged for 1 week or more and reweighed.


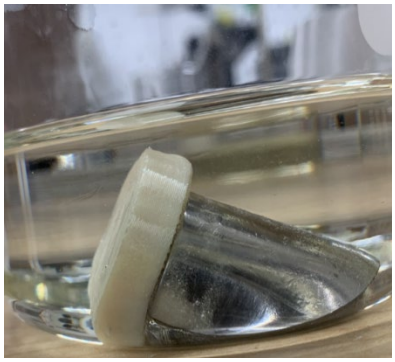


5.1.2. Preliminary Testing Plan

1) The IL is added, and humid air is sent through the sparger into the IL. The absorption capacity is tested first via the relative humidity/pressure readings at the air inlet and outlet. These results are recorded and tabulated to show the change from “dry” to saturated, the mass of water absorbed, and a plot showing % absolute humidity change over time. This test is repeated twice.

2) The IL is then heated to 70°C, and the relative humidity and pressure are read over increments of time. These results are recorded and tabulated to show the mass of water lost and the absolute humidity at exit over time.

5.1.3. Prototype Assembly Testing Plan

LabVIEW and Sensirion ControlCenter are used to log data, and Excel are used to collect the data and present the performance results in tabular format.

1) First set of tests using water – Checking for leaks and sensor reading.

2) Second set of tests using water – Functionality testing, resulting in structural improvements for fluid dynamics and to achieve the vortices inside the chambers.

5.2. Instrumentation and Data Acquisition

The prototype requires acquiring data for temperature, pressure, relative humidity (RH), and air/liquid flowrates. The testing plan involves using hardware, including:

1. 9 thermocouples
2. 5 pressure transducers
3. 3 RH sensors
4. 1 Air flowmeter
5. 2 Liquid flowmeters

The testing plan also uses software, including *LabVIEW* for temperature and pressure data and *Sensirion Control Center* for relative humidity data. For temperature and pressure data, a National Instruments NI cDAQ-9174 is required to transfer readings from thermocouples and pressure transducers to a computer for LabVIEW. *National Instruments NI Device Monitor* software is required to connect/identify *National Instruments NI cDAQ-9174* to *LabVIEW.* A *Sensirion SEK-SensorBridge* is required to transfer readings from relative humidity sensors to a computer for *Sensirion Control Center.* A full sensor schematic is shown to characterize the location of each sensor, and how each connects to the modules which connect them to the data acquisition software.

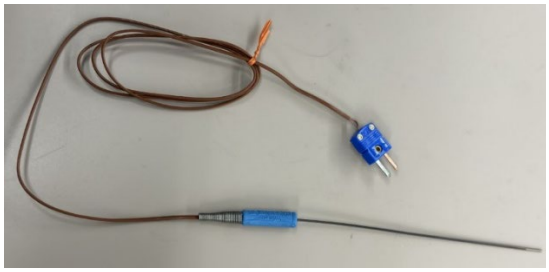

From left to right: OMEGA T-type Thermocouple, OMEGA Pressure Transducer, NI cDAQ-9174, with thermocouple and pressure modules.

From left to right: Sensirion RH sensor, Sensirion SEK-SensorBridge

A full sensor schematic is shown to characterize the location of each sensor, and how each connects to the modules which connect them to the data acquisition software.

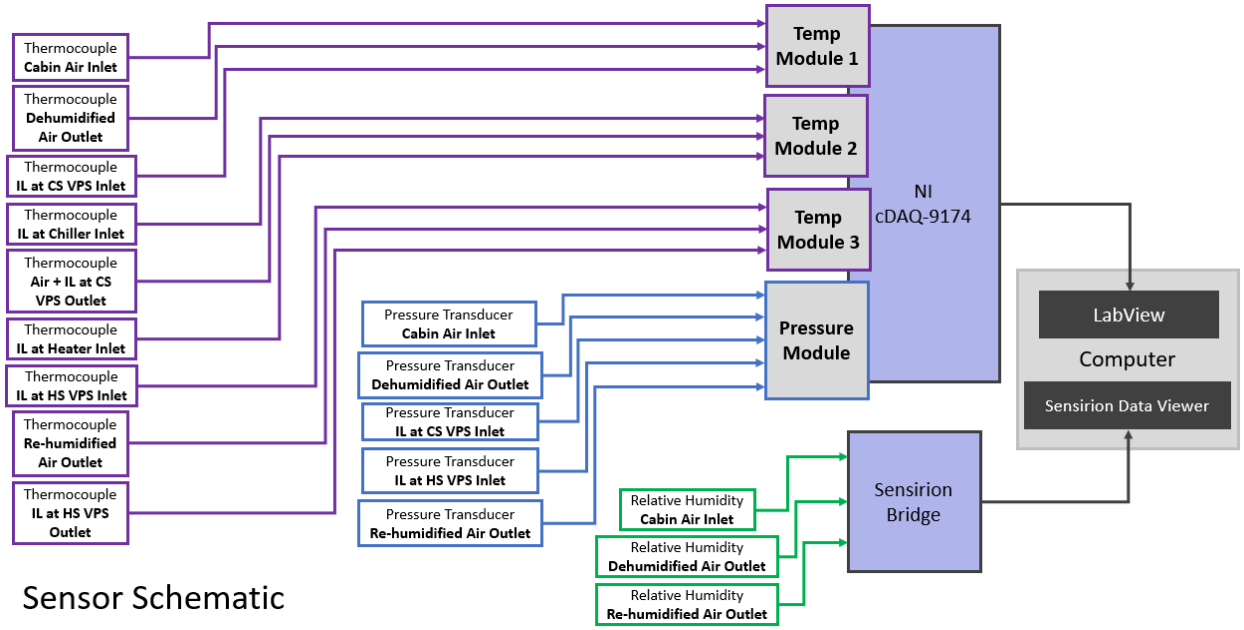

Figure 32: Sensor Schematic

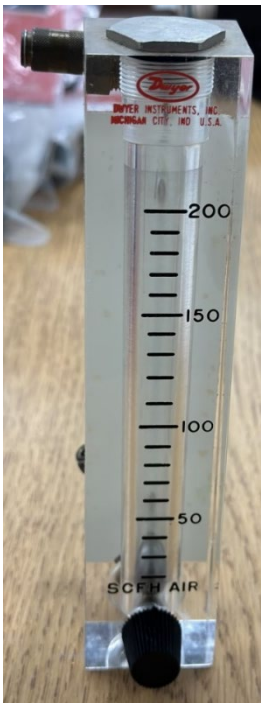

The system's incoming airflow is monitored manually via an air flowmeter (left), and the liquid fluid flow is monitored at each VPS chamber outlet using a liquid flowmeter (right).

A preliminary test was performed to test the functionality of pressure transducers. Testing instruments involved with this test include an Omega Pressure Transducer, Mastech DC Power Supply, Fluke Voltmeter, and Fluke Pressure Gauge. A DC power supply provides voltage to the pressure transducer that's connected to a pressure gauge which excites it by sending air from the hand-operated pressure pump. Instead of a psi value, the pressure transducer gives a voltage reading, so a voltmeter will be used to display the data. When the values displayed on the voltmeter increase simultaneously while the pump is being pressed, the pressure transducers are considered appropriate for use. The voltage data gathered from the pressure transducers will be converted to psi using the provided calibration instructions from OMEGA.

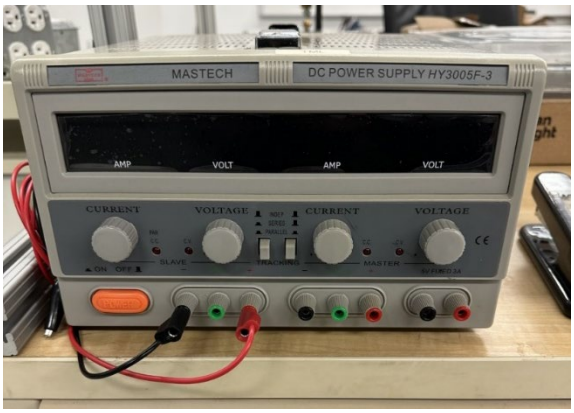


Left to Right: Mastech DC Power Supply, Fluke Voltmeter, Fluke Pressure Gauge/Pump.

Preliminary Pressure Transducer Testing Setup

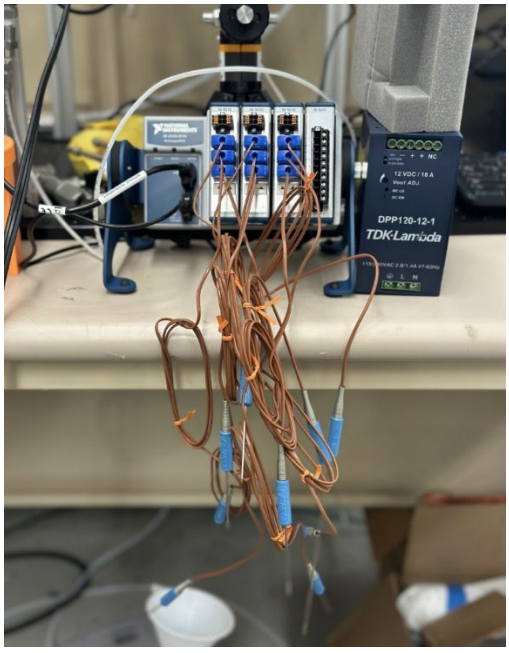

1. DAQ Preliminary Setup

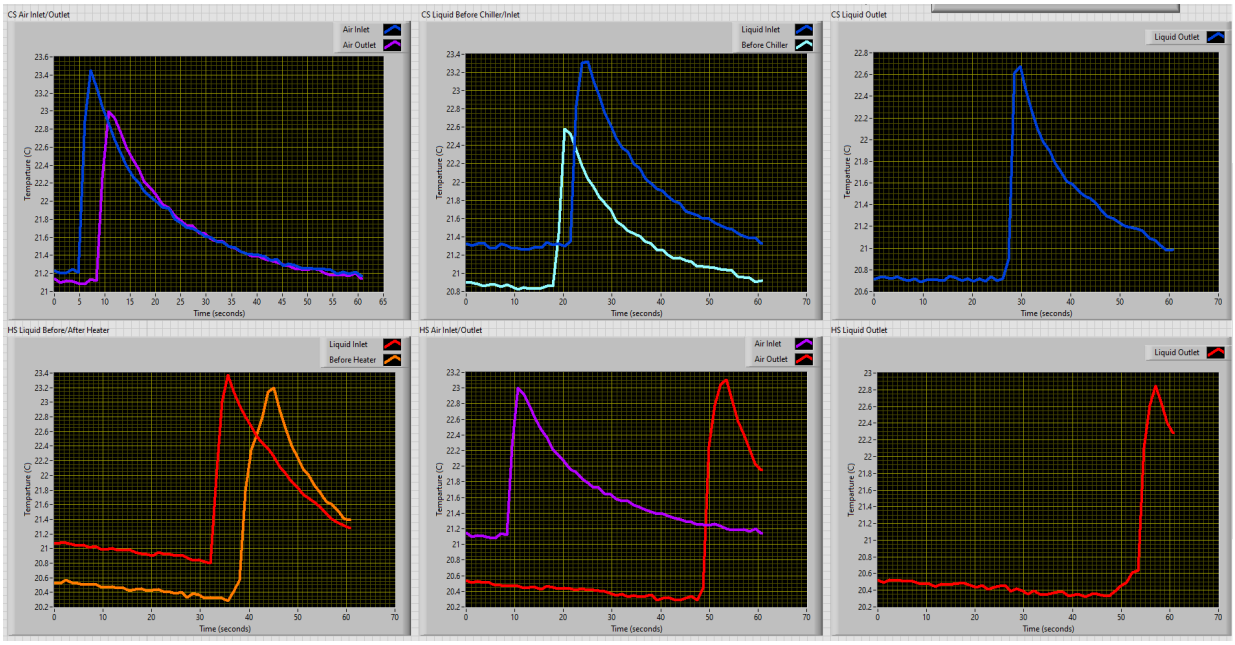

2. LabVIEW Prototype Temperature Graphs – Preliminary Testing

This diagram displays six graphs containing ten lines that represent nine separate thermocouples (violet lines share reading from a single thermocouple). The graphs are plotting temperature (°C) vs time (s).

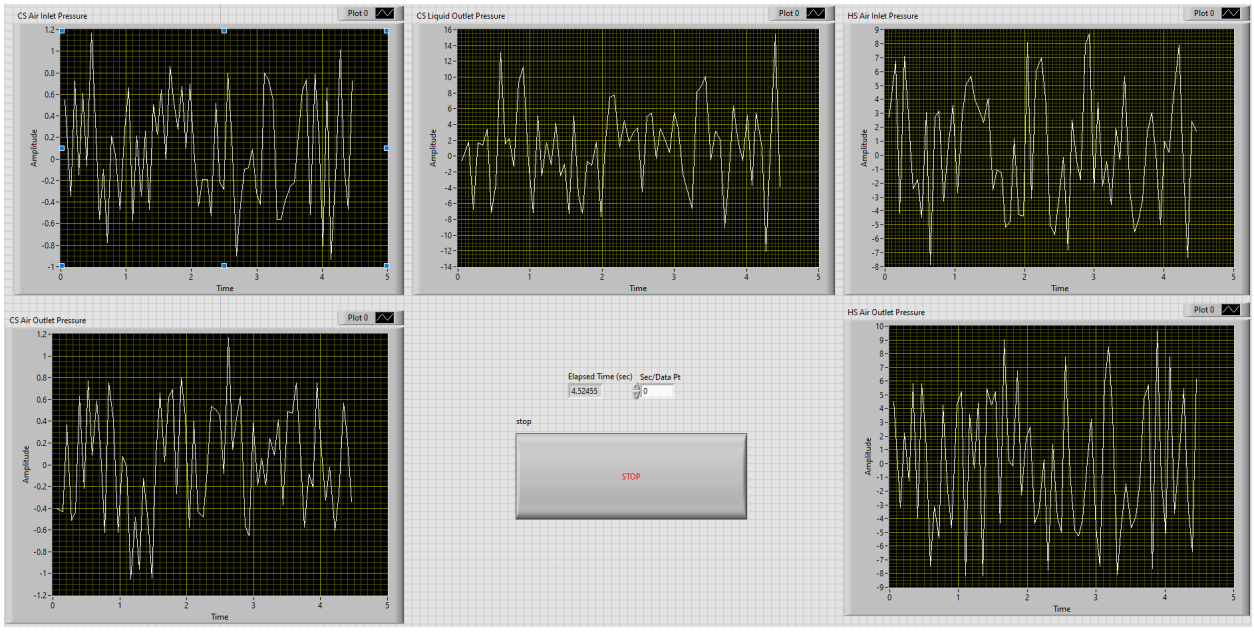

3. LabVIEW Prototype Pressure Graphs – Preliminary Testing

This diagram displays five graphs/lines that represent five individual pressure transducer data. The graphs are plotting amplitude (psi) and time (s).

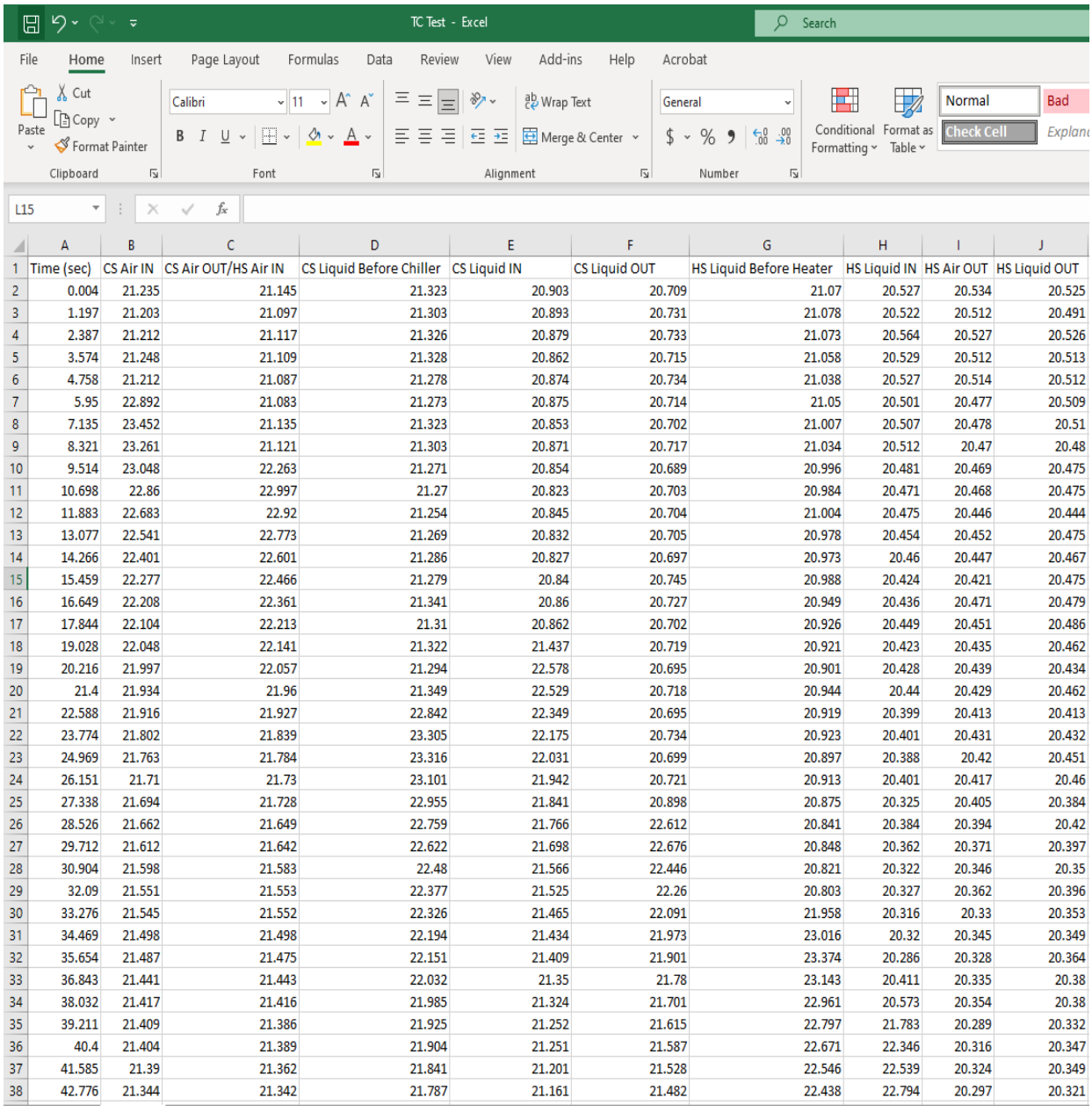

	A	B	C	D	E	F	G	H	I	J
1	Time (sec)	CS Air IN	CS Air OUT/HS Air IN	CS Liquid Before Chiller	CS Liquid IN	CS Liquid OUT	HS Liquid Before Heater	HS Liquid IN	HS Air OUT	HS Liquid OUT
2	0.004	21.235	21.145	21.323	20.903	20.709	21.07	20.527	20.534	20.525
3	1.197	21.203	21.097	21.303	20.893	20.731	21.078	20.522	20.512	20.491
4	2.387	21.212	21.117	21.326	20.879	20.733	21.073	20.564	20.527	20.526
5	3.574	21.248	21.109	21.328	20.862	20.715	21.058	20.529	20.512	20.513
6	4.758	21.212	21.087	21.278	20.874	20.734	21.038	20.527	20.514	20.512
7	5.95	22.892	21.083	21.273	20.875	20.714	21.05	20.501	20.477	20.509
8	7.135	23.452	21.135	21.323	20.853	20.702	21.007	20.507	20.478	20.51
9	8.321	23.261	21.121	21.303	20.871	20.717	21.034	20.512	20.47	20.48
10	9.514	23.048	22.263	21.271	20.854	20.689	20.996	20.481	20.469	20.475
11	10.698	22.86	22.997	21.27	20.823	20.703	20.984	20.471	20.468	20.475
12	11.883	22.683	22.92	21.254	20.845	20.704	21.004	20.475	20.446	20.444
13	13.077	22.541	22.773	21.269	20.832	20.705	20.978	20.454	20.452	20.475
14	14.266	22.401	22.601	21.286	20.827	20.697	20.973	20.46	20.447	20.467
15	15.459	22.277	22.466	21.279	20.84	20.745	20.988	20.424	20.421	20.475
16	16.649	22.208	22.361	21.341	20.86	20.727	20.949	20.436	20.471	20.479
17	17.844	22.104	22.213	21.31	20.862	20.702	20.926	20.449	20.451	20.486
18	19.028	22.048	22.141	21.322	21.437	20.719	20.921	20.423	20.435	20.462
19	20.216	21.997	22.057	21.294	22.578	20.695	20.901	20.428	20.439	20.434
20	21.4	21.934	21.96	21.349	22.529	20.718	20.944	20.44	20.429	20.462
21	22.588	21.916	21.927	22.842	22.349	20.695	20.919	20.399	20.413	20.413
22	23.774	21.802	21.839	23.305	22.175	20.734	20.923	20.401	20.431	20.432
23	24.969	21.763	21.784	23.316	22.031	20.699	20.897	20.388	20.42	20.451
24	26.151	21.71	21.73	23.101	21.942	20.721	20.913	20.401	20.417	20.46
25	27.338	21.694	21.728	22.955	21.841	20.898	20.875	20.325	20.405	20.384
26	28.526	21.662	21.649	22.759	21.766	22.612	20.841	20.384	20.394	20.42
27	29.712	21.612	21.642	22.622	21.698	22.676	20.848	20.362	20.371	20.397
28	30.904	21.598	21.583	22.48	21.566	22.446	20.821	20.322	20.346	20.35
29	32.09	21.551	21.553	22.377	21.525	22.26	20.803	20.327	20.362	20.396
30	33.276	21.545	21.552	22.326	21.465	22.091	21.958	20.316	20.33	20.353
31	34.469	21.498	21.498	22.194	21.434	21.973	23.016	20.32	20.345	20.349
32	35.654	21.487	21.475	22.151	21.409	21.901	23.374	20.286	20.328	20.364
33	36.843	21.441	21.443	22.032	21.35	21.78	23.143	20.411	20.335	20.38
34	38.032	21.417	21.416	21.985	21.324	21.701	22.961	20.573	20.354	20.38
35	39.211	21.409	21.386	21.925	21.252	21.615	22.797	21.783	20.289	20.332
36	40.4	21.404	21.389	21.904	21.251	21.587	22.671	22.346	20.316	20.347
37	41.585	21.39	21.362	21.841	21.201	21.528	22.546	22.539	20.324	20.349
38	42.776	21.344	21.342	21.787	21.161	21.482	22.438	22.794	20.297	20.321

Table 23: Exported EXCEL File from LabVIEW Program

4. LabVIEW Prototype Excel Data Acquisition – Preliminary Testing

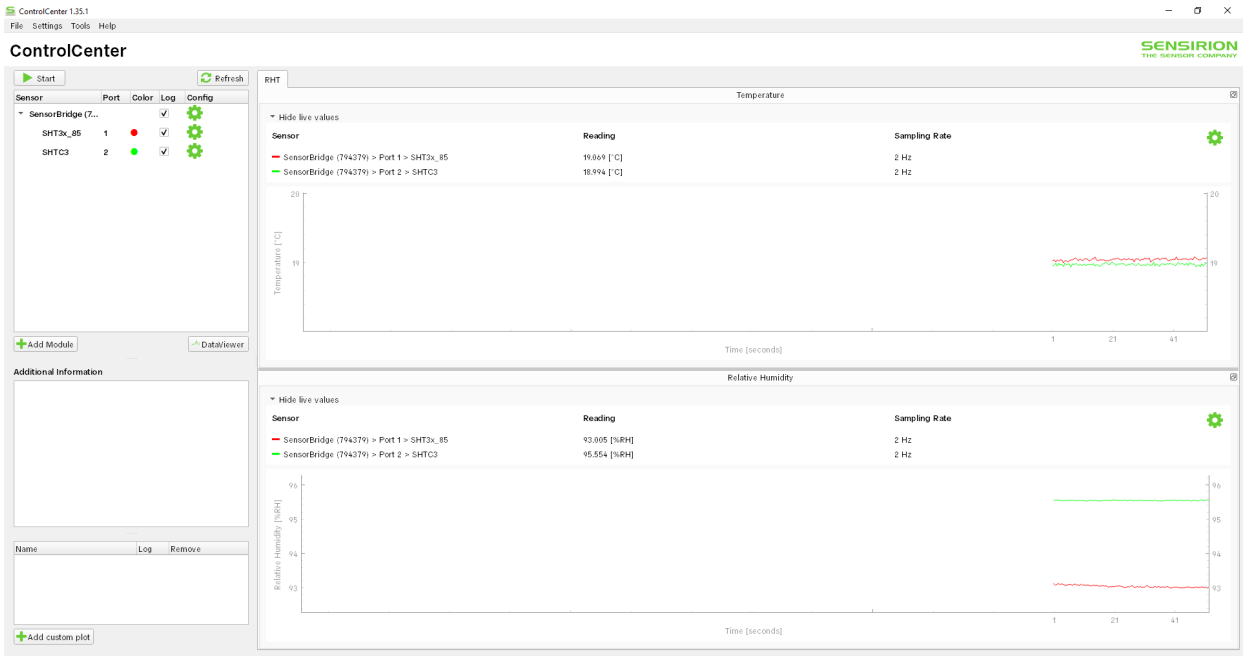

5. Sensirion ControlCenter

The window displays two graphs of data from two relative humidity sensors. The top graph displays temperature (°C) vs time (s) and the bottom graph displays relative humidity (%RH) vs time (s).

6. Sensirion DataViewer

This window displays the same data from Sensirion ControlCenter, except that these graphs are a more detailed view.

5.3. Results

The results of leak and functionality testing using distilled water indicated that, to avoid significant carry-under, the VPS chambers each require much more infill volume than was found in theoretical calculations. The flow rate was also significantly increased to achieve flow results characterizing a vortex in each chamber.

Because the regenerating temperature for IL is at least 30°C higher than initially predicted, the heating method was improved from a rope heater to a heat tank powered by the MINCO cartridge heating system. This increased the fluid volume by an additional 200mL. This caused the re-humidifying (HS) chamber to fill and empty periodically as the fluid would have to refill the chamber periodically before flowing into the liquid inlet nozzle. Thus, an additional pump was added after the heat tank, and the heat tank was raised to encourage the fluid to flow down into the HS chamber. Further methods will be strategically implemented and tested to improve the system's fluid flow conditions, including:

1. Trying different charge-up sequences to decrease time needed during charge-up to achieve synchronicity.

2. Running the pumps in series and/ or increasing pump size

5.3.1. Final Results of Material Compatibility Testing

The results are tabulated below:

Nylon 12 CF no Epoxy in [EMIM EtSO4]: Test Began 02/17/2023 at 4:17 p.m.		1	2	3
Puck Geometry	mass (g)	3.7000	3.7000	3.7000
	diameter (in)	1.0015	0.999	0.9945
	thickness (in)	0.2525	0.2530	0.2530
Nylon 12 CF removed from [EMIM EtSO4]: 02/28/2023 at 6:00 p.m.				
Puck Geometry	Mass (g)	3.7000	3.7000	3.7500
	diameter (in)	.9995	1.0000	.9990
	thickness(in)	.2550	.2520	.2530

Table 24: Nylon 12 CF Vs [EMIM] [EtSO4] Compatability Test

After about 11 days of the Nylon 12 CF being submerged in [EMIM EtS04] it did not show any physical change in diameter, thickness nor weight. The small fluctuation that can be seen in the results is due to the pucks not being perfectly printed, as they will have some rough edges from separation of the 3D printer.

Nylon 12 CF no Epoxy in KCOOH: Test Began 02/17/2023 at 4:17 p.m.		1	2	3
Puck Geometry	mass (g)	3.7000	3.7000	3.6500
	diameter (in)	0.9985	0.9975	0.9900
	thickness (in)	0.2575	0.2600	0.2605
Nylon 12 CF removed from KCOOH: 05/05/2023				
Puck Geometry	mass (g)	3.690	3.6800	3.6800
	diameter (in)	0.9945	0.9980	0.9995
	thickness (in)	0.2580	0.2580	0.2580

Table 25: Nylon 12 CF Vs KCOOH Compatability Test

The nylon 12 CF was left submerged in 75% Aq sol. of KCOOH for over 2 months and did not show significant change in weight, thickness, or diameter. This data supports the idea of Nylon 12 carbon fiber being compatible with KCOOH and [EMIM EtS04].

Ultem No Epoxy in [EMIM] [EtSO4]: Test began 03/21/2023 4:24 p.m.		1	2	3
Puck Geometry	Mass (g)	3.9000	3.9500	3.9500
	Diameter (in)	0.9895	0.985	0.9905
	Thickness (in)	0.2675	0.2765	0.2720
Removed from IL: 4/07/2023				
Puck Geometry	Mass (g)	4.0000	3.900	4.0000
	Diameter(in)	0.9930	0.9875	0.9914
	Thickness (in)	0.2720	0.2675	0.2660

Table 26: Ultem No Epoxy Vs [EMIM] [EtSO4]

Ultem No Epoxy in KCOOH: Test began 02/20/2023		1	2	3
Puck Geometry	Mass (g)	3.9000	4.0000	4.0000
	Diameter (in)	0.9903	0.9890	0.9900
	Thickness (in)	0.2697	0.2683	0.2748
Removed from KCOOH: 03/01/2023				
Puck Geometry	Mass (g)	4.0000	3.9000	4.0000
	Diameter(in)	0.9895	0.9908	0.9873
	Thickness (in)	0.2758	0.2762	0.2653

Table 27: Ultem No Eposy Vs KCOOH

The Ultem 9085 pucks also did not change in weight, diameter, and thickness after being submerged in the IL for a long period of time. The small fluctuations are made from the puck not being perfectly made and from not having a smooth surface. The reason for choosing Ultem 9085 is since it can withstand high temperatures. Ultem 9085 will be right for our nozzles because the IL jetting out of it will regenerate at high temperatures.

The Ultem puck was bonded and sealed with stainless steel (SS) using TotalBoat Resin. Nylon 12 CF was coated and bonded using JB weld. The epoxies were left for 24 hours to cure/ hardened. Then the bonded piece was submerged in the desiccant for a period of time. When removed from the desiccant, the bonded pieces were weighed to identify deterioration and pulled on to ensure bonding wasn't weakened. Results are shown below:

		Ultem with SS and Epoxy (Total Boat)	Nylon 12 CF (JB Weld)
April 8, 2023	m(g)	57	57.18
April 15, 2023	m(g)	57.25	57.19
May 3,2023	m(g)	57.1	57.15

Table 28: Weight of 3D Print with Epoxy or JB Weld

5.3.1 Final Results of Preliminary Experiments

The data from this experiment was collected over time using the handheld RH/temp sensors and LabView. The results were output into Excel spreadsheet.

Initial conditions are tabulated below.

Initial Condition	**Unit**	**Value**
Initial Charge Level	mL	166.5
Average Relative Humidity of Air at Inlet	%	89.8
Average Temperature of Air at Inlet	^{o}C	17.98
Average Temperature of IL at Inlet	^{o}C	17.98
Average Pressure of Air at Inlet	psia	20.6
Flow Rate of Air at Inlet	LPM	11.22

Table 29: Preliminary Experimment Initial Conditions

For water-absorption capacity: Humid air from a humidity tank enters the desiccant through a sparger at the bottom air inlet, which disperses the air into the desiccant inside the chamber. Here, the humidity of the incoming air is recorded over time while the desiccant absorbs the moisture from the incoming air. Once the absolute humidity of air at the inlet and outlet approaches indicating the IL is getting saturated, the chamber is weighed.

Absorption capacity of IL is characterized by the % change in absolute humidity of air:

% Change = (Air Inlet Abs. Humidity – Air Outlet Abs. Humidity) / Air Inlet Abs. Humidity

The data from this experiment with [EMIM][EtSO4] are collected over time using the handheld RH/temp sensors and LabView. The results are tabulated and presented in Table 30. Water absorption capacity of [EMIM][EtSO4] over time is also shown in Figure 30.

Time (Hr)	Inlet RH (%)	Inlet temperature (C)	Inlet pressure (psia)	Outlet RH (%)	Outlet temperature (C)	Outlet pressure (psia)	Inlet absolute humidity (kg/m3)	Outlet absolute humidity (kg/m3)	% change
0	91.00	18.63	20.60	13.72	20.03	14.78	0.01408	0.00243	82.75
0.5	92.20	18.38	20.60	10.78	21.04	14.78	0.01456	0.00203	86.10
1	93.52	18.09	20.60	13.42	21.85	14.78	0.01488	0.00251	83.16
1.5	87.25	18.18	20.60	15.75	22.10	14.78	0.01449	0.00313	78.40
2	87.92	18.35	20.60	18.31	21.72	14.78	0.01371	0.00345	74.87
2.5	88.42	18.46	20.60	20.04	22.19	14.78	0.01394	0.00393	71.79
3	89.55	18.50	20.60	21.47	21.46	14.78	0.01398	0.00396	71.67
3.5	90.85	18.36	20.60	22.96	21.08	14.78	0.01386	0.00424	69.39
4	91.65	18.60	20.60	24.28	21.48	14.78	0.01406	0.00453	67.77
4.5	91.89	18.79	20.60	25.79	21.23	14.78	0.01422	0.00484	65.97
5	92.55	18.71	20.60	27.29	21.50	14.78	0.01415	0.00510	63.94
5.5	92.87	18.45	20.60	29.11	21.29	14.78	0.01394	0.00542	61.14
6	93.15	18.51	20.60	30.50	21.29	14.78	0.01399	0.00579	58.62
6.5	93.61	18.21	20.60	33.40	22.12	14.78	0.01468	0.00647	55.94
7	92.90	17.93	20.60	35.27	22.03	14.78	0.01428	0.00682	52.24
7.5	91.50	17.76	20.60	36.60	22.01	14.78	0.01379	0.00720	47.77
8	93.07	17.46	20.60	37.37	22.12	14.78	0.01388	0.00725	47.77
8.5	92.57	17.81	20.60	37.88	22.01	14.78	0.01417	0.00761	46.32
9	91.32	16.82	20.60	38.90	22.12	14.78	0.01308	0.00764	41.57
9.5	91.44	16.74	20.60	39.62	22.12	14.78	0.01302	0.00784	39.79
10	91.87	16.75	20.60	40.06	22.12	14.78	0.01316	0.00784	40.45
10.5	91.87	17.29	20.60	40.57	22.12	14.78	0.01360	0.00803	40.91
11	91.87	16.12	20.60	41.14	18.82	14.78	0.01268	0.00753	40.62
11.5	88.05	16.56	20.60	41.52	21.00	14.78	0.01245	0.00771	38.04
12	92.00	16.13	20.60	41.78	21.51	14.78	0.01268	0.00794	37.40
12.5	88.04	17.25	20.60	41.21	21.55	14.78	0.01298	0.00816	37.15
13	93.01	17.25	20.60	41.83	21.25	14.78	0.01371	0.00841	38.68
13.5	93.22	18.11	20.60	42.73	21.52	14.78	0.01429	0.00861	39.76
14	93.51	18.10	20.60	43.02	21.55	14.78	0.01457	0.00914	37.31

Table 30: Absorption Capacity for [EMIM][EtSO4]

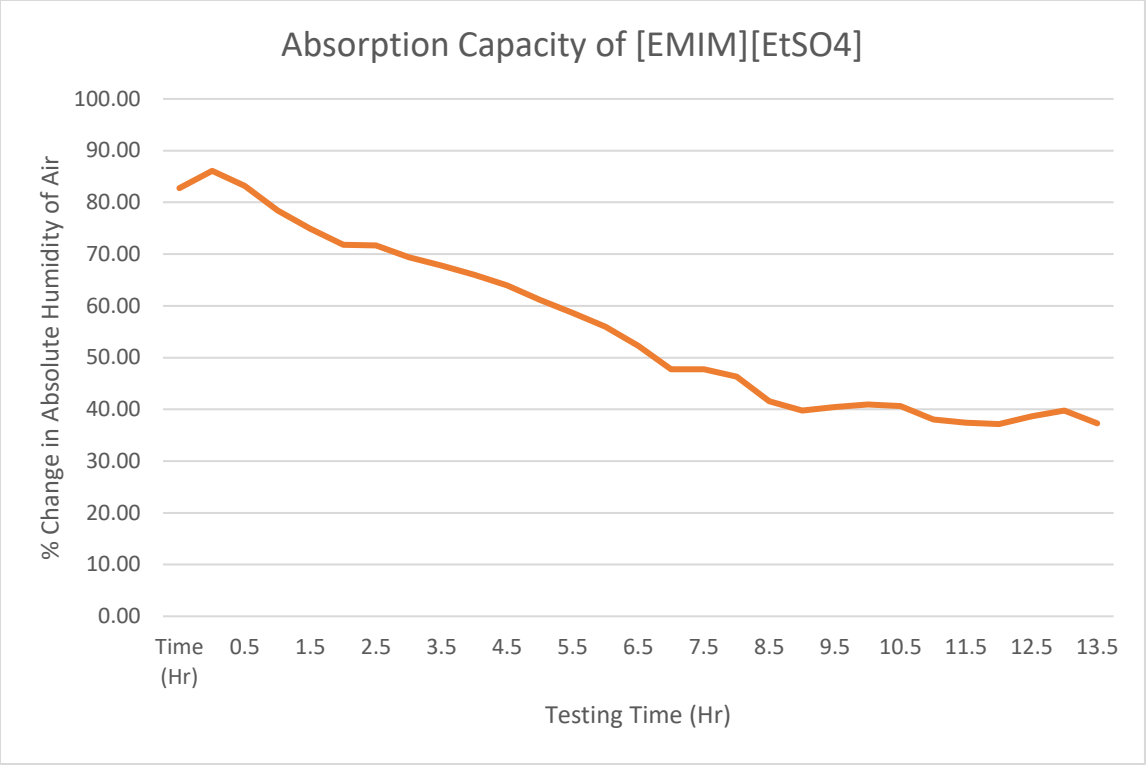

Figure 33: [EMIM][EtSO4] Water Absorption Capacity

As the IL absorbs more water and saturates, its ability to absorb more water declines over time. Such decrease in water absorption over 14-hour testing time is clearly illustrated in Figure 30. The data suggests that full saturation of the tested amount of IL will take much longer than 14 hours.

At room temperature, with an air flow rate of 11.22 LPM, KCOOH provided only 17% change in absolute humidity at the start of testing, and dropped after the first 4 minutes. This indicates that KCOOH is a significantly less capable desiccant than [EMIM][EtSO4], and thus, the KCOOH has been ruled out as a reasonable liquid desiccant making [EMIM][EtSO4] the preferred regenerable liquid desiccant for high-efficiency humidity control for this VPS system.

<u>For the ideal temperature for full regeneration:</u> The partially-saturated liquid desiccant from the earlier test is heated until a stable temperature reading of 70°C is met. Then, the top valve is opened, and relative humidity and pressure data are recorded at the inlet and outlet every minute up to 1 hour period. Then, the chamber is weighed again. The results are tabulated below in Table 31. Regenerability of [EMIM][EtSO4], characterized by the absolute humidity of air at the outlet of test chamber, is plotted in Figure 32.

Time (sec)	Time (Hr)	Outlet humidity (%)	Outlet temperature (C)	Outlet pressure (psia)	Outlet absolute humidity (kg/m3)
1860	0.516667	55.924	30.178	14.748	0.017192
1920	0.533333	55.716	30.176	14.748	0.01719
1980	0.55	55.491	30.277	14.748	0.016975
2040	0.566667	55.207	30.202	14.748	0.016906
2100	0.583333	55.108	30.346	14.748	0.017038
2160	0.6	54.7713	30.22	14.748	0.016923
2220	0.616667	54.369	30.127	14.748	0.016857
2280	0.633333	54.65	30.148	14.748	0.016857
2340	0.65	54.246	30.14	14.748	0.016544
2400	0.666667	54.003	29.961	14.748	0.016384
2460	0.683333	53.381	30.226	14.748	0.016313
2520	0.7	53.315	30.22	14.748	0.016308
2580	0.716667	53.275	30.119	14.748	0.016219
2640	0.733333	52.826	30.127	14.748	0.016226
2700	0.75	52.615	30.191	14.748	0.016282
2760	0.766667	52.029	30.172	14.748	0.015958
2820	0.783333	52.134	29.919	14.748	0.015733
2880	0.8	51.806	29.98	14.748	0.015794
2940	0.816667	51.846	29.924	14.748	0.015746
3000	0.833333	51.55	30.039	14.748	0.015844
3060	0.85	51.432	30.079	14.748	0.015573
3120	0.866667	51.146	29.994	14.748	0.015568
3180	0.883333	51.224	30.073	14.748	0.015568
3240	0.9	51.085	30.023	14.748	0.015526
3300	0.916667	50.627	30.365	14.748	0.015505
3360	0.933333	50.463	30.202	14.748	0.01537
3420	0.95	50.242	30.154	14.748	0.01533
3480	0.966667	49.763	30.397	14.748	0.015222
3540	0.983333	50.036	30.154	14.748	0.01533
3600	1	49.916	30.162	14.748	0.01503

Time (sec)	Time (Hr)	Outlet humidity (%)	Outlet temperature (C)	Outlet pressure (psia)	Outlet absolute humidity (kg/m3)
0	0.00	59.21	20.80	14.75	0.0107
60	0.02	56.81	21.20	14.75	0.0106
120	0.03	59.36	21.00	14.75	0.0179
180	0.05	59.43	21.04	14.75	0.0180
240	0.07	59.00	26.36	14.75	0.0188
300	0.08	60.55	25.82	14.75	0.0191
360	0.10	61.81	25.82	14.75	0.0197
420	0.12	63.80	26.28	14.75	0.0203
480	0.13	62.79	26.56	14.75	0.0203
540	0.15	62.77	26.50	14.75	0.0197
600	0.17	63.56	26.46	14.75	0.0199
660	0.18	63.16	26.85	14.75	0.0193
720	0.20	62.87	27.18	14.75	0.0193
780	0.22	62.13	27.66	14.75	0.0185
840	0.23	61.91	27.68	14.75	0.0185
900	0.25	61.58	27.87	14.75	0.0188
960	0.27	60.71	28.22	14.75	0.0178
1020	0.28	60.74	28.39	14.75	0.0189
1080	0.30	60.41	28.55	14.75	0.0188
1140	0.32	60.01	28.72	14.75	0.0190
1200	0.33	59.46	29.32	14.75	0.0173
1260	0.35	59.65	29.38	14.75	0.0173
1320	0.37	59.15	29.63	14.75	0.0176
1380	0.38	58.17	29.80	14.75	0.0174
1440	0.40	57.84	29.96	14.75	0.0176
1500	0.42	57.36	30.19	14.75	0.0175
1560	0.43	56.92	30.03	14.75	0.0174
1620	0.45	56.82	30.06	14.75	0.0174
1680	0.47	56.41	30.08	14.75	0.0171
1740	0.48	56.26	30.02	14.75	0.0170
1800	0.50	56.22	30.22	14.75	0.0172

Table 31: Regenerability Data for [EMIM][EtSO4]

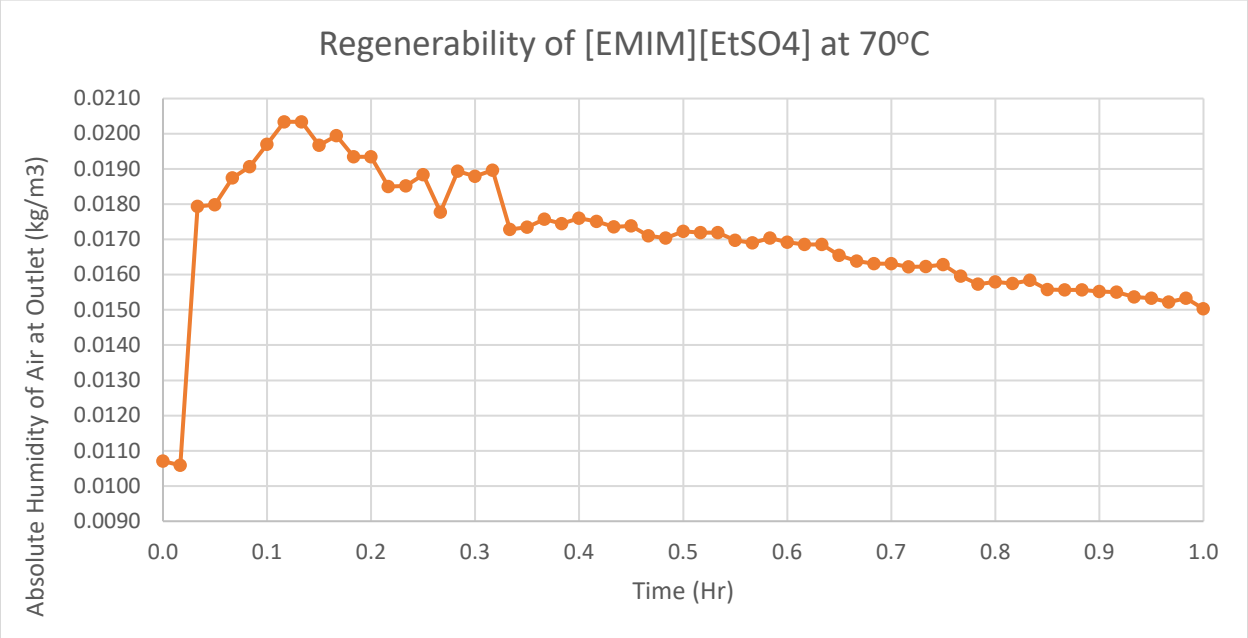

Figure 34: [EMIM][EtSO4] Regenerability at 70°C

The IL released ~57% of its absorbed water over 1 hour. Based on a study by Kiris et al. [34], in which an IL with similar thermodynamic properties was used, IL is regenerable at 70°C, and its regenerability is expected to improve as temperature increases.

After 14 hours of testing, Table 32 summarizes the weight of the chamber before testing, after saturation testing, and again after regeneration testing. The data shows that after 14 hours of water absorption test, the IL holds 6.04 g. After 1 hour of regeneration at 70°C, the IL released 3.43 g of water (56.8%).

Weight of Chamber with Fresh IL (g)	Weight of Chamber with Saturated IL (g)	Weight of Chamber with Regenerated IL (g)
3972.62	3978.66	3975.23

Table 32: Weight of Chamber at Varrying Stages of the Experiment

Because the [EMIM][EtSO4] had to be heated to 70°C to begin regenerating, the heating method was changed to regenerate the IL faster in the VPS system.

5.3.2 Final Assembly Iterations

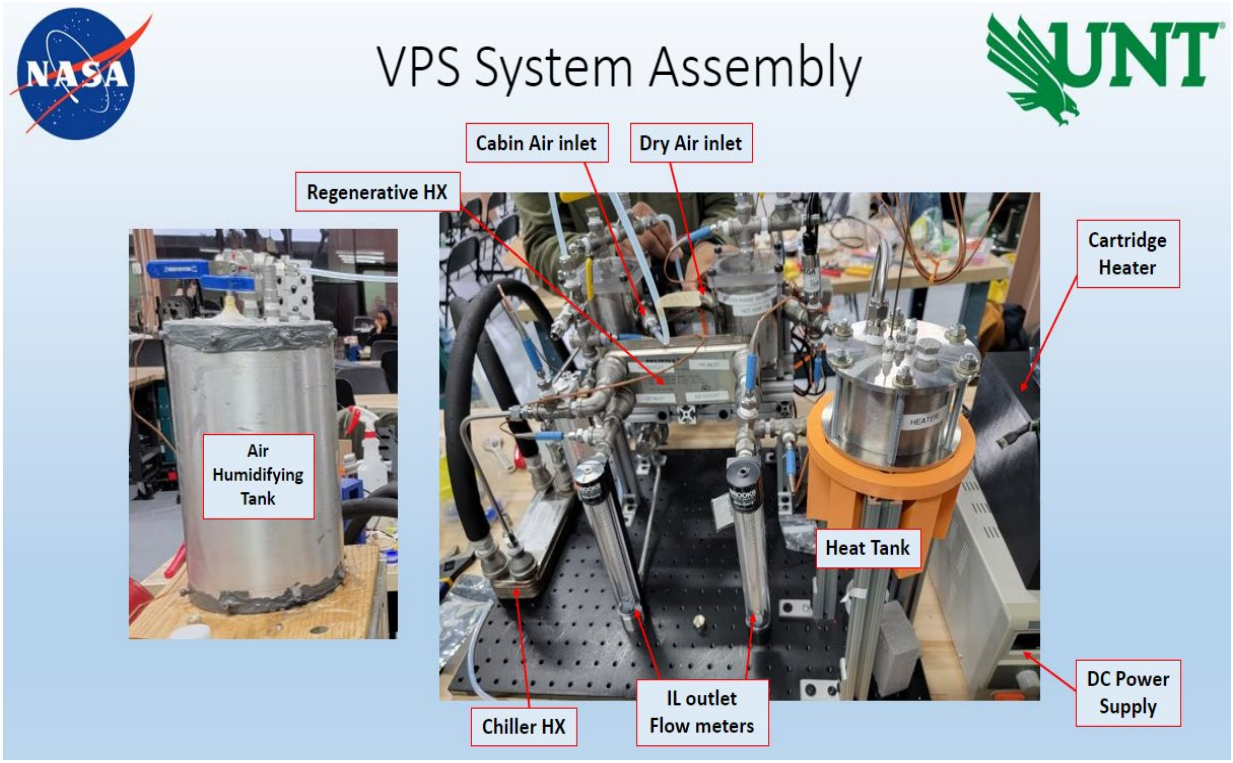

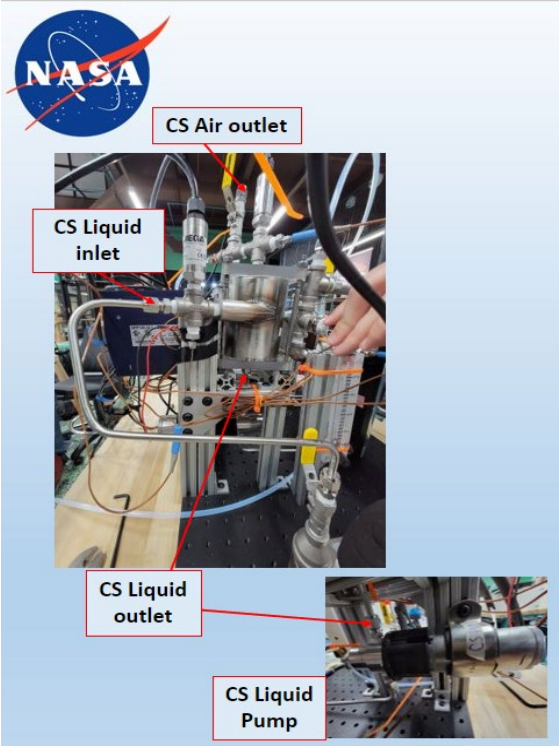

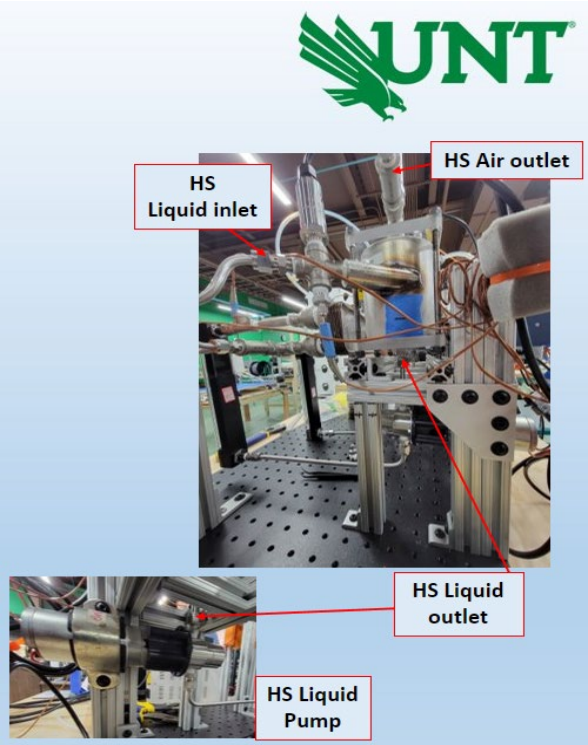

NI DAQ System:

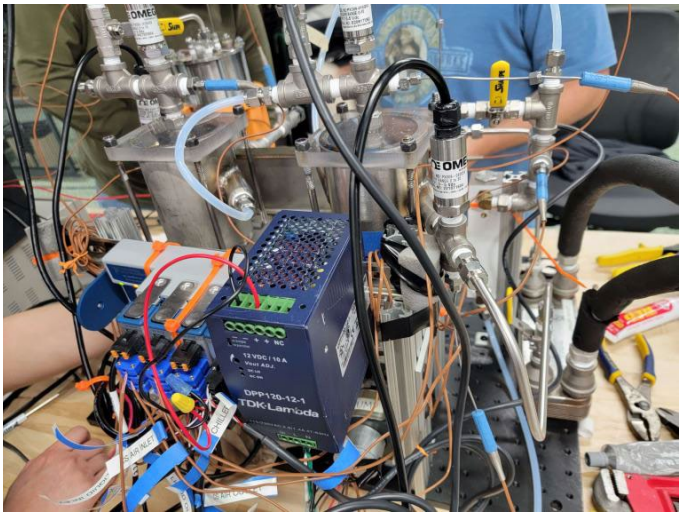

The regenerative heat exchanger was moved to a higher point on the system and needle valves were added to make the heat exchanger drainable. The heat tank was also lowered to allow for better flow into the top of the tank, solving a previous drainage issue. Furthermore, to allow for higher flow rates to reach the threshold of acquiring vortices, the 12V pumps were replaced with 24V pumps of the same type and brand, which required higher-range flowmeters:

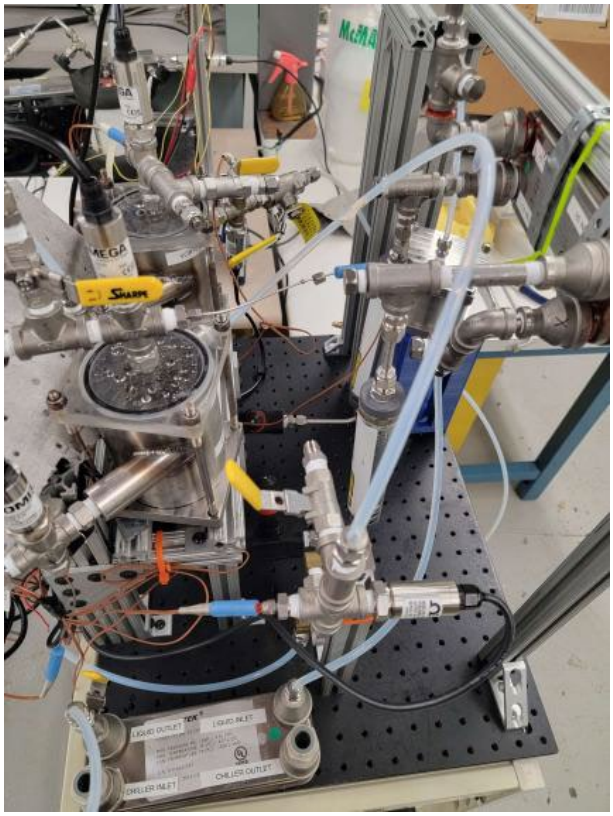

5.3.3 Final Prototype Operating Parameters Testing: Water

With water, the following testing results are shown for vortex formation.

At 200mL fill level in each VPS, 12V Pumps – No heat tank in system					
Air Flow (SCFH)	HS Pump (V)	CS Pump (V)	Avg. Flow Rate (LPM)	Consistent Fill Levels?	Results inside VPS
0	9.7	12	3.388	Y	Slight Rotation
0	12	14	4.487	N	No vortex
0	13.7	16	4.966	N	Slight Rotation
At 200mL fill level in each VPS, 24V Pumps – No heat tank in system					
Air Flow (SCFH)	HS Pump (V)	CS Pump (V)	Avg. Flow Rate (LPM)	Consistent Fill Levels?	Results inside VPS
0	13.7	16	4.966	N	Slight Rotation
At 200mL fill level in each VPS, 24V Pumps – Heat tank included in system					
Air Flow (SCFH)	HS Pump (V)	CS Pump (V)	Avg. Flow Rate (LPM)	Consistent Fill Levels?	Results inside VPS
70	17.5	18	5.925	Y	Significant Rotation, no vortices
50	18.85	19	6.244	Y	Vortices visible, but carry-under
At 350mL fill level in each VPS, 24V Pumps – Heat tank included in system					
Air Flow (SCFH)	HS Pump (V)	CS Pump (V)	Avg. Flow Rate (LPM)	Consistent Fill Levels?	Results inside VPS
25	19	18	6.244	Y	Vortices, no carry-under/over
25	18.53	19.7	6.404	N	CS Vortex only
40	19.7	19.2	6.564	Y	Vortices, no carry-under/over

Table 33: Tests performed on the VPS assembly to find optimal functionality for vortices – Water only

Thus, for successful vortices with water, the following parameters were found:

At 350mL fill level in each VPS, 24V Pumps					
Air Flow (SCFH)	HS Pump (V)	CS Pump (V)	Flow rate (LPM)	Tubing ID (in)	Flow velocity (m/s)
25	19	18	6.244	0.18	6.344
40	19.7	19.2	6.564	0.18	6.668

Table 34: Parameters for optimal operation to achieve vortices with water

For IL, the differences in viscosity and density as a function of temperature at the HS and CS VPS would likely require recalibration of the pumps to achieve the functional flowrates shown in table.

Volume Breakdown of the Assembly – Water

Locations of Volumes	Min. Vol. (mL)	Max. Vol. (mL)	Approx. Vol. (mL)
Total Volume drained	950	1050	1000
Inside CS VPS	350	350	350
Inside HS VPS	350	350	350
Inside Regenerative Heat Exchanger	256	256	256
Inside Cooling Heat Exchanger	128	128	128
Inside the Heat Tank	200	200	200
In Tubing, Pumps, Valves, and Fittings	334	234	284

Table 35: Volume Breakdown in System

5.4. Conclusions

The VPS assembly is fully prepared for IL testing. The system is leakproof, and the parameter testing showed that consistent vortices can be formed with water at the conditions listed in Table 34. When transitioning to IL, minor adjustments to the pump flow rates can be made to maintain consistent vortices and fill levels in both VPS chambers. The volume of the system is calculated, measured, and established.

The assembly is also modular – with standard fittings sizes, removable end caps, transparent end cap options, and a fully corrosion-resistant set-up made of 316 Stainless Steel and Ultem, a multitude of adjustments can be made to allow for parametric testing with [EMIM][EtSO4] and any other liquid desiccants viable for humidity absorption testing.

The instrumentation has been tested and validated for accurate readings, and the software programs have been validated to work with the sensors attached to the system.

The main assembly of the system is also small enough to fit on a rolling cart, allowing it to be moved easily. All attachments to the auxiliary systems are easily accessible, with standard, compatible fittings.

5.4.1 Further Developments:

Improvements could be made for the development of future iterations of this system. These are included in the following ways.

1. Acquire bubble testing footage from previous VPS models: these could provide key insights for establishing bubble dynamics in a real-world system, which could therefore improve theoretical calculations based on the experimentally verified bubble behaviors.

2. Assemble and test the system one sub-assembly at a time:

First, fully assemble the dehumidifying (CS) VPS chamber and connect the air inlet to the air compressor, and the CS pump at the liquid outlet back to the liquid inlet nozzle. This setup allows the ideal infill level to be established by increasing the fill level incrementally, and the vortex can be optimized. It also would allow for leaks to be mitigated before the CS VPS is added to the main assembly.

Next, fully assemble the re-humidifying (HS) VPS chamber and connect the air inlet to the air compressor, and the HS pump at the liquid outlet directly to the heat tank, and back to the liquid inlet nozzle. This setup allows the ideal infill level to be established by increasing the fill level incrementally while accounting for the heat tank's volume, and the vortex can be optimized. It also would allow for leaks to be mitigated before the HS VPS is added to the main assembly.

One method of achieving a separate-to-combined modular assembly is by installing fittings which connect the two VPS sections together efficiently.

Once these critical areas are calibrated to function adequately, the remainder of the system can be more readily tested for fluid flow functionality and efficiency.

3. Create more locations for system draining: Install bleed valves downstream of each pump and downstream of each heat exchanger outlet. This would decrease the idle time between tests and fluid replacements and improve system accessibility during testing.

4. Introduce a purge flow while welding the nozzles to the chamber. Purge flow is used to reduce oxidation in a weld. This is especially important when trying to produce a leak proof and corrosion resistant weld. To introduce purge flow, welding gas (most likely Argon) is directed to the backside of the welding area. The gas displaces the oxygen in that area. Oxidation results in a "dirty" weld. The resulting color of the weld looks like soot. Besides the negative aesthetic it also introduces porosity to the weld. This porosity can lead to welding leaks which could lead to major problems down the road.

5. Improve the consistency of the system's flow rate: This is directly correlated to the pump power supplied to the system. The DC power supply used for the pumps was often inconsistent due to the low voltage required and the condition of the power supply module itself, as well as the inconsistent pressure provided by the relatively low-voltage pumps. Improvements could be made to the pumps' power distribution with:

a. A better DC power supply

b. One DC power supply per pump, or

c. Ideally, constant-voltage or constant-pressure pumps connected to a single regulator. This allows for a more consistent voltage supply to the pumps, and thus creates a more reliable liquid flow rate throughout the system.

6. MARKETING PLAN

The VPS Humidity Control Module is designed as prototype and will not yet be sold in the commercial market. The National Aeronautics and Space Administration (NASA) posed the X-Hab challenge, so the team's marketing strategy is to provide NASA with proof-of-concept for high-efficiency regenerable liquid desiccant use in a VPS system for air dehumidification and re-humidification.

6.1. Project Logo

Figure *35*: Project Logo

6.2. Brochure

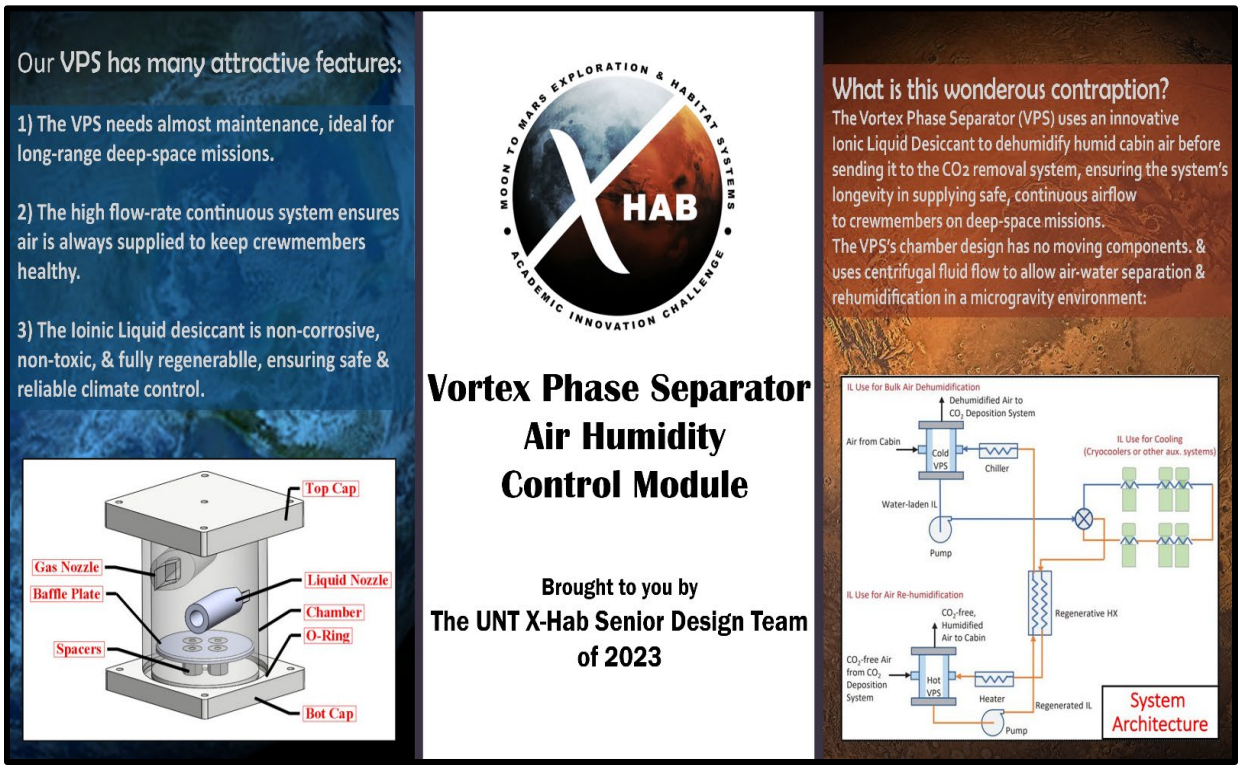

Figure 36: Project Brochure

6.3. Target Market

Because the project was a part of the NASA X-Hab Academic Innovation Challenge, the target customer of the High-Efficiency Humidity Control VPS Subsystem is NASA. The goal of marketing this prototype is to provide the customer with proof-of-concept for the VPS humidity control system and illustrate the effectiveness of desiccant use for air-water separation in microgravity.

6.4. Means of Accessing the Target Market

The team worked in direct contact with NASA representatives to develop the design and find innovative solutions to improve the prototype. The design and development process were presented to NASA's representatives in several milestone meetings, including:

1) System Design Review
2) Preliminary Design Review
3) Critical Design Review
4) Progress Checkpoint Review
5) Project Completion and Evaluation by NASA

7. TEAM PERSONNEL

This team has multiple skills that apply to this project. Thorough calculations, organization, focused and careful manufacturing, teamwork, communication, and leadership are all important to ensure that the team is effective. Below is a list of the responsibilities of each member and their resumé.

7.1. Team Personnel Responsibilities

Gerardo – Team Lead

- Determined material compatibility with desiccant
- Baffle plate calculations
- Researched reference documents for geometry and VPS design
- Determined the piping material
- Created and maintained Gantt Chart
- Helped to write the final report
- Programed and machined gas nozzle
- Made heater calculator for tape heater
- Helped assemble the prototype

Jeffery

- Worked on gas physics calculations and reference documentation
- Learned Ansys and worked on simulating the VPS system
- Slowed down the video footage of the bubble documentation
- Captured good quality video of the bubble footage
- Helped to write the final report
- Worked on LabView
- Helped assembled prototypes
- Helped with IL property experiment and material compatibility experiment

Laura

- Acquired Ionic Liquid properties and select desiccants for testing
- Built an Excel equation sheet
- Created the liquid desiccant selection lab report
- Worked on nozzle calculations reference documentation
- Designed gas nozzle, chamber, and chamber end caps
- Helped to write the final report
- Created a bill of materials
- Created CNC programs
- Fabricated baffle plates, end caps, gas nozzles, and liquid nozzles.
- Helped with assembly/ testing
- Created Excel calculators for testing

Joshua

- Learned Ansys and simulated the VPS system
- Machined baffle spacers
- Will machine the baffle plate
- Will machine the VPS chamber
- Created designs for the heater stand
- Helped with writing the final report

Martin

- Worked on prototype CAD in SolidWorks
- Worked on LabView Programs
- Tested testing instrumentation
- Worked on data acquisition hardware/software
- Worked on prototype assembly
- Helped with IL Properties experiment
- Helped with writing the final report

All team members

- Finished final prototype design in SolidWorks
- Identified necessary components to purchase
- Determined size and accompanying features of VPS
- Applied gathered data to calculations for bubble information
- Will manufacture and assemble 2 VPS systems
- Will complete the final subsystem assembly
- Will perform the testing of the prototype
- Helped with and presented the NASA milestones

7.2. Resumés

APPENDIX A: References

[1] Bostanci, H., Kurwitz, C. (2022.) *M2M X-Hab 2023 Academic Innovation Challenge Proposal, REGENERABLE LIQUID DESICCANTS FOR HIGH-EFFICIENCY HUMIDITY CONTROL IN MICROGRAVITY* .

[2] Sarvadi, A., Bostanci, H., Kurwitz, C., Belancik, G., Jan, D. (2022). *Preliminary Investigation of Microgravity Vortex Phase Separator for Liquid Amine CO2 Removal System," 51st International Conference on Environmental Systems (ICES 2022), Saint Paul, MN, July 10-14, 2022*.

[3] Sarvadi, A. *Dehumidification Using Vortex Phase Separator Technology (Summer 2021 VTE).*

[4] Sarvadi, A. (2022). *Microgravity Vortex Phase Separator for Liquid Amine CO_2 Removal System* (thesis). University of North Texas, Denton.

[5] Williams, D. E. (2007). (rep.). *International Space Station Temperature and Humidity Control Subsystem Verification for Node 1* (N.A., Vol. 1, Ser. N.A, pp. 1–12). Houston, TX: NASA, Lyndon B. Johnson Space Center.

[6] MacCallum, T. K. (2015, March 24). SPACE HUMIDITY CONTROL SYSTEMS

[7] Kurwitz, C. M. (2005). (rep.). Zero Gravity Proven Vortex Gas/Liquid Separator Accumulator (1st ed., Vol. 1, Ser. 1, pp. 1–10). San Diego, CA: Space Nuclear Conference.

[8] Ellis, M., Kurwitz, C., Best, F. (2005). Development of a unique, passive, microgravity vortex separator. Fluids Engineering. https://doi.org/10.1115/imece2005-81616

[9] Hasse, B., Lehmann, J., Assenbaum, D., Wasserscheid, P., Leipertz, A., & Fröba, A. P. (2009). Viscosity, interfacial tension, density, and refractive index of ionic liquids [emim][meso3], [emim][meohpo2], [emim][ocso4], and [BBIM][NTF2] in dependence on temperature at atmospheric pressure. *Journal of Chemical & Engineering Data*, *54*(9), 2576–2583. https://doi.org/10.1021/je900134z

[10] Keener, J. F., Anderson, M. S., & Ewert, M. K. (2018). (tech.). (V. Z. Untalan, N. M. Williams, & S. A. Swan, Eds.)*Life Support Baseline Values and Assumptions Document* (pp. 63–70). Hanover, MD: NASA Scientific and Technical Information.

[11] Jagtap, P., Grace Belancik, Darrell Jan, & Ryan Purdy. (2021). (tech.). *Numerical Characterization of Spacecraft Cabin Air Dehumidification System for CO_2 Removal* (pp. 2–8). Moffett Field, CA: NASA Ames Research Center

[12] Rodriguez, Hector, and Joan F. Brennecke. "Temperature and Composition Dependence of the Density and Viscosity of Binary Mixtures of Water + Ionic Liquid." Journal of Chemical and Engineering Data, vol. 51, no. 6, 2006.

[13] Melinder Åke. (2007). *Thermophysical properties of aqueous solutions used as secondary working fluids* (thesis). Division of Applied Thermodynamics and Refrigeration, Royal Institute of Technology, Stockholm.

[14] Xiangjie Chen , Saffa Riffat , Bai Hongyu , Xiaofeng Zheng , David Reay , Recent Progress in Liquid Desiccant Dehumidification and Air-conditioning: A Review, Energy and Built Environment (2019), doi: https://doi.org/10.1016/j.enbenv.2019.09.001

[15] Araújo, H. V., Massuchetto, L. H., Nascimento, R. B., Carvalho, S. M., & Dangelo, J. V. (2022). Thermodynamic performance analysis of a single-effect absorption refrigeration system operating with water and 1-ethyl-3-methylimidazolium-based ionic liquids mixtures. *ScienceDirect - Applied Thermal Engineering*, *201*, 117761. https://doi.org/10.1016/j.applthermaleng.2021.117761

[16] Wang, Y., Hatakeyama, M., Ogata, K., Wakabayashi, M., Jin, F., & Nakamura, S. (2015). Activation of CO_2 by Ionic Liquid Emim–BF4 in the electrochemical system: A theoretical study. *Physical Chemistry Chemical Physics*, *17*(36), 23521–23531. https://doi.org/10.1039/c5cp02008e

[17] Elena Gomez, Begona Gonzalez, Noelia Calvar, Emilia Tojo, and Angeles Domınguez. "Physical Properties of Pure 1-Ethyl-3-methylimidazolium Ethylsulfate and Its Binary Mixtures with Ethanol and Water at Several Temperatures." J. Chem. Eng. Data 2006, 51, 2096-2102

[18] José S. Torrecilla, Tatiana Rafione, Julián García, and Francisco Rodríguez. "Effect of Relative Humidity of Air on Density, Apparent Molar Volume, Viscosity, Surface Tension, and Water Content of 1-Ethyl-3-methylimidazolium Ethylsulfate Ionic Liquid." J. Chem. Eng. Data 2008, 53, 923–928.c

[19] Sohaib Qazi, Lucía Gómez-coma, Jonathan Albo, Stéphanie Druon-bocquet, Angel Irabien, et al.. Mathematical modeling of CO 2 absorption with ionic liquids in a membrane contactor, study of absorption kinetics and influence of temperature. Journal of Chemical Technology and Biotechnology, Wiley, 2020, 95 (7), pp.1844-1857. ff10.1002/jctb.6265ff. ffhal-02930318

[20] Yesudass, S., Olasunkanmi, L. O., Bahadur, I., Kabanda, M. M., Obot, I. B., & Ebenso, E. E. (2016). Experimental and theoretical studies on some selected ionic liquids with different cations/anions as corrosion inhibitors for mild steel in acidic medium. *Journal of the Taiwan Institute of Chemical Engineers*, *64*, 252–268. https://doi.org/10.1016/j.jtice.2016.04.006

[21] Qu, M., Abdelaziz, O., Sun, X.-G., & Yin, H. (2017). Aqueous solution of [emim][oac]: Property formulations for use in air conditioning equipment design. *Applied Thermal Engineering*, *124*, 271–278. https://doi.org/10.1016/j.applthermaleng.2017.05.167

[22] Römich, C., Merkel, N. C., Valbonesi, A., Schaber, K., Sauer, S., & Schubert, T. J. (2012). Thermodynamic properties of binary mixtures of water and room-temperature ionic

liquids: Vapor pressures, heat capacities, densities, and viscosities of water + 1-ethyl-3-methylimidazolium acetate and water + diethylmethylammonium methane sulfonate. *Journal of Chemical & Engineering Data*, *57*(8), 2258–2264. https://doi.org/10.1021/je300132e

[22] Ionic Liquids Technologies GmbH. (2016). (rep.). *Safety Data Sheet 1-Ethyl-3-methylimidazolium acetate* (Vol. SDS IL-0189, pp. 1–3). Heilbronn, Germany.

[23] Kühn, R., Meyer, T., & Ziegler, F. (2020). Experimental investigation of ionic liquids as substitute for lithium bromide in water absorption chillers. *Energy*, *205*, 117990. https://doi.org/10.1016/j.energy.2020.117990

[24] Krannich, M., Heym, F., & Jess, A. (2016). Characterization of six hygroscopic ionic liquids with regard to their suitability for gas dehydration: Density, viscosity, thermal and oxidative stability, vapor pressure, diffusion coefficient, and activity coefficient of water. *Journal of Chemical & Engineering Data*, *61*(3), 1162–1176. https://doi.org/10.1021/acs.jced.5b00806

[25] Fernández, A., Torrecilla, J. S., García, J., & Rodríguez, F. (2007). Thermophysical properties of 1-ethyl-3-methylimidazolium ethylsulfate and 1-butyl-3-methylimidazolium methylsulfate ionic liquids. *Journal of Chemical & Engineering Data*, *52*(5), 1979–1983. https://doi.org/10.1021/je7002786

[26] (n.d.). (rep.). *Safety Data Sheet: 1-Ethyl-3-methylimidazolium dimethyl phosphate*.

[27] Zheng, C., Zhou, J., Pei, Y., & Yang, B. (2020). Equilibrium thermodynamic properties of aqueous solutions of ionic liquid 1-ethyl-3-methylimidazolium methanesulfonate [emim][meso3]. *Scientific Reports*, *10*(1), 1–9. https://doi.org/10.1038/s41598-020-59702-z

[28] *1-ethyl-3-methylimidazolium chloride: 65039-09-0*. ChemicalBook. (n.d.). Retrieved October 5, 2022, from https://www.chemicalbook.com/ChemicalProductProperty_EN_CB5428700.htm

[29] Uerdingen, M., Treber, C., Balser, M., Schmitt, G., & Werner, C. (2005, March 29). *Corrosion behaviour of ionic liquids*. Green Chemistry. Retrieved October 14, 2022, from https://pubs.rsc.org/en/content/articlepdf/2005/gc/b419320m

[30] Roland, K. (2016). (rep.). *Safety Data Sheet acc. to Regulation (EC) No. 1907/2006 (REACH) 1-Ethyl-3-methylimidazolium methansulfonate* (pp. 1–3). Grambach, Austria: Prioionic GmbH Poisoning Information Center.

[31] Yoshii, K., Yamaji, K., Tsuda, T., Tsunashima, K., Yoshida, H., Ozaki, M., & Kuwabatta, S. (2013). Physicochemical Properties of Tri-n-butylalkylphosphonium Cation-Based Room-Temperature Ionic Liquids. *The Journal of Physical Chemistry*, *1*(117), 15051–15059. https://doi.org/dx.doi.org/10.1021/jp406791a

[32] Wen, T., Luo, Y., & Sheng, L. (2020). Experimental study on the corrosion behavior and regeneration performance of KCOOH Aqueous Solution. *Solar Energy*, *201*, 638–648. https://doi.org/10.1016/j.solener.2020.03.044

[33] S.; Saleel, C.A.; Aabid, A.; Baig, M. Comparative Analysis on Dehumidification Performance of KCOOH–LiCl Hybrid Liquid Desiccant Air-Conditioning System: An Energy-Saving Approach. Sustainability 2022, 14, 3441. https://doi.org/10.3390/su14063441

[34] Kiris, I. M. (1991, May 1). *Experimental development and investigation of a new liquid desiccant system for drying operations*. TTU DSpace Home. https://ttu-ir.tdl.org/handle/2346/59927

Supporting Documents

[35] NASA. (2022, January 27). *NASA Systems Engineering Handbook*. NASA.org. Retrieved December 9, 2022, from https://www.nasa.gov/sites/default/files/atoms/files/nasa_systems_engineering_handbook.pdf

[36] Sanglard, P., Vorlet, O., Marti, R., Naef, O., & Vanoli, E. (2013). CO_2 capture by Ionic liquids – an answer to anthropogenic CO_2 emissions? *CHIMIA*, *67*(10), 711–718. https://doi.org/10.2533/chimia.2013.711

[37] Gandolfi, O. R., Gonçalves, G. R., Pimentel, J. G., Fontan, R. C., S. Júnior, E. C., Bonomo, P., Barreto, C. L., Veloso, C. M., & Bonomo, R. C. (2019). Thermophysical properties of 1-ethyl-3-methylimidazolium chloride solution from 293.15 to 323.15 K. *Brazilian Journal of Chemical Engineering*, *36*(1), 599–608. https://doi.org/10.1590/0104-6632.20190361s20180117 https://app.amanote.com/v4.0.18/research/note-taking(modal:authentication-modal/modal/login)

[38] Longo, G. A., & Gasparella, A. (2015). Experimental measurement of thermophysical properties of H2O/KCOOH (potassium formate) desiccant. *International Journal of Refrigeration*, *62*, 106–113. https://doi.org/10.1016/j.ijrefrig.2015.10.004

[39] Watanabe, H., Komura, T., Matsumoto, R., Ito, K., Nakayama, H., Nokami, T., & Itoh, T. (2019). Design of ionic liquids as liquid desiccant for an air conditioning system. *Green Energy & Environment*, *4*(2), 139–145. https://doi.org/10.1016/j.gee.2018.12.005

[40] Worek, W. M., & Lowenstein, A. (2013). Status of liquid-desiccant technologies and systems. *Desiccant-Assisted Cooling*, 25–46. https://doi.org/10.1007/978-1-4471-5565-2_2

[41] Oladosu, T. L., Baheta, A. T., & Oumer, A. N. (2021). Desiccant solutions, membrane technologies, and regeneration techniques in liquid desiccant air conditioning system. *International Journal of Energy Research*, *45*(6), 8420–8447. https://doi.org/10.1002/er.6482

[42] Piemonte, V., Maschietti, M., & Gironi, F. (2012). A triethylene glycol–water system: A study of the TEG regeneration processes in natural gas dehydration plants. *Energy Sources, Part A: Recovery, Utilization, and Environmental Effects*, *34*(5), 456–464. https://doi.org/10.1080/15567031003627930

[43] Triethylene glycol Compound Summary. (n.d.). Retrieved from https://pubchem.ncbi.nlm.nih.gov/compound/Triethylene-glycol.

[44] Triethylene glycol - Mitsubishi Chemical Corporation. (n.d.). Retrieved from https://www.m-chemical.co.jp/en/products/departments/mcc/c2/product/1200985_7910.html.

[45] Tech, F. o. (2022, December 8). *Magnet Drive gear pumps MG200 series*. Fluid o Tech. Retrieved December 8, 2022, from https://www.fluidotech.cn/site/assets/files/1313/scheda_mg200-en-def03_2020may.pdf

[46] Anderson, M. S., Ewert, M. K., & Keener, J. F. (2015). (rep.). *Life Support Baseline Values and Assumptions Document* (1st ed., Vol. 1, Ser. 1, pp. 65–68). Springfield, VA: National Technical Information Service.

[47] Froba, Andreas P, et al. "Density, Refractive Index, Interfacial Tension, and Viscosity of Ionic Liquids [EMIM][EtSO4], [EMIM][NTf2], [EMIM][N(CN)2], and [OMA][NTf2] in Dependence on Temperature at Atmospheric Pressure." *ACS Publications*, The Journal of Phyiscal Chemistry, 4 Sept. 2008, https://pubs.acs.org/doi/10.1021/jp804319a.

APPENDIX B: Complete Specifications for Major Purchased Parts/Components

Component	*Material/ Brand*	*Dimensions/ Specs*
Chamber Material	304 Stainless Steel Pipe	3-1/2"OD x 3"ID x 48"OAL
End Caps	Clear Polycarbonate	6" x 6"x 1/2" thick
Chamber Connecting Rods	Grade 7 Steel Threaded Rod	1/4"-20 2A Thread Size X 4' Long
Lock Nuts	Grade 8 Steel Nylon-Insert	1/4"-20 2B Thread
Baffle Plates - Material	304 Stainless Steel Strip	3" x 12", 1/8" Thick
Baffle Spacers	18-8 Stainless Steel	1/2" Hex, 1/2" Long, 1/4"-20 2B Thread
Baffle to Cap Connecting Bolts	Corr-Res 316 Stainless Steel	1" Long 1/4"-20 2B Thread
Gas Nozzles - Material	304 Stainless Steel Rod	1" OD X 1' Long
Liquid Nozzles - Material	304 Stainless Steel Rod	3/4" OD X 1' Long
EMIM EtSO4	IL Desiccant	2L
KCOOH	IL Desiccant	2L
Milling Tools	AlTiN Coated Carbide	N/A
Pressure Transducers	OMEGA	5
DAQ Bridge and modules	NI-cDAQ 9174	3 temp and 1 pressure modules 4 channels each,
Thermocouples	Stainless steel	Various lengths, J-Type (LabView)
Liquidflow meters	KING acrylic flowmeter	0 – 2.0 GPM
pumps	316 SS housing/PTFE Gears Fluidotech	Max P 290psi, Max vacumm 724mmHg
motors	Zinc/ Kahlig Antriebstechnick	12V 22W Output Power 6.5 Ncm nom. Torque

Table 36: Major Purchased Parts/ Components

APPENDIX C: Drawings for Custom-Built or Fabricated Parts/Components/Sub-Assemblies

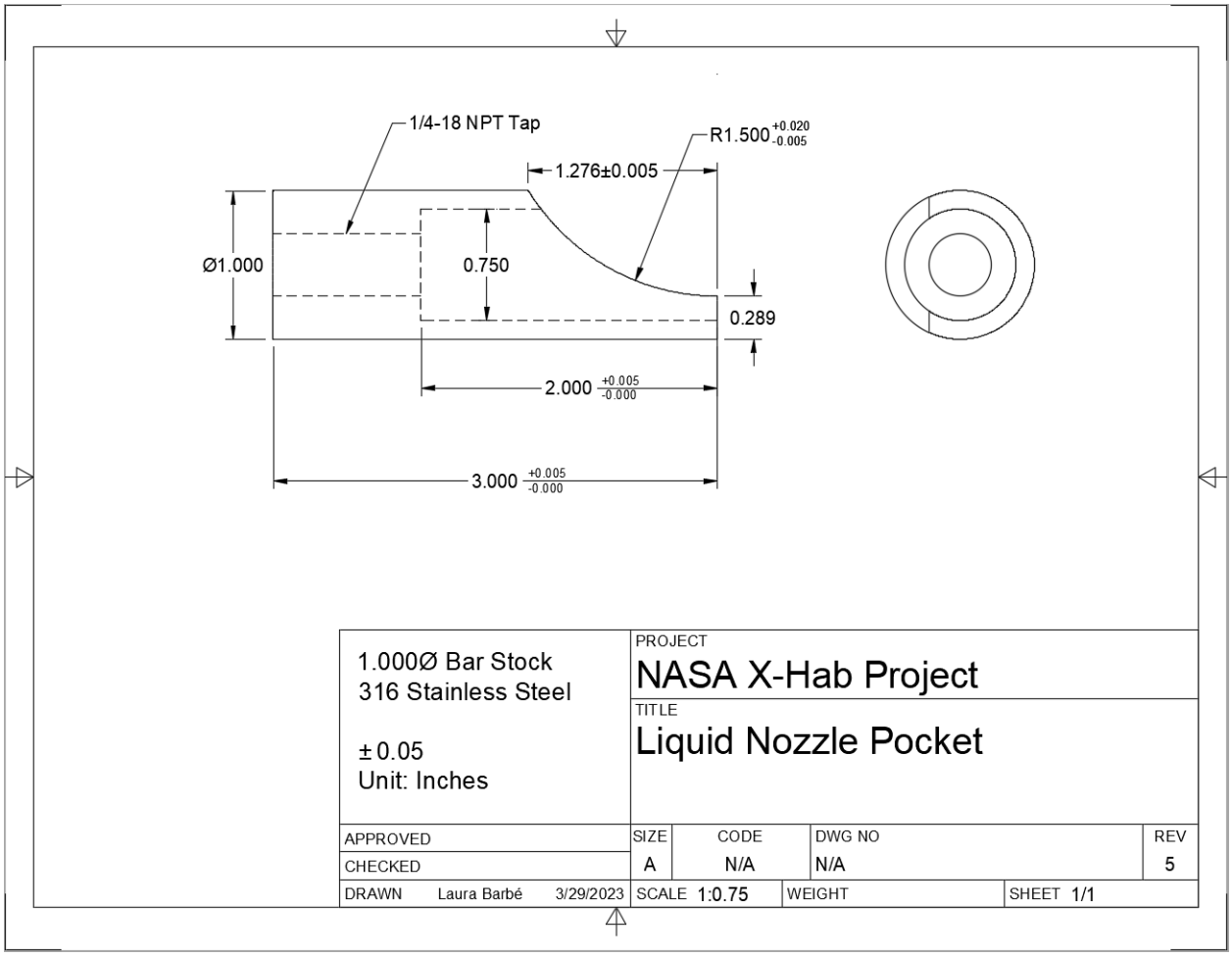

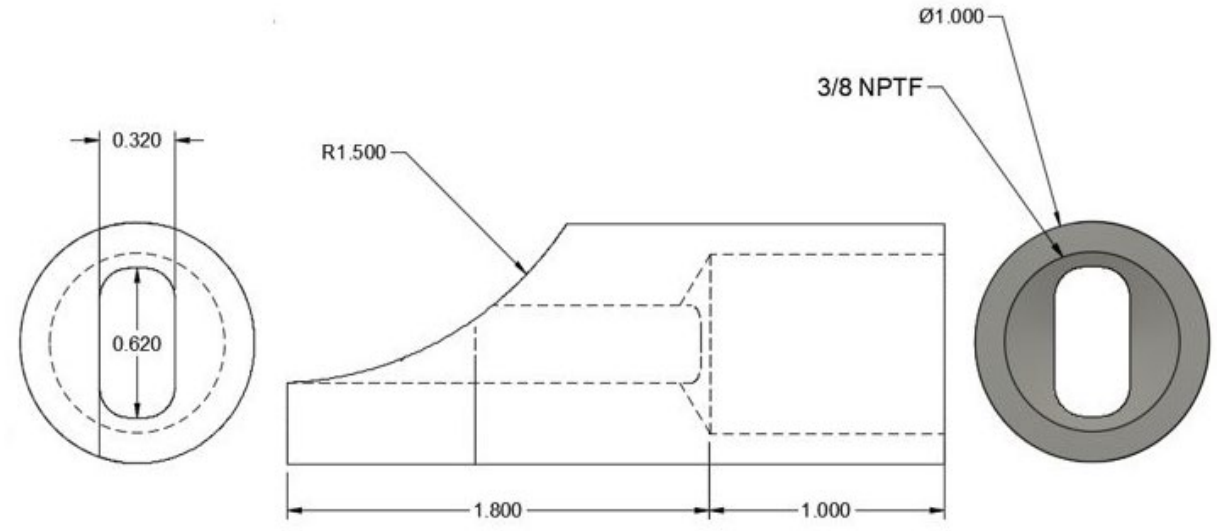

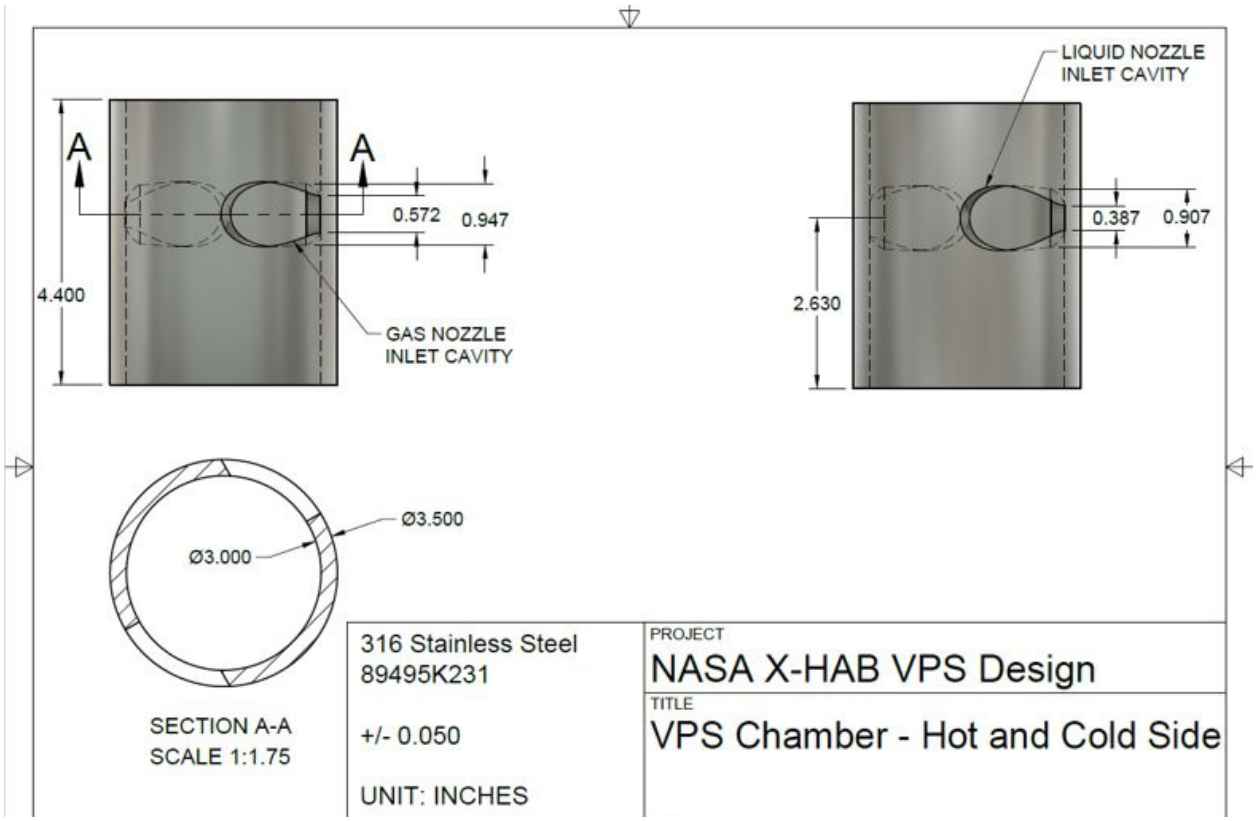
A
A
0.572
0.947
4.400
GAS NOZZLE
INLET CAVITY
LIQUID NOZZLE
INLET CAVITY
0.387
0.907
2.630
Ø3.500
Ø3.000
SECTION A-A
SCALE 1:1.75
316 Stainless Steel
89495K231
+/- 0.050
UNIT: INCHES
PROJECT
NASA X-HAB VPS Design
TITLE
VPS Chamber - Hot and Cold Side

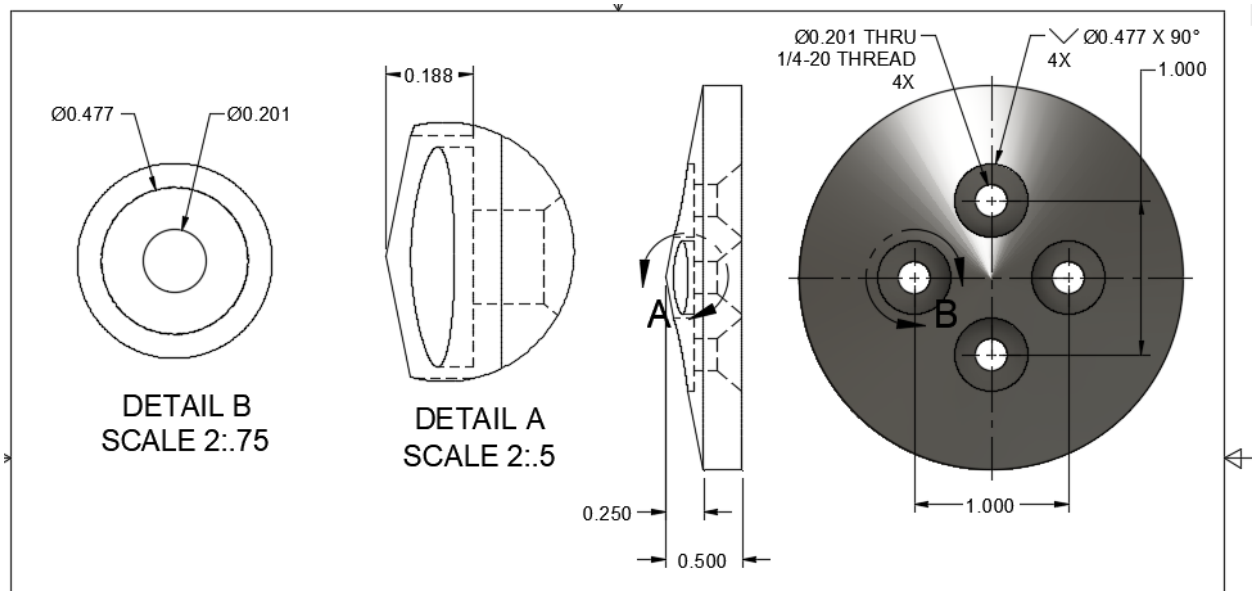
Ø0.477
Ø0.201
DETAIL B
SCALE 2:.75
0.188
DETAIL A
SCALE 2:.5
A
0.250
0.500
Ø0.201 THRU
1/4-20 THREAD
4X
Ø0.477 X 90°
4X
1.000
B
1.000

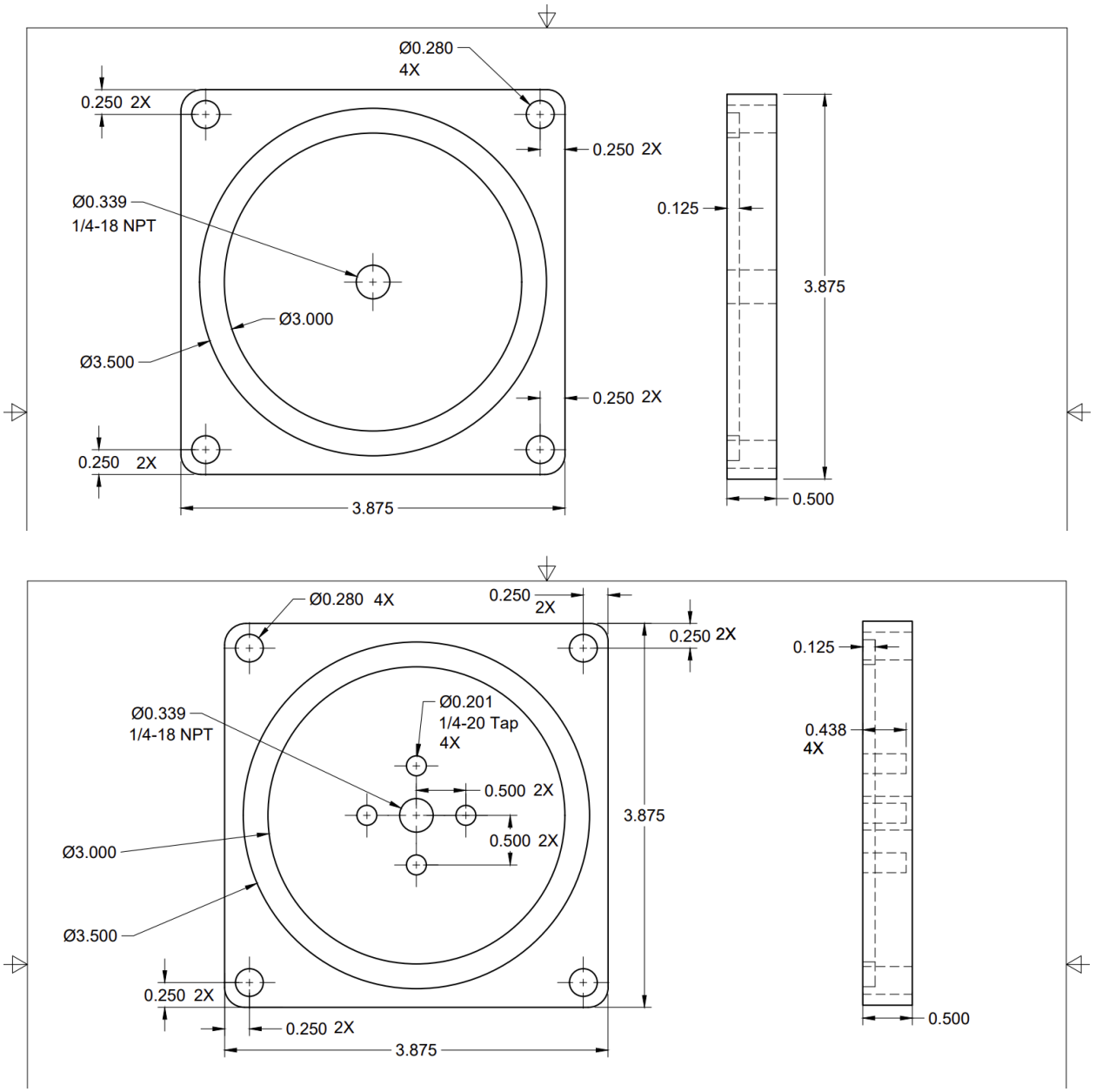
Ø0.280
4X
0.250 2X
0.250 2X
Ø0.339
1/4-18 NPT
Ø3.000
Ø3.500
0.250 2X
0.250 2X
3.875
0.125
3.875
0.500
Ø0.280 4X
0.250
2X
0.250 2X
Ø0.339
1/4-18 NPT
Ø0.201
1/4-20 Tap
4X
0.500 2X
0.500 2X
3.875
Ø3.000
Ø3.500
0.250 2X
0.250 2X
3.875
0.125
0.438
4X
0.500

APPENDIX D: Assembly Photos